

NUREG/CR-4792  
UCID-20914  
Vol. 4

---

---

# Probability of Failure in BWR Reactor Coolant Piping

Guillotine Break Indirectly Induced by Earthquakes

---

---

Prepared by G. S. Hardy, R. D. Campbell, M. K. Ravindra

NTS/Structural Mechanics Associates

Lawrence Livermore National Laboratory

Prepared for  
U.S. Nuclear Regulatory  
Commission

8701070592 861231  
PDR NUREG  
CR-4792 R PDR

## NOTICE

This report was prepared as an account of work sponsored by an agency of the United States Government. Neither the United States Government nor any agency thereof, or any of their employees, makes any warranty, expressed or implied, or assumes any legal liability of responsibility for any third party's use, or the results of such use, of any information, apparatus, product or process disclosed in this report, or represents that its use by such third party would not infringe privately owned rights.

## NOTICE

### Availability of Reference Materials Cited in NRC Publications

Most documents cited in NRC publications will be available from one of the following sources:

1. The NRC Public Document Room, 1717 H Street, N.W.  
Washington, DC 20555
2. The Superintendent of Documents, U.S. Government Printing Office, Post Office Box 37082,  
Washington, DC 20013-7082
3. The National Technical Information Service, Springfield, VA 22161

Although the listing that follows represents the majority of documents cited in NRC publications, it is not intended to be exhaustive.

Referenced documents available for inspection and copying for a fee from the NRC Public Document Room include NRC correspondence and internal NRC memoranda; NRC Office of Inspection and Enforcement bulletins, circulars, information notices, inspection and investigation notices; Licensee Event Reports; vendor reports and correspondence; Commission papers; and applicant and licensee documents and correspondence.

The following documents in the NUREG series are available for purchase from the GPO Sales Program: formal NRC staff and contractor reports, NRC-sponsored conference proceedings, and NRC booklets and brochures. Also available are Regulatory Guides, NRC regulations in the *Code of Federal Regulations*, and *Nuclear Regulatory Commission Issuances*.

Documents available from the National Technical Information Service include NUREG series reports and technical reports prepared by other federal agencies and reports prepared by the Atomic Energy Commission, forerunner agency to the Nuclear Regulatory Commission.

Documents available from public and special technical libraries include all open literature items, such as books, journal and periodical articles, and transactions. *Federal Register* notices, federal and state legislation, and congressional reports can usually be obtained from these libraries.

Documents such as theses, dissertations, foreign reports and translations, and non-NRC conference proceedings are available for purchase from the organization sponsoring the publication cited.

Single copies of NRC draft reports are available free, to the extent of supply, upon written request to the Division of Technical Information and Document Control, U.S. Nuclear Regulatory Commission, Washington, DC 20555.

Copies of industry codes and standards used in a substantive manner in the NRC regulatory process are maintained at the NRC Library, 7920 Norfolk Avenue, Bethesda, Maryland, and are available there for reference use by the public. Codes and standards are usually copyrighted and may be purchased from the originating organization or, if they are American National Standards, from the American National Standards Institute, 1430 Broadway, New York, NY 10018.



---

# Probability of Failure in BWR Reactor Coolant Piping

Guillotine Break Indirectly Induced by Earthquakes

---

Manuscript Completed: November 1986  
Date Published: December 1986

Prepared by  
G. S. Hardy, R. D. Campbell, M. K. Ravindra

NTS/Structural Mechanics Associates  
5160 Birch Street  
Newport Beach, CA 92660

Under Contract to:  
Lawrence Livermore National Laboratory  
Livermore, CA 94550

Prepared for  
Division of Engineering Safety  
Office of Nuclear Regulatory Research  
U.S. Nuclear Regulatory Commission  
Washington, DC 20555  
NRC FIN A0133

## ABSTRACT

The requirements to design nuclear power plants for the effects of an instantaneous double-ended guillotine break (DEGB) of the reactor coolant piping have led to excessive design costs, interference with normal plant operation and maintenance, and unnecessary radiation exposure of plant maintenance personnel. This report describes an aspect of the NRC/ Lawrence Livermore National Laboratory-sponsored research program aimed at investigating whether the probability of DEGB in Reactor Coolant Loop Piping of nuclear power plants is acceptably small such that the requirements to design for the DEGB effects (e.g., provision of pipe whip restraints) may be removed. This study estimates the probability of indirect DEGB in Reactor Coolant piping as a consequence of seismic-induced structural failures within the containment of the GE supplied boiling water reactor at the Brunswick nuclear power plant. The median probability of indirect DEGB was estimated to be  $2 \times 10^{-8}$  per year. Using conservative assumptions, the 90% subjective probability value (confidence) of  $P_{\text{DEGB}}$  was found to be less than  $5 \times 10^{-7}$  per year.

Key Words: Design; Fragility; Guillotine Break; Pipes; Pipe Whip Restraints; Boiling Water Reactor; Probabilistic Analysis; Reliability; Reactor Coolant Loop; Seismic Hazard; Seismic Response; GE Mark I.

# TABLE OF CONTENTS

<u>Section</u>	<u>Title</u>	<u>Page</u>
	ABSTRACT.....	iii
	FIGURES.....	vii
	TABLES.....	ix
	EXECUTIVE SUMMARY.....	xi
	ACKNOWLEDGEMENTS.....	xiii
1	INTRODUCTION.....	1-1
	1.1 Background.....	1-1
	1.1.1 Previous Studies on Westinghouse, Combustion Engineering and Babcock and Wilcox Reactors.....	1-2
	1.1.2 Reactor Recirculation and Primary Containment System Arrangements in GE Mark I Plants.....	1-5
	1.2 General Approach.....	1-6
	1.2.1 Objective and Scope.....	1-6
	1.2.2 Trial Plant Studies.....	1-6
2	METHODOLOGY .....	2-1
	2.1 General.....	2-1
	2.2 Seismic Fragility.....	2-2
	2.3 Seismic Hazard.....	2-9
	2.4 Calculation of DEGB Probability.....	2-9
3	SEISMIC FRAGILITY CALCULATIONS.....	3-1
	3.1 Capacity Factor Derivations.....	3-2
	3.1.1 Overhead Crane.....	3-2
	3.1.2 Primary Containment Structure (Drywell).....	3-3
	3.1.3 Star Truss.....	3-4
	3.1.4 Stabilizer Capacity.....	3-9
	3.1.5 Shield Wall.....	3-13
	3.1.6 RPV Pedestal.....	3-14
	3.1.7 RPV Lower Support Structure.....	3-16



## TABLE OF CONTENTS (Continued)

<u>Section</u>	<u>Title</u>	<u>Page</u>
3.2	Response Factors.....	3-18
3.2.1	Spectral Shape Factor, $F_{SS}$ .....	3-19
3.2.1.1	Background on Design Spectra and Median Spectra.....	3-20
3.2.1.2	Drywell and RPV System Response.....	3-21
3.2.1.3	Calculation of Spectral Shape Factors.....	3-22
3.2.2	Damping Factor, $F_D$ .....	3-23
3.2.3	Modeling Factor, $F_M$ .....	3-24
3.2.4	Soil-Structure Interaction, $F_{SSI}$ .....	3-24
3.2.5	Earthquake Component Combination Factor, $F_{EC}$ .....	3-25
3.3	Ground Acceleration Capacities for Critical Components $A_C$ .....	3-25
4	GENERIC SEISMIC HAZARD CURVES.....	4-1
4.1	Background.....	4-1
4.2	Curve Development Procedure.....	4-2
5	RESULTS AND CONCLUSIONS.....	5-1
5.1	Probability of an Indirect DEGB.....	5-1
5.2	Comparison with Previous Studies.....	5-2
5.3	Sensitivity of Results.....	5-2
5.3.1	Seismic Hazard.....	5-2
5.3.2	Design and Construction Errors.....	5-3
5.3.3	Low Fracture Toughness.....	5-5
5.3.4	Brunswick SSE Spectrum Application.....	5-6
5.4	Summary and Conclusions.....	5-6

REFERENCES

NOMENCLATURE

GLOSSARY

## FIGURES

- 1-1. Cross-section of a typical Mark I containment.
- 1-2. Schematic of a typical Mark I pressure suppression system.
- 1-3. Reactor recirculation loop arrangement.
- 1-4. Schematic of the drywell truss system.
- 1-5. Mathematical model used in the analysis of the reactor recirculation loop piping.
  
- 2-1. Fragility of structure or equipment.
- 2-2. Seismic hazard curves.
- 2-3. Distribution of the probability of indirectly-induced DEGB.
  
- 3-1. Brunswick containment structure and RPV support system.
- 3-2. Star truss configuration.
- 3-3. Resultant capacity vector for single "V" shaped pipe truss.
- 3-4. Ultimate load capacity for star truss.
- 3-5. Non-linear loading on star truss support system.
- 3-6. RPV stabilizer configuration.
- 3-7. Schematic of RPV stabilizer components.
- 3-8. RPV stabilizer clevis pin, clevis and draw bar.
- 3-9. RPV stabilizer gusset plate bracket.
- 3-10. Perspective view of containment structure.
- 3-11. Shield wall to pedestal interface.
- 3-12. Anchor bolt pattern for RPV ring girder and shield wall.
- 3-13. Anchor bolts for RPV ring girder and shield wall.
- 3-14. Summation of nodal shears for SSE condition - X direction.
- 3-15. Summation of nodal shears for SSE condition - Y direction.
- 3-16. Summation of nodal moments for SSE condition - Y direction.
- 3-17. Summation of nodal moments for SSE condition - X direction.
- 3-18. RPV support pedestal.
- 3-19. RPV ring girder to pedestal anchorage.
- 3-20. RPV support skirt configuration.
- 3-21. RPV ring girder and anchorage.
- 3-22. Brunswick OBE design ground response spectra.

## FIGURES (continued)

- 3-23. Containment structure model for soil-structure interaction.
- 3-24. Artificial time-history for Brunswick plant site.
- 3-25. Free-field surface response spectrum due to WASH-1255 spectrum applied at rock outcrop.
- 3-26. Free-field surface spectra due to a Brunswick design motion applied to the bedrock layer.
- 3-27. Dynamic model of reactor building.
- 3-28. Containment and RPV system mode shapes.
  
- 4-1. Region of applicability of generic seismic hazard curves.
- 4-2. Mean seismic hazard curves.
- 4-3. Normalized mean hazard curves.
- 4-4. Generic seismic hazard curves.
- 4-5. Generic seismic hazard curves - median and 10% and 90% curves.
  
- 5-1. Stabilizer fragility curves.
- 5-2. Star truss fragility curves.
- 5-3. Plant level fragility curves for Brunswick.
- 5-4. Plant level fragility curves for Brunswick.
- 5-5. Histogram of annual frequency of DEGB for Brunswick.



## TABLES

- 3-1. Sacrificial shield wall physical properties.
  - 3-2. Strength factor comparison for critical areas of the RPV lower support.
  - 3-3. Damping values used in Brunswick design analysis.
  - 3-4. Stabilizer fragility.
  - 3-5. Star truss fragility.
- 
- 5-1. Comparison of  $P_{DEGB}$  for different types of nuclear plants.

## EXECUTIVE SUMMARY

### BACKGROUND

Currently, nuclear power plants are required to be designed for the effects of the unlikely event of double-ended guillotine break (DEGB) of certain reactor coolant piping, with the DEGB and the Safe Shutdown Earthquake (SSE) events being considered to occur simultaneously. This requirement has led to excessive design costs (i.e., provision of pipe whip restraints), interference with normal plant operation and unnecessary radiation exposure of plant maintenance personnel. The present work is part of an NRC-directed research program, the Load Combination Research Program, at the Lawrence Livermore National Laboratory (LLNL), established to estimate the probability of a DEGB of reactor coolant piping. One objective of the program was to recommend changes to the current regulatory requirements if the probability of DEGB is found to be extremely small.

Two broad classes of DEGB have been identified in the LLNL evaluations. The "directly-induced" DEGB is defined as a double-ended pipe break of the RCL piping due to fatigue crack growth under the combined effects of thermal, pressure, seismic, and other cyclic loads while "indirectly-induced" DEGB is a RCL pipe break due to causes such as support structure failures, missiles, and transient events caused by earthquakes. The indirectly-induced DEGB is the topic of this report. Earthquakes are considered to be the only plausible cause for a DEGB of the reactor coolant piping considered in the evaluation described in this report.

### TECHNICAL APPROACH

A methodology for estimating the probability of a DEGB indirectly-induced by structural failures under earthquakes which was developed in a previous phase of the program has been applied to the Brunswick nuclear power plant. Brunswick is a General Electric boiling water reactor (BWR) with a Mark I containment. The key elements of the methodology are seismic hazard analysis, seismic response analysis, fragility evaluation for critical structural elements, and analysis of reactor coolant loop integrity following structural failures. The uncertainties in seismic hazard, seismic responses, and capacities are explicitly treated in this methodology to produce subjective probability bounds on the estimated probability of a DEGB. By reviewing the plant arrangement and design bases for the GE Mark I reactor configuration, it was concluded that failure of a primary equipment support (i.e., reactor pressure vessel or recirculation pump) would lead to a DEGB. Reactor pressure vessel support failure can potentially lead to failure of the recirculation loop or steam and feedwater lines inside of containment while recirculation pump support failure directly affects only the recirculation loop. LLNL is conducting a study of the recirculation piping and supports which includes the recirculation pump supports. The study discussed herein concentrates on the RPV support system which includes the RPV lower support, the RPV pedestal, the RPV stabilizer (upper support), the shield wall, the drywell and the star

truss that connects the top of the shield wall to the drywell. Fragility descriptions of the RPV support system have been developed using information on plant design criteria and by appropriately extrapolating the responses calculated at the design analysis stage to failure levels of the structural elements of the component supports. Fragility is expressed as a lognormally distributed conditional probability of failure. Fragility is defined as a median factor of safety over the SSE peak ground acceleration  $F$  and the variability estimates  $\beta_{F,R}$  and  $\beta_{F,U}$  representing randomness and uncertainty in the median estimate.

The probability of indirectly-induced DEGB in the reactor coolant piping has been estimated using the fragility descriptions and a set of generic seismic hazard curves developed in a previous phase of this research program (Ravindra, Campbell, 1984). The median probability of indirect DEGB for Brunswick was estimated to be  $2 \times 10^{-8}$  per year. Using conservative assumptions, the 90% subjective probability (confidence) value of  $P_{DEGB}$  was found to be less than  $5 \times 10^{-7}$  per year.

Based on the insights gained and the results of this study, the following conclusions are derived:

1. The probability of indirectly-induced DEGB in reactor coolant piping due to earthquakes is very small for the Brunswick plant.
2. Sensitivity studies have shown that only very unlikely design and construction errors of implausible magnitude may substantially change the probability of DEGB indirectly-induced by earthquakes calculated in this study.

The conclusions drawn from this study were made specifically for the Brunswick reactor and containment configuration. The Brunswick containment represents a transition between a Mark I design and a Mark II design. The Brunswick drywell is conical-shaped (typical for Mark II) instead of light-bulb-shaped (typical of Mark I) although the drywell design for suppressing steam discharges from safety relief valve openings and loss-of-coolant accidents is typical of a Mark I, i.e., steam discharges into a torus surrounding the drywell. The treatment of soil-structure interaction in the Brunswick design process was very conservative. This design conservatism resulted in Brunswick components and structures being overdesigned for seismic loading. Conservatism in design is common, but, the degree of conservatism in the soil-structure interaction analysis for Brunswick appeared to be more conservative than usual. Conclusions regarding probability of DEGB derived for Brunswick may, therefore, not be generally applicable to other Mark I designs. It is recommended that further study be conducted on the remaining GE nuclear plants to establish the range of indirect DEGB probabilities. The results of this pilot plant (Brunswick) study can be utilized to efficiently direct the resources of the continued study towards the most critical areas.



#### ACKNOWLEDGEMENTS

The study reported herein was performed by ITS/Structural Mechanics Associates, under a subcontract from the Lawrence Livermore National Laboratory. The authors acknowledge the guidance and valuable comments of Drs. C. K. Chou, G. S. Holman and T. Y. Lo of the Lawrence Livermore National Laboratory.

## 1. INTRODUCTION

### 1.1 BACKGROUND

The Code of Federal Regulations requires that structures, systems, and components important to the safety of nuclear power plants in the United States be designed to withstand appropriate combinations of effects of natural phenomena, normal situations, and accident conditions. One of the loading conditions that has been formulated on the basis of these Federal Regulations is the consideration of a double-ended guillotine break (DEGB) of the reactor coolant piping and the combination of its effects with those of the Safe Shutdown Earthquake (SSE). This requirement has led to high design costs (i.e., provision of pipe whip restraints), interference with normal plant operation and added radiation exposure of plant maintenance personnel. Since some of the operating plants have not been designed for this loading condition, extensive plant modifications may be necessary to meet this design requirement. In order to judge the need for DEGB requirements, the NRC directed a research program, the Load Combination Research Program, at the Lawrence Livermore National Laboratory (LLNL), to estimate the probability of a DEGB of the RCL piping. The first 3 phases of the program addressed the issue for Westinghouse (W), Combustion Engineering (CE), and Babcock and Wilcox (B&W) PWR plants. The present phase of the program concentrates on the BWRs supplied by General Electric (GE). One objective of the program is to estimate the probability of DEGB in certain reactor coolant piping and recommend changes in regulatory requirements. If the probability of DEGB is acceptably low (as judged by the NRC), it may no longer be necessary to 1) evaluate the asymmetric blowdown loading, 2) combine SSE and DEGB loads and 3) install and maintain pipe whip restraints for the affected piping.

Two broad classes of DEGB have been identified. The "directly-induced" DEGB is pipe break due to fatigue crack growth under combined effects of thermal, pressure, seismic, and other cyclic loads. The indirectly-induced DEGB is pipe break due to causes such as structural failures, missiles, electrical failures, and transient events caused by earthquakes. Of these, seismically-induced structural failures within containment generally

constitute the only credible source of indirect DEGB. This report discusses only the indirectly-induced DEGB of the piping.

#### 1.1.1 Previous Studies on Westinghouse, Combustion Engineering and Babcock and Wilcox Reactors

In the first phase of the Load Combination Research Program, the probability of an indirectly-induced DEGB in the reactor coolant loop (RCL) piping of Westinghouse reactors was evaluated (Ravindra, et al, 1984). A methodology for calculating this probability,  $P_{DEGB}$ , was developed using the Zion Nuclear Generating Station as a pilot plant. It was concluded that failure of the supports of the reactor pressure vessel, reactor coolant pump, or steam generator could potentially cause a DEGB of the reactor coolant loop piping. In the pilot study on the Zion Nuclear Generating Station, the median capacities and responses of these supports were calculated by conducting detailed seismic response analysis and failure mode evaluation. The variabilities representing inherent randomness and uncertainty were estimated. Using the site-specific hazard curves, the plant-specific probability of an indirect DEGB was evaluated for Zion. The median probability of an indirect DEGB was calculated to be  $1.3 \times 10^{-8}$  per year with the 10 and 90 percent subjective probability bounds estimated to be  $4.1 \times 10^{-10}$  and  $3.5 \times 10^{-7}$  per year, respectively.

A generic study on 46 Westinghouse-supplied PWRs was performed to extend the results of the Zion pilot study. A set of generic seismic hazard curves deemed applicable for sites located east of the Rocky Mountains was developed using the results of published site-specific seismic hazard studies. Westinghouse provided data on the seismic design parameters and SSE design margins for the reactor coolant loop design of each reactor unit. Since these units were designed for a variety of response spectra and zero period peak ground accelerations using different methods of analysis and damping values, the design margins were reassessed to put them on a consistent basis. The total population of Westinghouse reactor units were classified into two groups:



- Units with primary equipment supports designed by W.
- Units with primary equipment supports designed by the architect-engineer.

In each group, the plant with lowest margin was selected for further study. Detailed information on design of the plant and inherent safety margins in the ASME Code were used in estimating the factors of safety available against SSE for equipment supports in these selected plants. Using the generic seismic hazard curves and the factors of safety for equipment supports, the median annual probability of an indirect DEGB was calculated to  $3.3 \times 10^{-6}$  per year and  $2.4 \times 10^{-6}$  per year for the two selected plants. The 10% to 90% subjective probability bounds on this DEGB probability was approximately  $2.0 \times 10^{-7}$  to  $2.0 \times 10^{-5}$  per year.

From the plants located in the Western U.S., Diablo Canyon and San Onofre Unit 1 were selected for estimation of the indirect DEGB probability. Site-specific hazard curves and seismic margins calculated in the reevaluations of these plants were used for this purpose. The median probability of an indirect DEGB was calculated to be about  $3 \times 10^{-6}$  per year. The 10% to 90% subjective probability range of this probability was estimated as approximately  $2 \times 10^{-7}$  per year to  $6 \times 10^{-5}$  per year.

The study on Westinghouse reactors showed that the probability of an indirect DEGB in the RCL piping due to earthquakes is very low and that the failure of some major equipment supports has a high likelihood of rupturing the RCL piping inside the reactor cavity (i.e., between the shield wall and RPV).

In the second phase of this program, a similar but reduced scope evaluation of the probability of an indirect DEGB of the RCL piping was undertaken for Combustion Engineering supplied reactor systems. A total of 13 Combustion Engineering plants were investigated with Palo Verde Units 1, 2, and 3 being used as the reference plant. Six of the plants were characterized as "early" plants (three nozzle supports for the reactor vessel) and the

remaining seven were characterized as "modern" plants (four nozzle supports for the reactor vessel). The median probability of an indirect DEGB was calculated to be in the range of  $10^{-6}$  per year for early plants and less than  $10^{-8}$  for modern plants. Using very conservative assumptions, the 90% subjective probability (confidence) value of  $P_{DEGB}$  was found to be less than  $5 \times 10^{-5}$  per year for the older plants and less than  $3 \times 10^{-7}$  per year for the modern plants. Consistent with the results of the study of Westinghouse plants, the study of Combustion Engineering reactors showed that the probability of an indirect DEGB in the RCL piping due to earthquakes is very low.

In the third phase of the program, a scope of work similar to the one conducted in Phase 2 was undertaken. A total of ten plants whose NSSS was designed and fabricated by Babcock & Wilcox (B&W) were evaluated during the course of this study. The plants are separated into two groups on the basis of the reactor coolant loop configuration ("raised" or "lowered") as follows:

Lowered Loop Configuration

Midland 1 & 2 (Reference Plant)  
 Oconee 1, 2, & 3  
 Crystal River 3  
 Arkansas Nuclear One 1  
 Rancho Seco

Raised Loop Configuration

WPPSS 1 (Reference Plant)  
 Davis - Besse 1

For the first, designated the "lowered-loop" configuration, the reactor vessel and steam generators are both skirt-supported and are anchored to the base mat at essentially common elevations. The skirt flanges are fixed against translation. Thermal expansion is accommodated by means of the flexibility of the RCL piping and the freedom of movement allowed the reactor coolant pumps, which are snubbed.

For the second configuration, designated as the "raised-loop" configuration, the reactor vessel is supported on nozzle pads. The pads are an integral part of the four cold leg inlet nozzles and are set on lubrite

plates which allow radial expansion but essentially restrain lateral and vertical translation.

The median probability of indirect DEGB for both configurations was estimated to range between  $6 \times 10^{-11}$  and  $1 \times 10^{-7}$  per year. Using very conservative assumptions, the 90% subjective probability (confidence) value of  $P_{\text{DEGB}}$  was found to be less than  $1 \times 10^{-5}$  per year.

#### 1.1.2 Reactor Recirculation and Primary Containment System Arrangements in GE Mark I Plants

A cross-section of a typical Mark I containment system is shown in Figure 1-1. The primary containment system consists of the drywell, vent pipes, and a pool of water contained in the suppression chamber. The reactor building encloses the primary containment system, thereby providing a second containment. Figure 1-2 contains a schematic of the steel drywell together with the vent pipe/suppression chamber interface. The light-bulb-shaped drywell containment surrounds the reactor and the primary system piping. A toroidal suppression chamber is provided to condense steam in the event of a safety relief valve discharge or a Loss of Coolant Accident (LOCA), and is connected to the drywell by either eight or ten main vent pipes, depending upon the particular installation.

The reactor pressure vessel system in a typical Mark I plant comprises the vessel, the surrounding shield wall (a cylindrical concrete-filled steel shell), the vessel support system, and the concrete support pedestal. Figure 1-3 shows the recirculation pump and the recirculation piping system arrangement for a typical GE Mark I system. The RPV upper support system is shown schematically in Figure 1-4. The reactor vessel seismic loads are transmitted through the stabilizer and into the shield wall. The shield wall in turn, transmits these loads through the star truss on into the Drywell/Reactor Building. A typical mathematical model developed for a seismic analysis of a reactor recirculation system is shown in Figure 1-5. Not shown are the mass points representing the reactor vessel and the shield wall, or the springs representing the connecting structural



elements between the vessel and the shield, and between the shield and the reactor building.

## 1.2 GENERAL APPROACH

### 1.2.1 Objective and Scope

The objective of this present study has been to evaluate the probability of a seismically-induced indirect DEGB in the reactor coolant system piping of a trial plant GE Mark I containment system. The study consisted of the following major tasks:

1. Review available site-specific seismic hazard curves for the trial location to assess the validity of using generic seismic hazard curves in the proposed study.
2. Review the seismic design basis and the qualification analyses for the RPV support system at the trial plant.
3. Estimate the seismic fragilities of the RPV support system subassemblies whose seismic failure may lead to an indirect DEGB of the reactor recirculation piping for the selected trial plant.
4. Calculate the probability of an indirectly-induced DEGB in the recirculation piping of the trial plant using the generic seismic hazard curves.

### 1.2.2 Trial Plant Studied

The Carolina Power and Light Company's Brunswick Steam Electric Plant was chosen to be the trial plant for the DEGB study on Mark I nuclear power plants. The Brunswick site is located 19 miles south of Wilmington, North Carolina. The electrical capacity of the plant is 790 Mw and Units 1 and 2 have been in commercial operation since 1977 and 1975, respectively. General Electric is the reactor supplier for the plant while United Engineers and Constructors is the balance-of-plant engineers. As described in Section 3.1 of this report, the Brunswick Mark I drywell is slightly different than other earlier Mark I plants. The "light-bulb-shaped" steel drywell was not used at

Brunswick, instead, a cylinder-cone reinforced concrete drywell was used which is more characteristic of Mark II containments. The suppression chamber is, however, a steel torus surrounding the drywell, which is characteristic of Mark I containments.

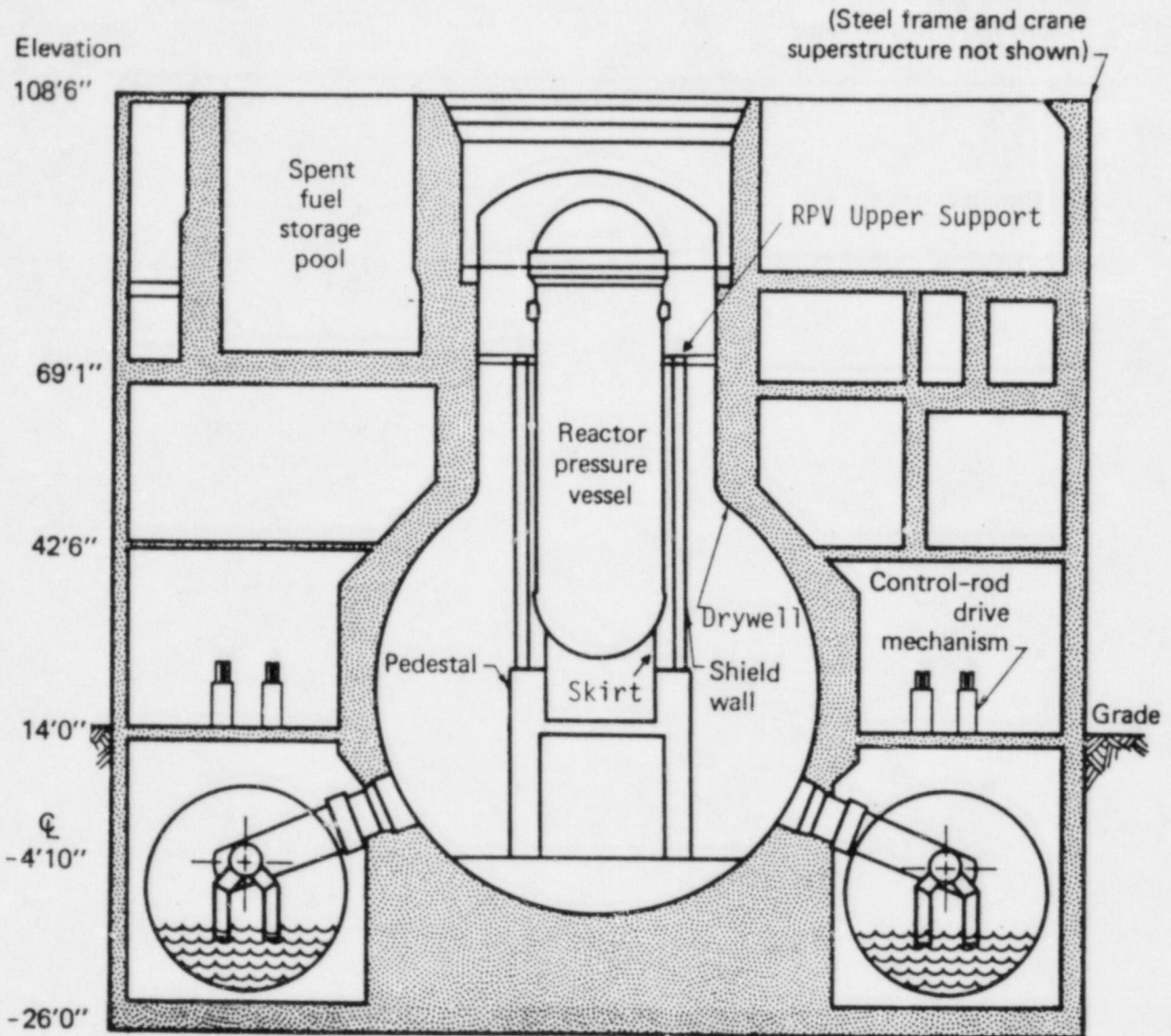


FIGURE 1-1. CROSS-SECTION OF A TYPICAL MARK I CONTAINMENT



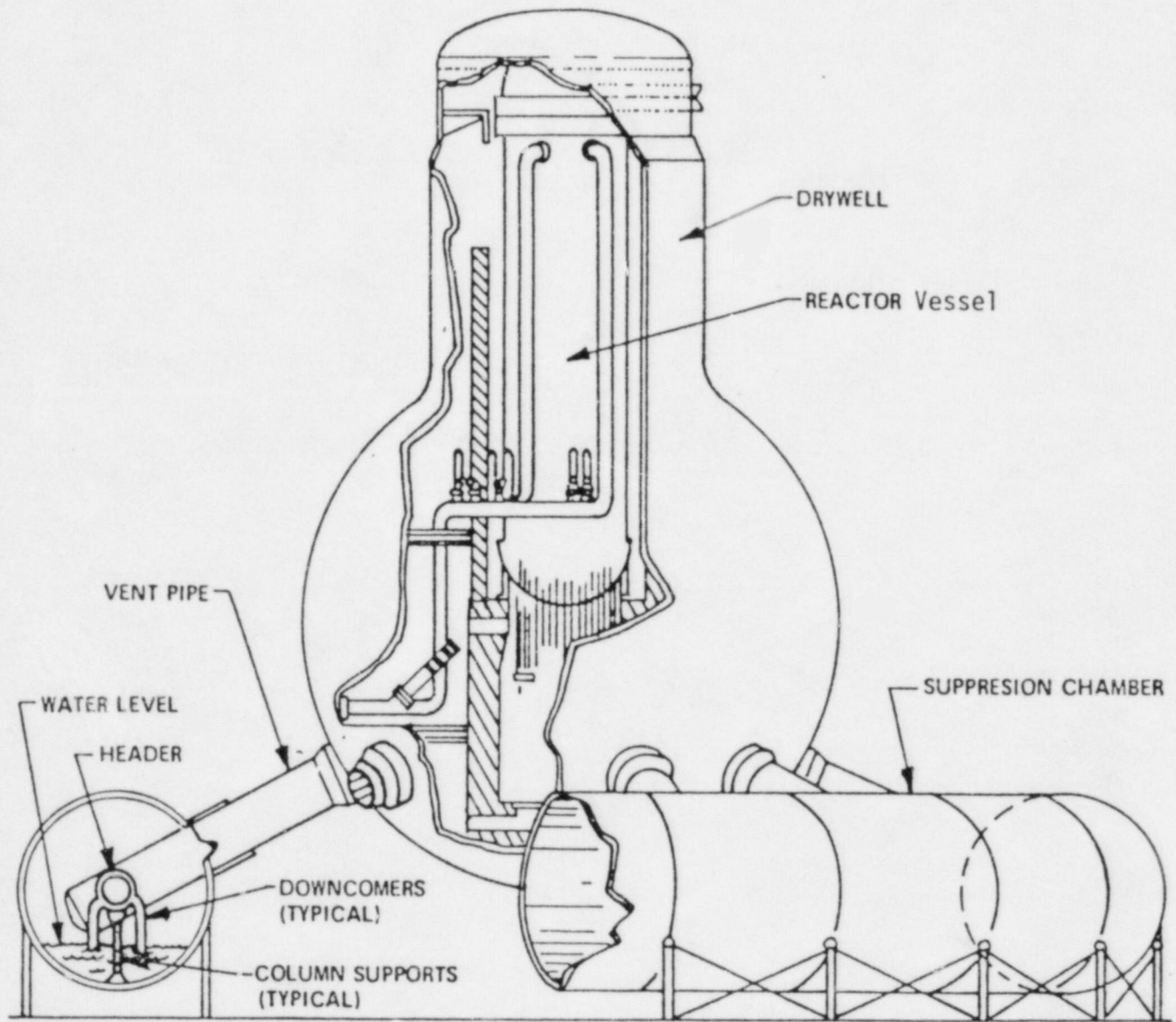


FIGURE 1-2. SCHEMATIC OF MARK I PRESSURE SUPPRESSION SYSTEM

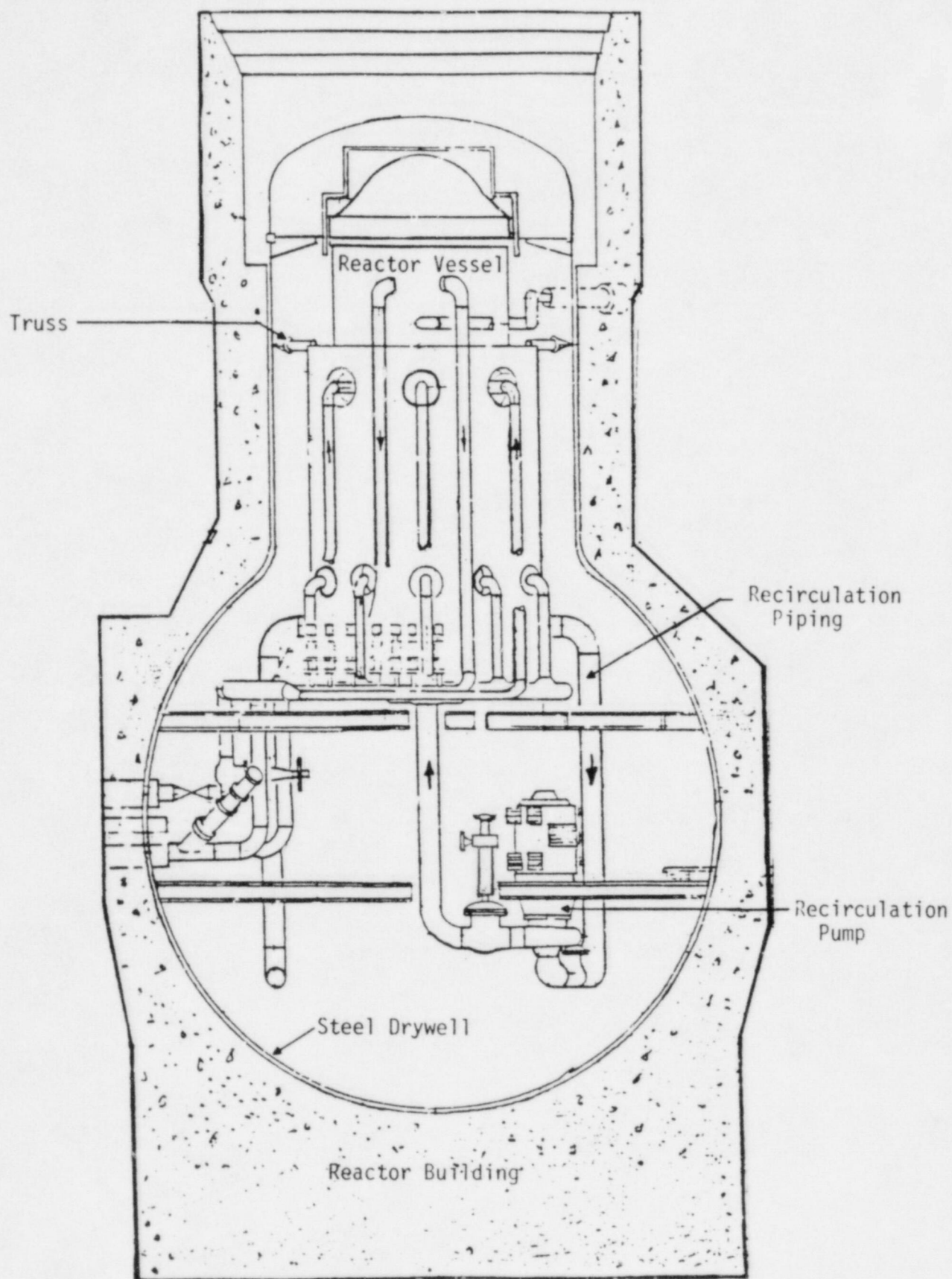


FIGURE 1-3. REACTOR RECIRCULATION LOOP ARRANGEMENT

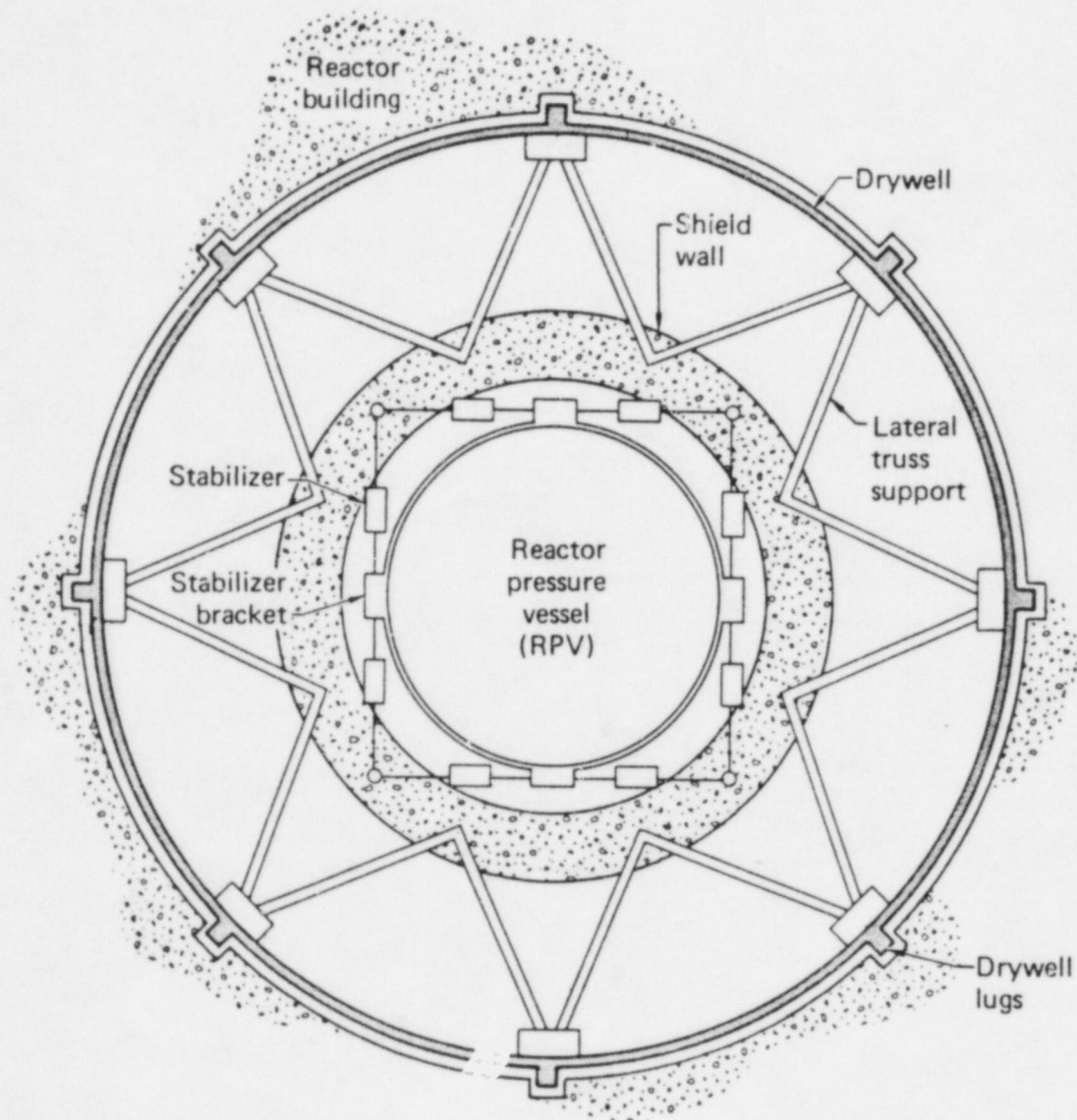


FIGURE 1-4. SCHEMATIC OF THE DRYWELL TRUSS SYSTEM



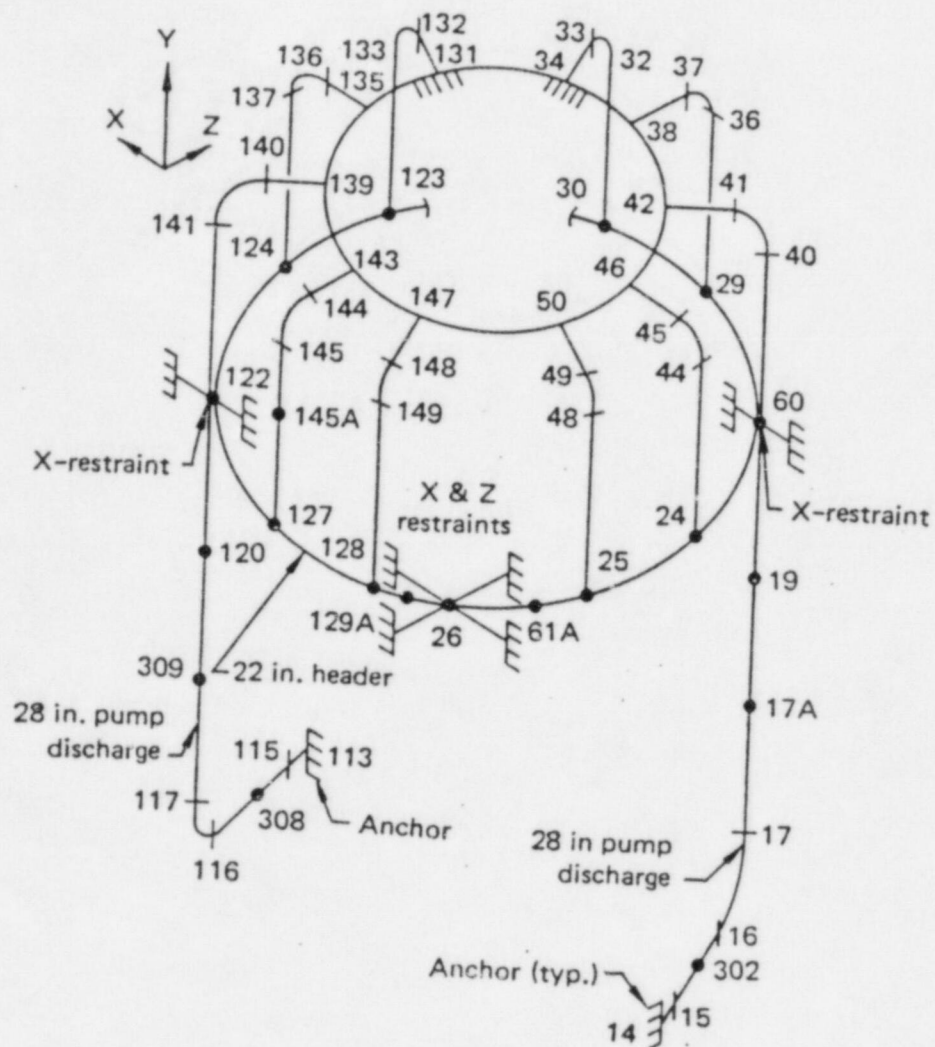


FIGURE 1-5. MATHEMATICAL MODEL USED IN THE ANALYSIS OF THE REACTOR RECIRCULATION LOOP PIPING.

## 2. METHODOLOGY

This chapter describes the general methodology utilized in the calculation of the probability of an indirect DEGB induced by structural failures under earthquakes. The key elements of the methodology are seismic hazard analysis and evaluation of the fragility of equipment supports whose failure might lead to a DEGB of the reactor coolant system piping.

### 2.1 GENERAL

The objective of the present study is to calculate the probability of a DEGB as a result of structural failures which are induced by an earthquake. This probability,  $P_{\text{DEGB}}$ , can be mathematically expressed as:

$$P_{\text{DEGB}} = \int_0^{\infty} P \left[ \bigcup_{i=1}^n (C_i < R_i) \mid A = a \right] f_A(a) da \quad (2-1)$$

where

- $C_i$  = Capacity of structural element  $i$  (e.g., reactor pressure vessel skirt, stabilizer, or reactor support pedestal, etc.);  $i=1, 2, \dots, n$ ; a random variable.
- $R_i$  = Seismic response of element  $i$  due to an earthquake of peak ground acceleration  $a$ ; a random variable.
- $\bigcup_{i=1}^n$  = "Union" symbol.
- $f_A(a)$  = Frequency of occurrence of a peak ground acceleration between  $a$  and  $a+da$  at the site.

Equation 2-1 is written assuming that there is perfect knowledge about the values of the parameters that define the probability terms. Since there is uncertainty in these parameter values, a subjective probability distribution on the probability of an indirectly-induced DEGB is obtained by appropriately varying the parameter values as will be subsequently described.

The first term within the integral of Equation 2-1 is the conditional probability of occurrence of a DEGB due to structural failures for a given peak ground acceleration,  $a$ . It is defined as the probability of failure of at least one of the structural elements which can lead to a DEGB of the reactor coolant piping. Therefore, the focus of this study is only on those structural elements within the containment whose failure can result in a DEGB. Among these, some elements may have large margins of safety against seismic failure and thus may not contribute significantly to the probability of a DEGB. Therefore, critical elements are defined as those whose failure could contribute significantly to the probability of an indirectly-induced DEGB.

The conditional probability of a DEGB is evaluated by treating the failure events of individual structural elements as statistically independent and is derived from the conditional probabilities of failure of these structural elements. This gives a conservative upper bound on the probability of a DEGB. Also, if one of the structural elements has a very high conditional probability of failure compared to other elements, the upper bound is a good approximation to the actual  $P_{\text{DEGB}}$ .

## 2.2 SEISMIC FRAGILITY

The conditional probability of failure of a structural element for a given peak ground acceleration is called the seismic fragility of the element (Figure 2-1). The fragility evaluation is accomplished in this study using information concerning the plant design bases and by appropriately extrapolating the responses calculated at the design analysis stage to the failure levels of the structural elements.

Evaluation of the fragility is simplified by defining a random variable called the ground acceleration capacity. The ground acceleration capacity,  $A_C$ , is expressed as:

$$A_C = F \cdot A_{\text{SSE}} \quad (2-2)$$



where  $F$  is the factor of safety on the design basis earthquake (e.g., safe shutdown earthquake) and  $A_{SSE}$  is the peak ground acceleration specified for the SSE. The factor of safety is defined as a ratio of the seismic capacity of the structural element,  $C_i$ , to the response,  $R_i$ , due to the SSE. Since  $C_i$  and  $R_i$  are random variables, the factor of safety,  $F$ , is also a random variable.

The factor of safety,  $F$ , is modeled as a lognormally distributed random variable with the parameters, median  $F$  and logarithmic standard deviation,  $\beta_F$ . Two basic types of variability are identified (Kennedy, et al, 1980) in describing the factor of safety; one that represents the inherent randomness and the other which represents the uncertainty in the parameter value, e.g., the median. These variabilities are quantified by the logarithmic standard deviations,  $\beta_{F,R}$  and  $\beta_{F,U}$ , respectively. Essentially,  $\beta_{F,R}$  represents the variability due to randomness of earthquake characteristics for the same peak ground acceleration and to the randomness of the structural response parameters which relate to these characteristics. The dispersion represented by  $\beta_{F,U}$  is due to such factors as:

1. Lack of understanding of structural material properties such as strength, inelastic energy absorption capacity and damping, and
2. Errors in calculated response due to use of approximate modeling of the structure and equipment and inaccuracies in mass and stiffness representations.

For equipment supports, the factor of safety can be modeled as the product of the two random variables (Kennedy and Ravindra, 1983):

$$F = F_C \cdot F_R = F_C \cdot F_{RS} \cdot F_{RE} \quad (2-3)$$

The capacity factor,  $F_C$ , for the equipment support is a product of a strength factor,  $F_S$ , and an inelastic energy absorption factor,  $F_\mu$ . The response factor,  $F_R$ , is the product of structural response factor,  $F_{RS}$ , and the equipment response factor,  $F_{RE}$ , which will be discussed later.

The strength factor,  $F_S$ , represents the ratio of ultimate strength to the stress calculated for  $A_{SSE}$ . In calculating the value of  $F_S$ , the non-seismic portion of the total load acting on the support is subtracted from the strength as follows:

$$F_S = \frac{S - P_N}{P_T - P_N} \quad (2-4)$$

where  $S$  is the ultimate structural strength for the specific failure mode,  $P_N$  is the stress due to the normal operating load (i.e., dead load, restraint of thermal expansion load, etc.) and  $P_T$  is the stress resulting from the total load on the support (i.e., sum of the seismic load for  $A_{SSE}$  and the normal operating load). For higher levels of earthquake, other transients (e.g., turbine trip) may have a high probability of occurring simultaneously with the earthquake; the definition of  $P_N$  in such cases should be extended to include the stress due to these transients.

The strength,  $S$ , is a function of the failure mode (i.e., brittle or ductile modes). Brittle failures are defined as those failure modes which exhibit little or no system inelastic energy absorption capability. Examples are:

1. Anchor bolt failures
2. Support weld failures
3. Shear pin failures
4. Buckling

Each of these failure modes has the ability to absorb some inelastic energy on the component level, but the plastic zone is very localized, and the system ductility for an anchor bolt or a support weld is very small. The strength of the component failing in a brittle mode is therefore calculated using the ultimate strength of the material.

Ductile failure modes are those in which the structural system can absorb a significant amount of energy through inelastic deformation. Examples include:

1. Pressure boundary failure of piping
2. Primary equipment supports failing in tension or bending

The strength of the element failing in a ductile mode is taken to be the yield strength of the material for tensile loading while for flexural loading, the strength is defined as the stress at which a plastic hinge is developed.

The inelastic energy absorption factor,  $F_\mu$ , for an equipment support is a function of the ductility ratio,  $\mu$  and damping,  $\delta$ . The median value  $\bar{F}_\mu$  is considered to be close to 1.0 for brittle and functional failure modes. For ductile failure modes of equipment supports that respond in the amplified acceleration region of the design spectrum (i.e., 2 to 8 Hz), the inelastic energy absorption factor is calculated using the procedure given in Riddell and Newmark (1979).

The median  $\bar{F}_C$  and the variability estimates,  $\beta_{C,R}$  and  $\beta_{C,U}$  of the capacity factor are obtained as follows:

$$\bar{F}_C = \bar{F}_S \cdot \bar{F}_\mu \quad (2-5)$$

$$\beta_{C,R} = (\beta_{S,R}^2 + \beta_{\mu,R}^2)^{1/2} \quad (2-6)$$

$$\beta_{C,U} = (\beta_{S,U}^2 + \beta_{\mu,U}^2)^{1/2} \quad (2-7)$$

where

- $\bar{F}_S$  = Median strength factor
- $\bar{F}_\mu$  = Median inelastic energy absorption factor
- $\beta_{S,R}$  = Logarithmic standard deviation of the randomness in the strength factor.
- $\beta_{S,U}$  = Logarithmic standard deviation of the uncertainty in the median value of strength factor.



$\beta_{\mu,R}$  = Logarithmic standard deviation of the randomness in the inelastic energy absorption factor.

$\beta_{\mu,U}$  = Logarithmic standard deviation of the uncertainty in the median value of the inelastic energy absorption factor.

In developing the structural response factor,  $F_{RS}$ , it is recognized that in the design analysis, the structural response was computed using specific (often conservative) deterministic response parameters for the structure. Because many of these parameters are random (often with a wide variability), the actual response may differ substantially from the response calculated in the design analysis for a given peak ground acceleration level.

The structural response factor,  $F_{RS}$ , is expressed as a product of factors representing each of the parameters that influence response.

$$F_{RS} = F_{SS} \cdot F_D \cdot F_M \cdot F_{SSI} \quad (2-8)$$

where

$F_{SS}$  = Spectral shape factor representing the relation between ground motion defined by the median site-specific ground response spectra and the ground spectra used for design.

$F_D$  = Damping factor representing the ratio of response between the best estimate damping and design damping.

$F_M$  = Factor accounting for conservatisms or unconservatisms in response due to modeling assumptions.

$F_{SSI}$  = Soil-Structure Interaction Factor which represents the ratio of response resulting from median-centered SSI modeling versus SSI modeling used in design.

Each of the factors is a random variable and has variability characterized by randomness,  $\beta_R$ , and uncertainty,  $\beta_U$ .

The median  $F_{RS}$  and the variability estimates  $\beta_{RS,R}$  and  $\beta_{RS,U}$  are calculated using Equations 2-8 and the lognormal probability law:

$$F_{RS} = F_{SS} \cdot F_D \cdot F_M \cdot F_{SSI} \quad (2-9)$$

$$\beta_{RS,R} = (\beta_{SS,R}^2 + \beta_{D,R}^2 + \beta_{M,R}^2 + \beta_{SSI,R}^2)^{1/2} \quad (2-10)$$

A similar expression exists for  $\beta_{RS,U}$ .

Similarly, the equipment response factor,  $F_{RE}$ , is a measure of the conservatism inherent in the calculation of equipment response in the design analyses.  $F_{RE}$  is equal to the ratio of the equipment response calculated during design to the best estimate equipment response to a median-centered floor response spectrum. The equipment response factor is also expressed as a product of factors representing each of the parameters that influences response.

$$F_{RE} = F_{SS} \cdot F_D \cdot F_M \cdot F_{MC} \cdot F_{EC} \quad (2-11)$$

$F_{SS}$  = Spectral shape factor - including the effects of peak broadening and smoothing, and artificial time history generation.

$F_D$  = Damping factor.

$F_M$  = Modeling factor (affects mode shape and frequency results).

$F_{MC}$  = Factor to account for conservatism in method used to combine modal responses.

$F_{EC}$  = Factor to account for conservatism in method used to combine earthquake components.

The median  $F$  and the variability estimates,  $\beta_R$  and  $\beta_U$  of the equipment response factor are obtained using forms of Equations 2-9 through 2-11 and the properties of the lognormal probability law as described above.

The overall factor of safety  $F$  is calculated using Equation 2-3 as the product of the capacity factor and the equipment and structural response factors. Using Equation 2-2, the ground acceleration capacity of the structural element then becomes:

$$\bar{A}_C = \bar{F} \cdot \bar{A}_{SSE} \quad (2-12)$$

where

$$\bar{F} = \bar{F}_C \cdot \bar{F}_{RS} \cdot \bar{F}_{RE} \quad (2-13)$$

$$\beta_{A,R} = \beta_{F,R} = (\beta_{C,R}^2 + \beta_{RS,R}^2 + \beta_{RE,R}^2)^{1/2} \quad (2-14)$$

$$\beta_{A,U} = \beta_{F,U} = (\beta_{C,U}^2 + \beta_{RS,U}^2 + \beta_{RE,U}^2)^{1/2} \quad (2-15)$$

The overall factor of safety is thus decomposed into factors that can be modeled and for which data and information exist. In some instances, evaluating values exactly would require detailed analysis and/or more extensive data than are available. For these cases, it is sometimes necessary and justifiable to use subjective evaluations and engineering judgment to evaluate the  $\beta$  values. As an example, consider the case for which a median value of a factor is reasonably well estimated and a lower bound value, below which it is fairly unlikely that the factor will fall, is also known. Assuming that the factor is lognormally distributed, the  $\beta$  may be evaluated by assuming the lower bound to be, say, a 5 percentile value. Although this procedure is subjective, it is generally observed that changes in the  $\beta$  value resulting from a different assumption for the lower bound probability value, have a small effect on the final probabilities calculated (Ravindra, et al, 1984). This results from the fact that the  $\beta$ 's of the overall safety factor are the SRSS of many  $\beta$ 's (Equations 2-14, 2-15) of similar magnitude and therefore, insensitive to minor variations in the individuals  $\beta$ 's. Also, the seismic hazard uncertainty tends to dominate the final analysis variability, making the calculated probabilities relatively insensitive to minor changes in the values estimated.

The ground acceleration capacity of the support for each major equipment component has been expressed in this study as the lowest capacity for all credible failure modes of the component support. This is a realistic assumption since the failure modes are highly correlated due to common



earthquake input, structural material and method of fabrication. Again, if one of the failure modes of the structural element has a very low capacity compared to other modes, this assumption leads to a good approximation of the probability distribution of the capacity.

### 2.3 SEISMIC HAZARD

The last term within the integral of Equation 2-1,  $f_A(a)da$ , is the annual probability that the peak ground acceleration at the site is between  $a$  and  $a+da$ . This is usually described by a set of seismic hazard curves (Figure 2-2) where each curve is a plot of the annual exceedance probability versus peak ground acceleration. The uncertainty in the hazard is presented by developing a family of curves and assigning a subjective weighting factor (or probability) to each curve.

### 2.4 CALCULATION OF DEGB PROBABILITY

Equation 2-1 has been evaluated in this study applying the SMA computer program SEISRISK. The program first combines the individual component fragilities into a plant level fragility (i.e., union operation in this case) and then convolves the plant level fragility with the family of seismic hazard curves to obtain the subjective probability distribution of the probability of DEGB indirectly-induced by earthquake (Figure 2-3). Site-specific seismic hazard curves were not available for the Brunswick plant. The generic curves which were used in the earlier studies of Westinghouse, Combustion Engineering, and Babcock and Wilcox plants were utilized for this study.

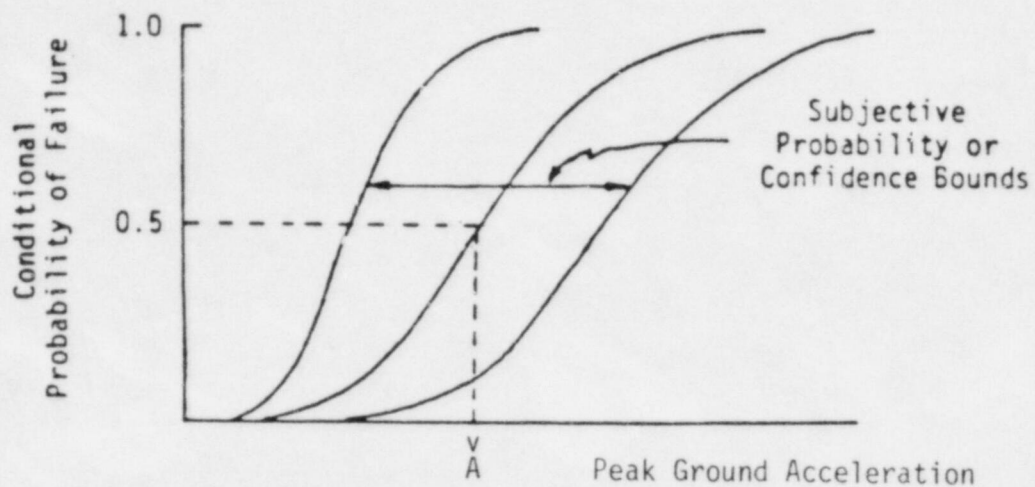


FIGURE 2-1: FRAGILITY OF STRUCTURE OR EQUIPMENT

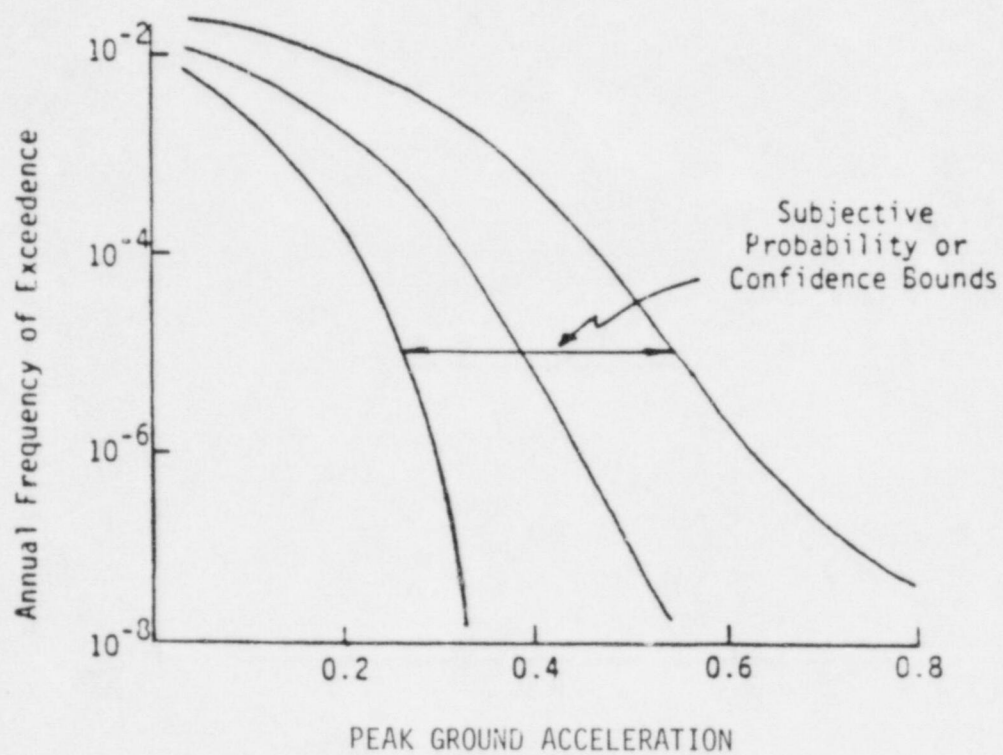


FIGURE 2-2. SEISMIC HAZARD CURVES

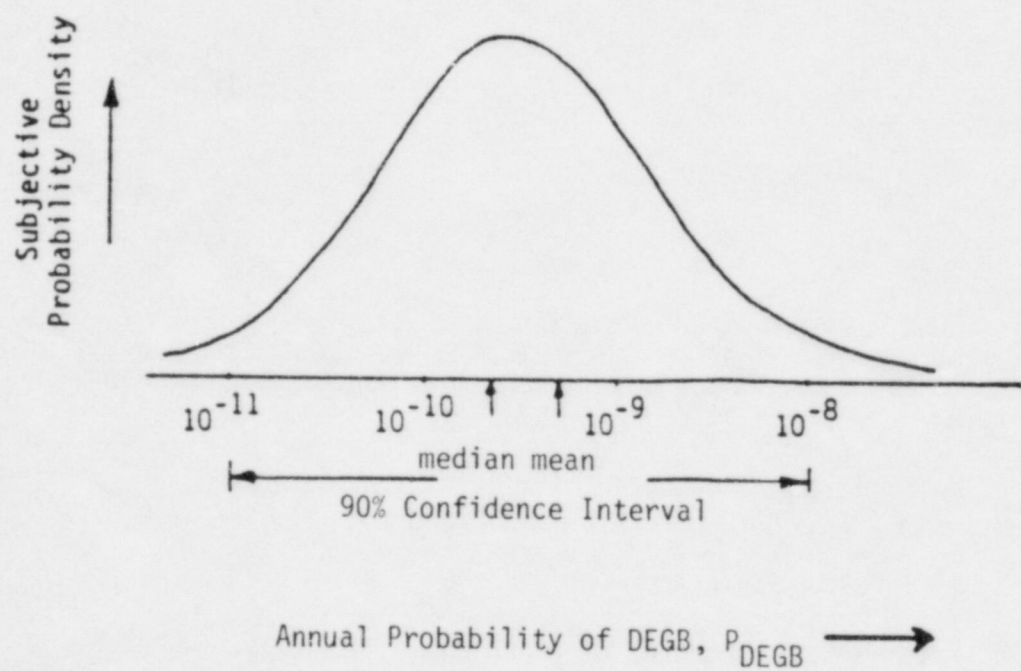


FIGURE 2-3. DISTRIBUTION OF THE PROBABILITY OF INDIRECTLY-INDUCED DEGB



### 3. SEISMIC FRAGILITY CALCULATIONS

The containment structure and the reactor vessel support system for Brunswick are depicted in Figure 3-1. The overall reactor building unit is made up of three units: The Reactor Building (secondary containment), the Drywell (primary containment) and the RPV System (RPV, sacrificial shield and pedestal). All of these units are supported (and hence, coupled) upon a massive, rigid foundation mat. The RPV, sacrificial shield wall and drywell are also coupled by the stabilizer and star truss as shown in Figure 3-1. The foundation mat is rectangular, approximately 190 ft (X-direction) x 154 ft (Y-direction) in plan. The Reactor Building is square in plan (142 ft x 142 ft) for most of its height. The Drywell and the RPV System are approximately axisymmetric about a vertical axis. As noted earlier, the primary containment structure for Brunswick varies slightly from other Mark I containments in that the structure itself is reinforced concrete and not steel. In addition, the shape is roughly conical (similar to the Mark II) and not light-bulb-shaped.

For the Brunswick containment configuration, eight different critical areas were identified where failures could cause an indirect DEGB. These eight areas are:

1. Overhead Crane
2. Primary Containment
3. Star Truss
4. Stabilizer
5. Sacrificial Shield Wall
6. RPV Pedestal
7. RPV Lower Support
8. Reactor Recirculation Pump Supports

The last of these components (Reactor Recirculation Pump Supports) is being addressed by LLNL in their probabilistic fracture mechanics study and is not a part of this study. The first 7 components were examined to determine which components were the primary contributors to the probability of DEGB.

It is assumed that seismic failure of any component of the RPV support system (stabilizer, shield wall, star truss, primary containment, RPV lower support or the RPV pedestal) would unconditionally result in a DEGB of the recirculation, steam or feedwater piping. Failure of the overhead crane would have to be coincident with a high conditional probability of the crane striking the piping given that the crane falls. It is assumed that failure of the four stabilizer brackets is perfectly dependent. Thus, the fragility description of only one stabilizer bracket is considered in the fragility development. This is a realistic assumption because the stabilizers are all identical and responses are correlated. Additionally, the various possible failure modes for a component are assumed dependent, thus, the fragility description of each component is governed by its lowest capacity failure mode. Section 3.1 contains a summary of the capacity derivation for these components, while Section 3.2 contains both the structural response factors and the equipment response factors. Section 3.3 documents the overall fragility calculations for the controlling failure modes.

### 3.1 CAPACITY FACTOR DERIVATIONS

DEGB of the reactor coolant system piping is judged to occur if any one of the above systems fails catastrophically. Based on SMA's past experience with seismic capacity evaluations of BWR components and structures, several of these critical areas can be shown to have a very low probability of failure. For these high capacity items, further analysis is judged unnecessary. Seismic capacity evaluations were conducted on the remaining critical areas in order to determine which failure modes controlled the probability of DEGB. In the following, the procedure for evaluating the median and the variability estimates ( $\beta_R$  and  $\beta_U$ ) for the capacity of the above equipment support elements is described.

#### 3.1.1 Overhead Crane

The Brunswick overhead crane is mounted on a crane rail immediately above the refueling platform area. These cranes are typically parked to the side of the reactor building whenever they are not in use. Thus, even if the

crane could somehow jump off of the track during an earthquake, it would not be feasible for it to be thrown over to the primary containment area. In addition, massive reinforced concrete beams are placed over the drywell head to protect the RPV from possible missiles. These beams are assumed to provide significant resistance against the crane or any other missile penetrating the primary containment. Thus, based on both the normal operation configuration and on the reinforced concrete shielding, the overhead crane failure is judged to have a very low probability of DEGB and is not addressed further in the study.

### 3.1.2 Primary Containment Structure (Drywell)

The Brunswick drywell is composed of vertical right cylinders and truncated cones with inside diameters varying between 36'-0" and 65'-0". The overall height from the top of the foundation mat to the drywell head flange connection is approximately 111'-0". The steel dome covering the top of the drywell is furnished with double-gasketed flanges and is securely fastened to the reinforced drywell liner extension, which is in turn anchored to the top of the reinforced concrete portion of the drywell with 84 uniformly spaced pretensioned bolts.

The drywell pedestal is a 17'-0" thick solid cylindrical concrete disk and contains top and bottom reinforcing over the total plan area. In addition to the top and bottom reinforcing, a band of closed hoop bars, evenly spaced through the full depth of the pedestal, runs along the outside face. The drywell wall reinforcing consists of circumferential closed hoops on each face along its full height, continuous meridional reinforcing on each face, diagonal seismic reinforcing on the outside face, and shear reinforcing.

The drywell supports the star truss arrangement that provides a load path between the shield wall and the drywell for seismic loads on the RPV and the shield wall. Failure of the drywell would eliminate this load path and require all of the RPV load to be taken out at the base of the shield wall. This added loading would be well in excess of the shield wall's capacity and failure of the RPV is expected to result. Thus, failure of the drywell is judged to cause unconditional DEGB due to the RPV supports failing.



A cursory review of the Brunswick drywell drawings revealed a large seismic capacity. Past PRA studies on five BWR primary containment structures gave a range of ground acceleration capacities from 2.5 g's to over 10 g's with a mean of approximately 6 g's. Failure of primary containment structures has never entered into the seismic risk picture in past PRAs and based on our experience, and a quick review of Brunswick drywell drawings, drywell failure is not considered to contribute to the probability of DEGB.

### 3.1.3 Star Truss

The top of the shield wall is effectively pinned by a truss system consisting of eight "V"-beams spaced  $45^{\circ}$  around the circumference. Figure 3-2 shows a schematic of one of the eight "V" beams. The "V" beams are constructed of 10" extra strong pipe which are welded to embedded plates at the top of the shield wall. The two 10" pipes are connected to a "Y"-type pipe fitting with bolted flange joints. The "Y"-type pipe fitting has a bumper connection with the drywell that can carry compression loads only.

Seismic qualification analyses for the star truss system was not available for Brunswick, so SMA conducted a capacity analysis of the critical portions of the truss system. The areas addressed for criticality were:

1. Weld of the 10" pipes to the plate embedded in the shield wall.
2. Buckling of the 10" extra strong pipe
3. Compression failure of the bumper

The most critical failure mode was determined to be buckling of the pipe members. The buckling capacity of the star truss system was first determined, and then the capacity factor was derived based on the compression loads produced by an SSE.

The properties of 10" extra strong pipe are shown below. A-106B was assumed for the material (drawings do not specify the material) since it is typical for piping.

Outer Diameter	= 10.75"
Thickness	= 0.5"
Yield Strength	= 35 ksi
Tensile Strength	= 60 ksi
Elongation	= 30% (minimum strain from ASTM specifications)
Modulus of Elasticity	= 29x10 <sup>6</sup> psi

The yield and tensile strengths shown above are minimum properties based on the ASME code. Median properties are given in NUREG/CR-2137 (Rodabaugh, 1981) to be:

$$\begin{aligned}\bar{\sigma}_y &= 47.5 \text{ ksi} \\ \bar{\sigma}_u &= 71.9 \text{ ksi}\end{aligned}$$

The ASME Code minimum properties are 95% confidence values and thus, the uncertainty on yield strength was calculated to be:

$$\beta_{y,u} = \frac{1}{1.65} \ln \left( \frac{47.5}{35} \right) = 0.19$$

The plastic buckling equation from the NASA Space Vehicle Design Criteria (NASA 1965) is:

$$\sigma = 0.6 \times \gamma \times \eta \times E \ t/r \quad (3-1)$$

where

$\eta$  = plasticity correction factor

$\gamma$  = experimental correction factor

$E$  = modulus of elasticity

t = shell thickness

r = mean radius

The plasticity correction factor,  $\eta$ , is defined as:

$$\eta = \frac{\sqrt{E_{SEC} \cdot E_{TAN}}}{E} \quad (3-2)$$

By defining the stress-strain curve in a power law formation ( $\sigma = \sigma_0 \epsilon^\eta$ ) which represents the yield strength, ultimate strength and elongation at failure, the stress-strain relation was defined as:

$$\sigma = 81357 \cdot \epsilon^{0.1025} \quad (3-3)$$

The equation was solved for the secant modulus and the tangent modulus:

$$E_{SEC} = 81357 \times \epsilon^{-0.8975} \quad (3-4)$$

$$E_{TAN} = 8339 \times \epsilon^{-0.8975} \quad (3-5)$$

Substituting Equation 3-4 and 3-5 into 3-2:

$$\eta = 0.000898 \times \epsilon^{-0.8975} \quad (3-6)$$

The experimental correction factor,  $\gamma$ , is based on the results of a large number of buckling tests on cylinders and accounts for the difference between the experimental results and the classical theoretical equation. The NASA buckling criteria (NASA, 1965) shows that for  $\lambda/\lambda_c$  of less than 5,  $\gamma = 0.85$ .

Substituting  $\gamma$ ,  $\eta$ ,  $t$ ,  $E$  and  $R$  into the plastic buckling Equation 3-1, we find:



$$\begin{aligned}\sigma_{cr} &= 0.6 \times 0.85 \times (8.98 \times 10^{-4} \times \epsilon^{-0.8975}) \times (29 \times 10^6) \times 0.5/5.125 \\ &= 1280 \times \epsilon^{-0.8975}\end{aligned}\quad (3-7)$$

Equations 3-3 and 3-7 now provide two equations with two unknowns. The critical buckling stress and the corresponding strain are calculated to be:

$$\sigma_{cr} = 53 \text{ ksi}$$

$$\epsilon_{cr} = 1.57\%$$

This critical buckling stress of 53 ksi is a lower bound on the median buckling capacity since Equation 3-1 was developed for design applications. A 15% bump-up factor to obtain median capacity is judged as reasonable based on inspection of the NASA data, thus:

$$\sigma_{cr} = 61 \text{ ksi}$$

The uncertainty on this bump-up factor is:

$$\beta_{1.15} = \frac{1}{1.65} \ln \left( \frac{1.15}{1.0} \right) = 0.09$$

The overall uncertainty of the critical buckling stress is calculated by taking the SRSS of the related uncertainties (this is based on the properties of a logarithmic distribution):

$$\beta_{\sigma_{cr}} = (0.19^2 + 0.09^2)^{1/2} = 0.21$$

The critical buckling load of the entire star truss system will be reached when three of the "V-shaped" pipe trusses have reached the critical buckling stress. At that point, the shield wall will displace without any increase in load and total failure/DEGB will occur. The remaining five pipe trusses around the circumference will not resist the motion of the shield wall since trusses can only resist compressive loadings. The ultimate load

capacity of a single "V-shaped" pipe truss was calculated to be 1,613 kips in the radial direction as shown in Figure 3-3.

Due to the fact that two of the three trusses are situated at  $45^{\circ}$  from the direction of lateral motion of the shield wall, the overall star truss capacity is (see Figure 3-4):

$$P_{ULT} = 1,613 \text{ kips} + 2 \times 0.707 \times 1,613 \text{ kips}$$

$$P_{ULT} = 3,894 \text{ kips}$$

The strength factor for the star truss is:

$$F_S = \frac{\text{Ultimate Load Capacity}}{\text{Load due to an SSE}} = \frac{P_{ULT}}{P_{SSE}}$$

The SSE load is given in a GE analysis summary (GE, 1980) as 594 kips. Thus,

$$F_S = \frac{3894 \text{ kips}}{594 \text{ kips}} = 6.56$$

This strength factor is based on the assumption that the loads remain linear up to the point of failure. As will be shown in Section 3.1.7, this assumption is not completely valid since the RPV lower support will form a plastic hinge at a lower acceleration level and the load will redistribute to the upper support. The RPV lower support hinges at a ground acceleration level of 2.55 SSE's (see Section 3.1.7). At this point, an additional 62 kips/SSE (which had previously been taken out as a moment at the RPV base) will be placed on the star truss. Figure 3-5 depicts the nonlinear loading arrangement. The corrected strength factor for the star truss is calculated to be:

$$3894 \text{ kips} = 2.55 \times 594 \text{ kips} + (F_S - 2.55) \times 656 \text{ kips}$$

$$F_S = 6.18$$

The uncertainty on this strength factor remains the 0.21 calculated previously.

Since the failure mode was buckling of the pipe members, ductility is not applicable. Thus, the capacity factor and variability are identical to the strength factor.

$$F_C = F_S = 6.18$$

$$\beta_{C,R} = \beta_{S,R} = 0.0$$

$$\beta_{C,U} = \beta_{S,U} = 0.21$$

#### 3.1.4 Stabilizer Capacity

The stabilizer is a strut-type support assembly which is designed to transfer the horizontal accident loads (seismic and LOCA) from the RPV to the top of the shield wall. There are four stabilizer assemblies located 90° from each other as depicted in Figure 3-6. Each stabilizer is attached at one end to an RPV support lug which is integral with the RPV cylindrical wall. The other end of the stabilizer is attached to a gusseted bracket assembly which is welded to the top of the shield wall. Figure 3-7 contains a schematic of the individual components which make up the stabilizer assembly. Each of the stabilizer components were examined to determine how a failure of the stabilizer function could occur. Five different areas were identified as possible failure modes:

1. Clevis Pin
2. Clevis
3. Draw Bar
4. Gusset Plate
5. Nut for Draw Bar

The clevis pin (Figure 3-8) is a 4" diameter AISI 4140 pin which reacts the stabilizer load in double shear. The capacity is conservatively calculated in



single shear to be 1696 kips. The clevis itself (Figure 3-8) is a connection device between the shear pin and the threaded draw bar. The clevis end which interfaces with the shear pin was analyzed for both tensile and bearing failures and found to have an ultimate capacity of 4,050 kips. The opposite end with the female threads was analyzed to have a capacity of 2475 kips.

The draw bar (Figure 3-8) is an AISI 4340 threaded rod which runs the span between the clevis and the gusset plate bracket. The capacity of the draw bar was calculated to be 1374 kips in tension. The welded steel bracket assembly attaches the draw bar to the shield wall as shown in Figure 3-9. The two critical areas which were analyzed were the welds between the 4" thick face plate and the two 1" thick side plates, and the weld which anchors the bracket to the shield wall. The base weld capacity was conservatively calculated to be 1,555 kips, while the 4" plate to 1" plate welds have a median capacity of 1,440 kips.

The draw bar nut is 3-1/2" - 4UNC nut which is made from ASTM A-307 Grade B material. This material has an ASME Code minimum tensile strength of 60 ksi, which is much less than the 150 ksi ultimate strength of the draw bar itself. Generally, the nut threads will not govern the design of a joint connection, but, in this case, they do govern because the nut threads have a tensile strength of less than 50% of that of the draw bar. The ultimate load capacity of the draw bar nut was calculated to be 1100 kips.

The ultimate load capacity for each of the critical stabilizer components is listed below.

	<u>Component</u>	<u>Failure Mode</u>	<u>Ultimate Load Capacity</u>
1.	Clevis	Shear	1865 kips
2.	Clevis	Threads	2475 kips
3.	Draw Bar	Tensile	1374 kips
4.	Gusset Plate	Welds	1440 kips
5.	Nut	Threads	1100 kips

The loading within these components is perfectly correlated and, thus, only the most critical of the failures needs to be addressed. The nut has the lowest capacity and was used as the basis for stabilizer capacity calculations.

The 1100 kip nut capacity was calculated based on the shear failure of the nut threads. Median ultimate strength of the ASTM A-307 material is estimated to be 72 ksi based on studies presented in NUREG/CR-2137 (Rodabaugh, 1981). The uncertainty is calculated based on the ASME code minimum of 60 ksi being the  $-1.65\beta$  value:

$$\beta_{U1} = \frac{1}{1.65} \ln \left( \frac{72}{60} \right) = 0.11$$

The median shear ultimate was estimated to be 60% of the tensile ultimate with a 50% value representing the  $-1.65\beta$  lower bound.

$$\tau_{ult} = 0.6 \times 72 \text{ ksi} = 43.2 \text{ ksi}$$

$$\beta_{U2} = \frac{1}{1.65} \ln \left( \frac{0.6}{0.5} \right) = 0.11$$

The effective shear area of the threads is based on the location where ultimate stresses are reached in both the nut thread and the draw bar threads. By balancing forces, the effective shear area in the nut is calculated to be 25.5 in<sup>2</sup> with an uncertainty  $\beta_{U3}$  equal to 0.20.

The ultimate load and its corresponding uncertainty are calculated to be:

$$P_{ult} = 43.2 \text{ ksi} \times 25.5 \text{ in}^2 = 1,100 \text{ kips}$$

$$\beta_{S,U} = (0.11^2 + 0.11^2 + 0.2^2)^{1/2} = 0.25$$

The loading on the stabilizer due to an SSE is 199 kips (GE, 1980). The worst case condition represents the load being split equally by two stabilizers, thus the SSE load on an individual stabilizer is 100 kips. This

100 kip loading is linear up until the RPV lower support forms a plastic hinge, then the loading rate increases. The additional load which must be reacted at the upper support is the load that will produce the moment which had previously been carried at the RPV base. The distance from the RPV base to the upper support is 544 inches and this is the moment arm over which this added load will resist the overturning moment. Thus, the additional load per SSE on the two stabilizers as a result of the lower support being unable to carry additional moment is:

$$P_{\text{add}} = \frac{33,720 \text{ in-kips}}{544 \text{ in.}} = 62 \text{ kips/SSE}$$

Thus, the loading rate on the stabilizer increases, to 131 kips after the lower support hinges at 2.55 SSE's. The strength factor was calculated to be:

$$1100 \text{ kips} = 2.55 \times 100 \text{ kips} + (F_S - 2.55) \times 131 \text{ kips}$$

$$F_S = 9.0$$

The uncertainty on the strength factor is the uncertainty on the capacity factor which equals 0.25.

The capacity factor and variabilities will equal those of the strength factor since a shear failure of threads will not have any ductility associated with it.

$$F_C = F_S = 9.0$$

$$\beta_{C,R} = \beta_{S,R} = 0.0$$

$$\beta_{C,U} = \beta_{S,U} = 0.25$$



### 3.1.5 Shield Wall

The sacrificial shield is a cylindrical structural steel frame consisting of beams and columns. Steel plates line the inside and outside surfaces of the structure and act as a form for fill concrete which is provided for shielding purposes. Figure 3-10 shows a perspective view of the shield wall and its location relative to the pedestal and RPV. The sacrificial shield also supports pipe restraints and miscellaneous platforms. RPV stabilizers connect the reactor vessel with the top of the sacrificial shield and transmit seismic forces from the reactor vessel to the shield wall. In addition, a series of pipe trusses between the sacrificial shield and the drywell permit the transfer of seismic forces from the reactor vessel and shield wall to the drywell. This system of lateral supports is designed to act only under asymmetric or antisymmetric loading situations. The sacrificial shield wall is connected to the reactor pedestal with anchor bolts and a portion of the reactor pedestal meridional reinforcing is connected to the sacrificial shield base plate. This layer of meridional reinforcing is extended from the shield wall and anchored into the drywell pedestal to aid in resisting extreme loadings such as seismic. The reactor vessel and its sacrificial shield are supported on a cylindrical reinforced concrete pedestal at the center of the drywell and the reactor pedestal is in turn supported on a 4'-0" thick reinforced concrete mat. Table 3-1 contains the physical properties of the Brunswick sacrificial shield wall.

Shield wall capacity evaluations on previous PRA studies have consistently shown the most critical area of the shield wall to be the connection with the RPV pedestal. Figure 3-11 shows a blowup of this connection for the Brunswick plant. The connection consists of a double ring of anchor bolts (see Figures 3-12 and 3-13), a single ring of #14 rebar anchored to the pedestal, and a double ring of shear keys. This connection has a much more rugged design than is typical for other BWRs studied. Many plants anchor the shield wall using anchor bolts alone.

The Brunswick shield wall lower support connection was analyzed and the tensile failure of the anchor bolts and #14 rebar were found to be the

critical failure mode for seismic loading. The rebar and bolting capacities were calculated based on classical strength of materials derivations. The uplift load capacity of the shield wall bolts and rebar were determined to be 2,400 kips. The ultimate moment capacity of the shield wall connection corresponding to this 2,400 kip load was calculated to be 346,000 kip-ft. The SSE loads on the shield wall are shown in Figures 3-14 through 3-17 which are based on the Brunswick FSAR. The maximum moment at the base is shown to be 25,605 kip-ft from Figure 3-16. The strength factor is then calculated to be:

$$F_S = \frac{346,000 \text{ kip-ft}}{25,605 \text{ kip-ft}} = 13.5$$

This strength factor is much higher than both the star truss and the stabilizer and, thus, the shield wall will not contribute substantially to the probability of DEGB. In addition, failure of some of the shield wall anchor bolts and rebar is not, by itself, expected to cause a DEGB. The double ring of shear keys will prevent the shield wall from separating from the pedestal, and the star truss assembly would resist overturning. Thus, the shield wall was not included as a critical element in the indirectly-induced DEGB study.

#### 3.1.6 RPV Pedestal

The reactor pedestal is a hollow reinforced concrete cylinder which supports the reactor vessel and sacrificial shield. The pedestal additionally provides support for platforms, pipe restraints and the control rod system. Meridional and hoop reinforcing is provided on each face of the structure. To aid in resisting the loads, one layer of meridional reinforcing is extended into the drywell pedestal and anchored. The pedestal is supported on a 4'-0" thick reinforced concrete mat. Mat reinforcement is provided by top and bottom layers of orthogonal bars.

RPV pedestal capacity evaluations in previous SMA Probabilistic Risk Assessments have shown the pedestal to possess a generically high seismic capacity. The lower cylindrical portion of the pedestal is 3 feet 3 inches thick and has a seismic capacity well beyond the levels of interest for the DEGB study. Experience has shown that the only possible areas of concern are

the reinforced concrete sections directly under the RPV ring girder and the shield wall. Figure 3-18 depicts the overall pedestal dimensions as well as its interface locations with the ring girder and shield wall.

The shield wall connection to the pedestal consists of 52 three-foot anchor bolts and 92 five-foot anchor bolts as depicted in Figure 3-12. The shorter bolts are anchored above piping penetrations where the full five foot length cannot be developed. The concrete failure path over a penetration has to cross five #6 rebars, two at right angles and three at  $45^{\circ}$  angles. The failure surface for the longer bolts will cross a #8 rebar at a right angle, three #8 rebars at  $45^{\circ}$  angles, and two #6 rebars at  $45^{\circ}$  angles. The #6 and #8 rebars have a minimum yield strength of 60 ksi and the concrete has a 28-day compressive strength of 3,000 psi. A capacity analysis shows the pedestal to have a minimum concrete pullout strength of 2,863 kips at the shield wall. This exceeds the 2,400 kip capacity derived in Section 3.1.5 for the shield wall bolts and #14 rebar. Thus, since the shield wall was determined not to contribute to the probability of DEGB, the pedestal at the shield wall interface will not contribute either.

The RPV ring girder interface to the pedestal is shown in Figure 3-19. There are 60 sets of 2'-7" anchor bolts which are oriented as shown in Figure 3-12. The failure surface under the ring girder will cross four #6 rebars, two at right angles and two at  $45^{\circ}$  angles. In addition, there is also a #8 rebar in the sections between penetrations which the failure surface crosses at right angles. Both the #6 and the #8 rebars are A-516 Grade 60 material with a 60 ksi yield strength. The pullout strength of the rebar and concrete at the ring girder in terms of an overall moment at the RPV was calculated to be 174,000 kip-ft. This capacity is greater than that of the ring girder anchor bolts (see Section 3.1.7) and, thus, is not the critical failure mode.

Based on calculations for the base of the RPV pedestal and on calculations for the top portions interfacing with the ring girder and the shield wall, the RPV pedestal has a sufficiently high seismic capacity that it will not contribute substantially to the probability of indirectly-induced DEGB.



### 3.1.7 RPV Lower Support Structure

The reactor vessel support assembly consists of a ring girder and the various bolts, shims, and set screws necessary to position and secure the assembly between the reactor vessel support skirt and the support pedestal. The concrete support pedestal is constructed integrally with the building foundation. Steel anchor bolts are set in the concrete with the threads extending above the surface. The anchor bolts extend through the ring girder bottom flange. High strength bolts are used to bolt the flange of the reactor vessel support skirt to the top flange of the ring girder. The ring girder is fabricated of ASTM A36 structural steel.

The capacity evaluation of the RPV lower support included the following critical areas:

1. RPV skirt knuckle
2. RPV skirt cylinder
3. RPV skirt base ring (flange)
4. Bolting from skirt to ring girder
5. RPV ring girder top flange
6. RPV ring girder bottom flange
7. Bolting from ring girder to pedestal

Figure 3-20 shows the RPV support skirt and notes the locations of Items 1, 2, and 3 above. Figure 3-21 shows the ring girder and its associated bolting (Items 4 through 7 above). Each of these seven areas were analyzed to determine which was the most critical for seismic events. Table 3-2 contains the calculated strength factors for the seven critical areas listed above. The bolting from the RPV skirt to the ring girder has the lowest strength factor at  $F_S = 2.55$ . Since all of these seven strength factors are perfectly correlated in the loading and also highly correlated in the limit load capacity, the lowest value was used as the basis for the RPV lower support fragility description.

The strength factor for the skirt to ring girder bolting was based on summary information supplied in Table C-12 of the Brunswick FSAR. The bolt material is specified in the FSAR to have a yield strength of 125 ksi. For bolting materials such as A354 Grade BD which have yield strengths of 125 ksi, the ASME code specifies a minimum ultimate of 150 ksi. This ultimate strength was increased by 10% to obtain a median strength. The 10% increase was based on similar high strength steel properties (Rodabaugh, 1981). The median and uncertainty are:

$$\sigma_{ult} = 1.1 \times 150 \text{ ksi} = 165 \text{ ksi}$$

$$\beta_{U1} = \frac{1}{1.65} \ln \left( \frac{165}{150} \right) = 0.06$$

Based on the data presented in FSAR Table C-12, the following seismic and normal bolt stresses were calculated:

$$\sigma_{SSE} = 65 \text{ ksi}$$

$$\tau_{SSE} = 10 \text{ ksi}$$

$$\sigma_N = -7.5 \text{ ksi}$$

$$\tau_N = 0 \text{ ksi}$$

The normal stress of 7.5 ksi is taken as negative because this is the resisting force to the seismic loads caused by the RPV deadweight forces. The strength factor was calculated based on the shear and tension interaction equation specified by the AISC code.

$$\frac{(\tau_N + F_S \cdot \tau_{SSE})^2}{F_V^2} + \frac{(\sigma_N + F_S \cdot \sigma_{SSE})^2}{F_T^2} = 1.0 \quad (3-8)$$

where

$F_V$  = ultimate shear capacity (60%  $F_T$ )

$F_T$  = ultimate tensile capacity (165 ksi)

Inserting the correct stresses into Equation 3-8 and solving by trial and error, the strength factor was calculated to be 2.55. Ductility is not applicable because the anchor bolt failure was assumed to be brittle.

The strength factor calculated for the RPV lower support bolts does not represent catastrophic failure of the RPV and subsequent onset of a DEGB. This threshold of 2.55 times the SSE merely identifies the point where the bottom support can no longer carry increased moment. By the time that the outermost of the skirt to ring girder bolts is strained up to its ultimate failure level, the RPV will have rotated significantly at its upper support such that the stabilizer will be carrying a significantly higher percentage of the load. Thus, at this point where the lower support can no longer carry increasing moment from the seismic loads, an increasing load distribution will occur in the upper support (see Figure 3-5). The shear load in the RPV lower support will continue to increase at seismic levels greater than 2.55 times the SSE, but the shear loads are small in comparison to the uplift loads due to the overturning moment. It was reasoned that sufficient bolts will remain unbroken to carry the increased shear load up to the point of upper stabilizer failure.

### 3.2 RESPONSE FACTORS

As described in Section 2 of this report, the response factors for a component are typically separated into two groups: structural response factors and equipment (or subsystem) response factors. The structural response factors take into account the conservatism/unconservatism and variabilities involved with deriving the response of structures and includes the propagation of the earthquake motion up through the soil and into the structure. The equipment response factors take into account the conservatism/unconservatism and variability involved in performing a subsystem analysis using floor response spectra which were generated from the original



structure analysis. In the case of the design analysis of Brunswick, however, all of the components addressed within this study (RPV, Shield Wall, Pedestal, Drywell) were analyzed using a coupled time history model such that separate subsystem analyses were not performed. Consequently, overall factors for the variables influencing response of the coupled model are developed.

The overall response factor,  $F_R$ , for the coupled model is defined as a product of five factors.

$$F_R = F_{SS} \cdot F_D \cdot F_M \cdot F_{SSI} \cdot F_{EC}$$

where the factors are as defined in Section 2.2. The evaluation of each of these factors is discussed in the following sections.

### 3.2.1 Spectral Shape Factor, $F_{SS}$

The spectral shape factor is a measure of the conservatism/unconservatism involved in using the design ground response spectrum in lieu of a median ground response spectra. The design ground response spectra for Brunswick is a smoothed 1940 North-South El Centro spectrum normalized by a factor of 0.08g/0.33g for the OBE as shown in Figure 3-22. The SSE was scaled up by a factor of 2 resulting in a peak ground acceleration of 0.16 g's. The median spectrum for the Brunswick site is judged to be a WASH 1255 median rock site spectrum. Since the generic hazard curves used within this study are tied to earthquake motion at the free-field, the median spectrum is also required to be tied to the free-field. The spectral shape factor thus accounts for two different conditions:

1. The difference between the El Centro Design Spectrum and the median WASH 1255 spectrum at the primary frequency of interest.
2. The conservatism involved in placing the ground response spectrum at bedrock (as was done on the Brunswick design analysis) instead of evaluating structural response for seismic motion occurring at free-field.

#### 3.2.1.1 Background on Design Spectra and Median Spectra

The Brunswick site is underlined with loose layers of sands and silts between existing grade at Elevation 24.0 ft and approximately Elevation -26.0 ft. A very dense sand occurs between Elevation -26.0 ft and bedrock at Elevation -52 feet. The reactor building foundations bear directly on the very dense sand strata. The remainder of the plant bears on a structural fill supported on this dense sand. The entire plant area, including a perimeter ring, was excavated to Elevation -25.0 ft and refilled with granular material compacted to relative densities consistent with bearing pressure requirements. Figure 3-23 contains a schematic of the containment structure embedment together with the model used to represent the soil springs.

The design analysis placed a time history (Figure 3-24) into the bedrock and computed the response as it amplified through the dense sand layer and into the structure. This artificial time history envelopes the design ground spectrum throughout the amplified frequency range. A median-centered analysis would have placed a site-specific ground spectrum at the free-field and computed the deconvolution effects of the ground motion to the base mat of the containment. Since a site-specific median ground spectrum has yet to be developed for the Brunswick site, the WASH 1255 spectrum was judged to be appropriate. The WASH 1255 spectrum for alluvium is appropriate for deep soil sites, but Brunswick has a shallow soil layer. The WASH 1255 rock spectrum is not appropriate for Brunswick either because of the shallow soil layer. Consequently, the median ground spectrum was derived based on placing a WASH 1255 rock spectra at a rock outcrop location, and then calculating an appropriate free-field median spectrum using the CLASSI computer program. Figure 3-25 shows the median WASH 1255 spectrum together with the resulting free-field spectrum that was calculated from it. This free-field spectrum was utilized as the median Brunswick SSE ground spectrum. The spectra in Figure 3-25 are all for 7% spectral damping and the free-field spectrum was derived using a median soil damping of 10%. It should be noted that this median free-field spectrum is scaled to a zero period acceleration (ZPA) of 0.27 g's. In order to put this spectrum in terms of the 0.16g SSE, the entire curve needs to be scaled by 16/27.

In order to compare the median free-field ground motion to the design ground motion, an equivalent free-field design spectrum was developed from the smoothed El Centro spectrum which was applied at bedrock. The Brunswick design motion (smoothed El Centro, Figure 3-22) was placed at bedrock and a CLASSI analysis was conducted to calculate the corresponding free-field design spectra for three different soil damping cases (4%, 7% and 10%). The design analysis used 7% soil damping for the SSE response analyses, but 10% soil damping is considered median. The spectral shape factor was calculated by comparing the 10% soil damping design free-field spectrum (Figure 3-26) and the 10% soil damping median free-field spectrum (Figure 3-24), at the frequency which drives the response for the component being addressed. The next section addresses the dominant frequencies of response of the drywell structure and the major structures within the drywell.

#### 3.2.1.2 Drywell and RPV System Response

The RPV system dynamic model used in the Brunswick design analysis is shown in Figure 3-27. The model includes the soil, reactor building, primary containment (drywell), shield wall, RPV pedestal and the reactor vessel. The response of these systems is shown in Figure 3-28 in terms of the first 4 mode shapes. The following conclusions can be derived from these mode shapes:

- a. Mode 1 - This mode is essentially the fundamental mode of the soil layer. Node 44, which represents the soil mass at the side of the Reactor Building, is the only node undergoing significant displacement. The structural response is not appreciably influenced by this mode.
- b. Mode 2 - This mode is the fundamental mode of the soil-structure system. It consists of horizontal relative translation between the rock and the foundation, and distortion of the Reactor Building. This mode is viewed as driving the primary response of the drywell and pedestal.
- c. Mode 3 - This mode primarily affects the Reactor Building structural steel framing above the refueling floor. The balance of the Reactor Building, Drywell, suppression chamber, RPV System, and foundation are influenced significantly less.



- d. Mode 4 - This mode is the fundamental mode of the RPV System. The Reactor Building, Drywell, suppression chamber, and foundation are least influenced.

There are higher and more complicated modes, but they contribute little to the overall response of the drywell and RPV system. These mode shapes show that Mode 2 (3.3 Hz) is associated with the drywell and reactor building response, while Mode 4 (5.62 Hz) is primarily associated with the RPV system response.

#### 3.2.1.3 Calculation of Spectral Shape Factors

The median spectral accelerations for Modes 2 and 4 are taken from Figure 3-25 to be:

$$S_a (3.3 \text{ Hz}) = 0.84 \text{ g's}$$

$$S_a (5.6 \text{ Hz}) = 0.58 \text{ g's}$$

These values must be scaled by 0.16/0.27 in order to be anchored to the SSE ZPA of 0.16 g's.

$$S_a (3.3 \text{ Hz}) = 0.50 \text{ g's}$$

$$S_a (5.6 \text{ Hz}) = 0.34 \text{ g's}$$

The spectral accelerations used in the design are taken from the 10% soil damping curves of Figure 3-25 (note, the conservatism of using 7% soil damping in the design analysis will be accounted for in the SSI factor):

$$S_a (3.3 \text{ Hz}) = 0.98 \text{ g's}$$

$$S_a (5.5 \text{ Hz}) = 0.41 \text{ g's}$$

The spectral shape factor for the star truss failure mode is primarily based on the Mode 2 response since the drywell and shield wall are the major contributors to loading.

$$F_{SS} = \frac{0.98 \text{ g}}{0.50 \text{ g}} = 1.96 \quad (\text{star truss})$$

The randomness on the median spectrum are given in the WASH 1255 study in terms of a standard deviation from the median:

$$\beta_{SS,R} = \ln \left( \frac{2.36}{1.89} \right) = 0.22$$

where 2.36 and 1.89 are the plus one standard deviation and the median 7% damped spectral accelerations.

The uncertainty is estimated to be two-thirds of the randomness:

$$\beta_{SS,U} = 2/3 (.22) = 0.15$$

The spectral shape factor for the stabilizer failure is primarily based on the RPV response which is Mode 4.

$$F_{SS} = \frac{0.41 \text{ g}}{0.34 \text{ g}} = 1.21$$

The randomness and uncertainty are identical to those calculated for Mode 2 since the WASH 1255 spectra are of constant acceleration amplitude in the 2.7 Hz - 6 Hz range.

### 3.2.2 Damping Factor, $F_D$

Table 3-3 contains the damping values utilized on the Brunswick structural analyses. The 7% structural damping utilized on the primary containment structures is considered median since the structures themselves are not in the inelastic range at the level of projected DEGB failure. Based on Newmark's recommendations, 7% will be estimated as median and 5% will be taken as a -1 value. Therefore, using the WASH 1255 spectra:

$$F_D = 1.0$$

$$\beta_{D, \text{Composite}} = \ln \left( \frac{S_{a5\%}}{S_{a7\%}} \right) = \ln \left( \frac{2.12}{1.90} \right) = 0.11$$

$$\beta_{D,U} = \beta_{D,R} = \frac{0.11}{\sqrt{2}} = 0.08$$

### 3.2.3 Modeling Factor, $F_M$

A state-of-the-art dynamic analysis was performed on the soil and structure, thus, the modeling is assumed to be median-centered and  $F_M = 1.0$ . The system is complex warranting a  $\beta_{M,U}$  of 0.15.  $\beta_{M,R}$  is taken as zero.

### 3.2.4 Soil-Structure Interaction, $F_{SSI}$

The site of the Brunswick Steam Electric Plant is located approximately 2-1/2 miles north of Southport and 1-1/2 miles west of the Cape Fear River in southeastern North Carolina. Physiographically, the site is located on the Atlantic Coastal Plain about 90 miles southeast of the boundary between the flat-lying deposits of the Coastal Plain and the folded formations of the Piedmont and Appalachian regions. This boundary is known as the Fall Line. In the vicinity of the site, the Coastal Plain consists of approximately 1,500 feet of Cretaceous and younger deposits. In general, hard limestone exists from a depth of approximately 70 feet below existing ground surface and extends to a depth of 230 feet or more. The crystalline or metamorphic basement rock has been broadly warped into a tectonic feature known as the Cape Fear Arch.

The Brunswick design analysis included a fairly sophisticated soil-structure interaction analysis (Figure 3-27) and the soil spring properties were derived from Brunswick specific geological information. The deconvolution with depth was previously addressed in Section 3.2.1. It is impossible to verify the results of that analysis without undertaking a major study of our own, but we have no reason to believe that the analysis is biased. Thus, the soil-structure interaction analysis is considered as median-centered except for soil damping. Median damping is estimated to be 10% for soil instead of the 7% used in design. Using the free-field spectra from Figure 3-26:



at 3.3 Hz       $S_a$  (7% soil damping) = 1.35 g's  
                   $S_a$  (10% soil damping) = 0.98 g's

at 5.5 Hz       $S_a$  (7% soil damping) = 0.45 g's  
                   $S_a$  (10% soil damping) = 0.41 g's

Therefore,

$$F_{SSI} = \frac{1.35}{0.98} = 1.38 \quad (\text{star truss})$$

$$F_{SSI} = \frac{0.45}{0.41} = 1.10 \quad (\text{stabilizer})$$

The uncertainty on the soil-structure interaction is estimated to be  $\beta_{SSI,U} = 0.30$  based on past experience, and the randomness is zero.

### 3.2.5 Earthquake Component Combination Factor, $F_{EC}$

The earthquake component combination methods used in the capacity evaluation are considered median-centered, thus:

$$F_{EC} = 1.0$$

There is some randomness in the phasing of the earthquake components which is estimated to be 0.10.

$$\beta_{EC,R} = 0.10$$

$$\beta_{EC,U} = 0.00$$

### 3.3 GROUND ACCELERATION CAPACITIES FOR CRITICAL COMPONENTS, $A_C$

The strength factor calculations in Section 3.1 indicate that Brunswick has two seismic failure modes which are expected to be the dominant contributors to the probability of indirect DEGB. These two failure modes are

the RPV stabilizer and the star truss separating the shield wall from the drywell. Tables 3-4 and 3-5 contain the capacity factors and response factors derived for these components along with the calculated ground acceleration capacities and variabilities.

The median ground acceleration capacity of each component was calculated using the formula:

$$\check{A}_C = \check{A}_{SSE} F_C \check{F}_R$$

the variability estimates are:

$$\beta_{A,R} = (\beta_{C,R}^2 + \beta_{R,R}^2)^{1/2}$$

$$\beta_{A,U} = (\beta_{C,U}^2 + \beta_{R,U}^2)^{1/2}$$

The resulting fragilities are:

$$\left. \begin{array}{l} \check{A}_C = 1.92 \text{ g's} \\ \beta_R = 0.25 \\ \beta_U = 0.45 \end{array} \right\} \text{ (stabilizer)}$$

$$\left. \begin{array}{l} \check{A}_C = 2.67 \text{ g's} \\ \beta_R = 0.25 \\ \beta_U = 0.42 \end{array} \right\} \text{ (star truss)}$$

TABLES AND FIGURES FOR SECTION III.



TABLE 3-1

SACRIFICIAL SHIELD WALL PHYSICAL PROPERTIESPHYSICAL PROPERTIES OF CONTAINMENT STRUCTURE  
REFUELING CONDITIONDATA FOR SACRIFICIAL SHIELD

Modulus of Elasticity = 29000.00 kip/sq in.  
 Poisson Ratio = 0.30

<u>Segment No.</u>	<u>Outer Radius (ft)</u>	<u>Inner Radius (ft)</u>	<u>Length (ft)</u>	<u>Weight (kip)</u>
15	12.064	12.000	6.25	240.00
16	12.099	12.000	8.00	241.00
17	12.099	12.000	7.00	246.00
18	12.099	12.000	7.00	246.00
19	12.064	12.000	9.50	293.00
20	12.099	12.000	9.50	342.00

TABLE 3-2

STRENGTH FACTOR COMPARISON FOR CRITICAL AREAS OF THE RPV LOWER SUPPORT

AREA	MODE OF LIMIT CAPACITY	STRENGTH FACTOR
1.) RPV Skirt Knuckle	Bending	8.9
2.) RPV Skirt Cylinder	Buckling	12.1
3.) RPV Skirt Flange	Bending	12.4
4.) Bolting: Skirt to Ring Girder	Tensile and shear	2.5 *
5.) Ring Girder Top Flange	Bending	2.7 *
6.) Ring Girder Bottom Flange	Bending	3.4 *
7.) Bolting: Ring Girder to Pedestal	Tensile and shear	2.7
* Based on FSAR summaries on seismic qualification results		

TABLE 3-3

DAMPING VALUES USED IN BRUNSWICK DESIGN ANALYSES

<u>ITEM</u>	<u>DAMPING FACTORS</u>	
	<u>PERCENT OF CRITICAL DAMPING</u>	
	<u>OBE</u>	<u>DBE</u>
Reinforced Concrete:		
(a) Primary Containment Structure	4	7
(b) Reactor Building and other Class I Structures	4	7
Steel Structures and Assemblies:		
(Reactor Building & other Class I structures)		
(a) Bolted or Riveted	5	10
(b) Welded	2	5
Vital Piping	0.5	2
Equipment	1	2
Soil - Structure Interaction Damping	4	7



TABLE 3-4  
STABILIZER FRAGILITY

Item	Median F.S.	$\beta_R$	$\beta_u$	$\beta_c$
Strength	9.0	0.0	0.25	
Inelastic Energy Absorption	1.0	0.0	0.0	
Spectral Shape	1.21	0.22	0.15	
Damping	1.0	0.08	0.08	
Modelling	1.0	0.0	0.15	
Modal Combination	1.0	0.0	0.0	
Combination of Earthquake Components	1.0	0.10	0.0	
Soil-Structure Interaction	1.10	0.0	0.30	
TOTAL	12.0	0.25	0.45	0.51

Median Acceleration Capacity =  $0.16g's \times 12 = 1.92g's$

TABLE 3-5  
STAR TRUSS FRAGILITY

Item	Median F.S.	$\beta_R$	$\beta_U$	$\beta_C$
Strength	6.18	0.0	0.21	
Inelastic Energy Absorption	1.0	0.0	0.0	
Spectral Shape	1.96	0.22	0.15	
Damping	1.0	0.08	0.08	
Modelling	1.0	0.0	0.15	
Modal Combination	1.0	0.0	0.0	
Combination of Earthquake Components	1.0	0.10	0.0	
Soil-Structure Interaction	1.38	0.0	0.30	
TOTAL	16.7	0.25	0.42	0.49

Median Acceleration Capacity =  $0.16 \text{ g's} \times 16.7 = 2.67 \text{ g's}$

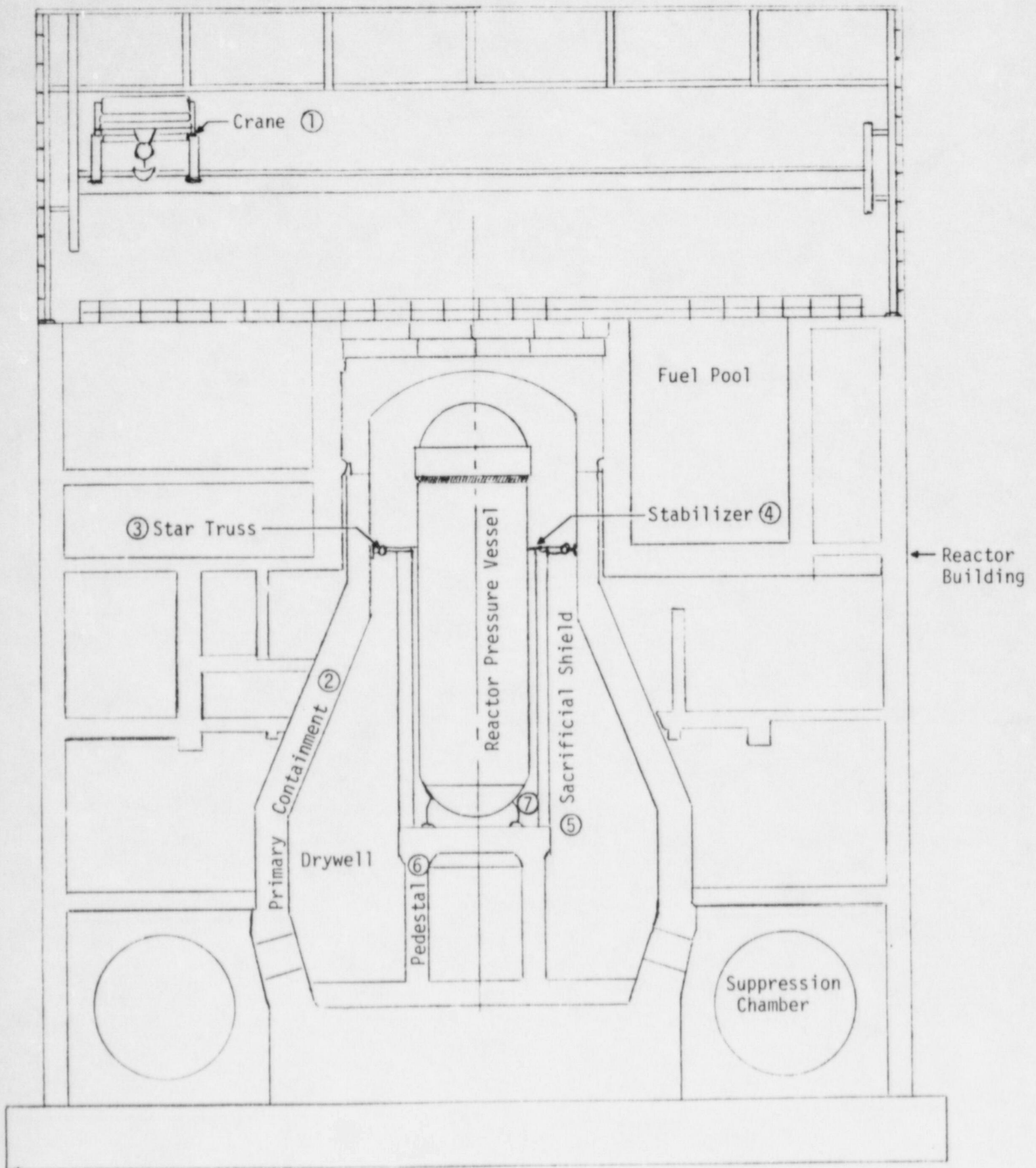


FIGURE 3-1. BRUNSWICK CONTAINMENT STRUCTURE AND RPV SUPPORT SYSTEM



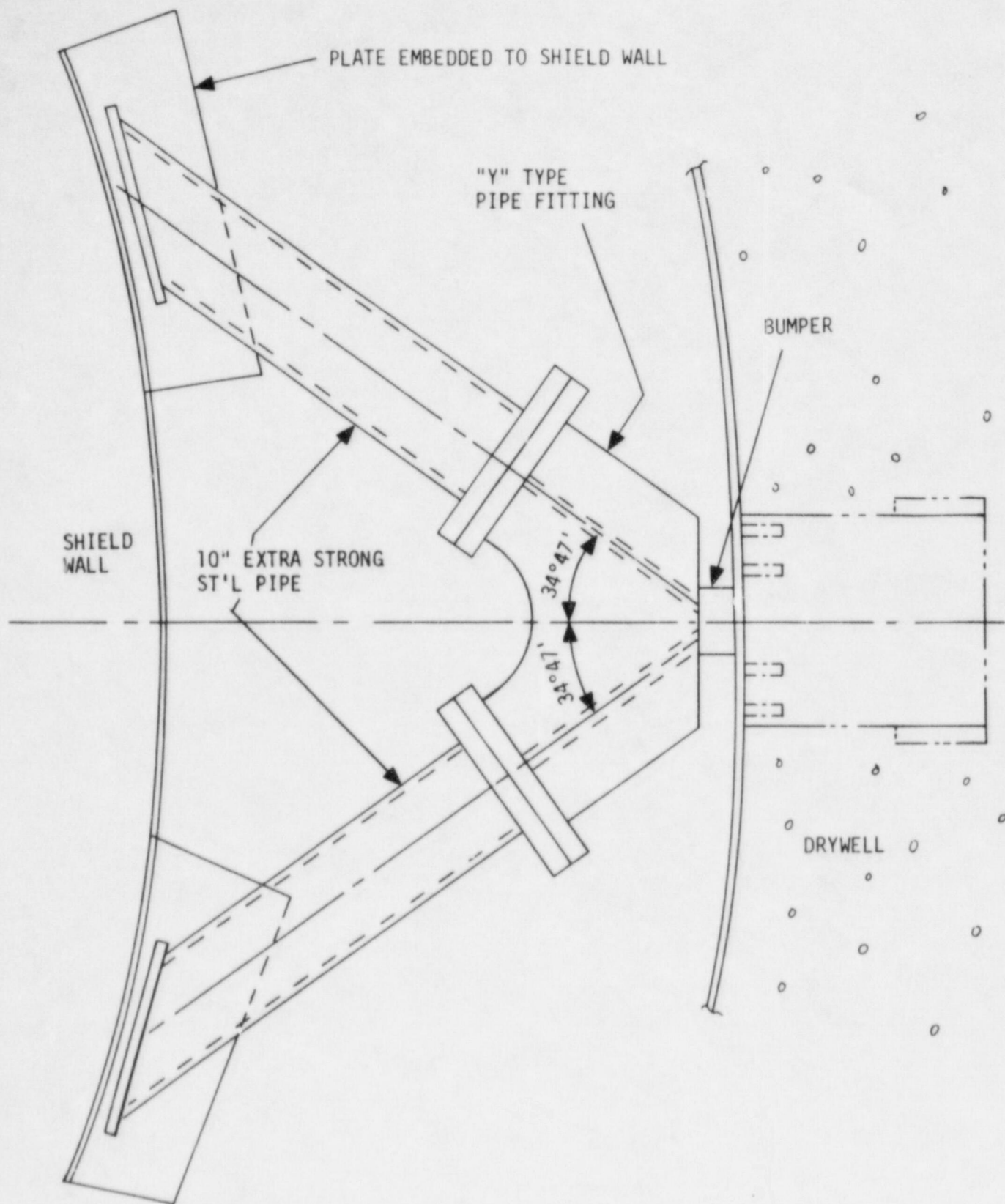


FIGURE 3-2. STAR TRUSS CONFIGURATION

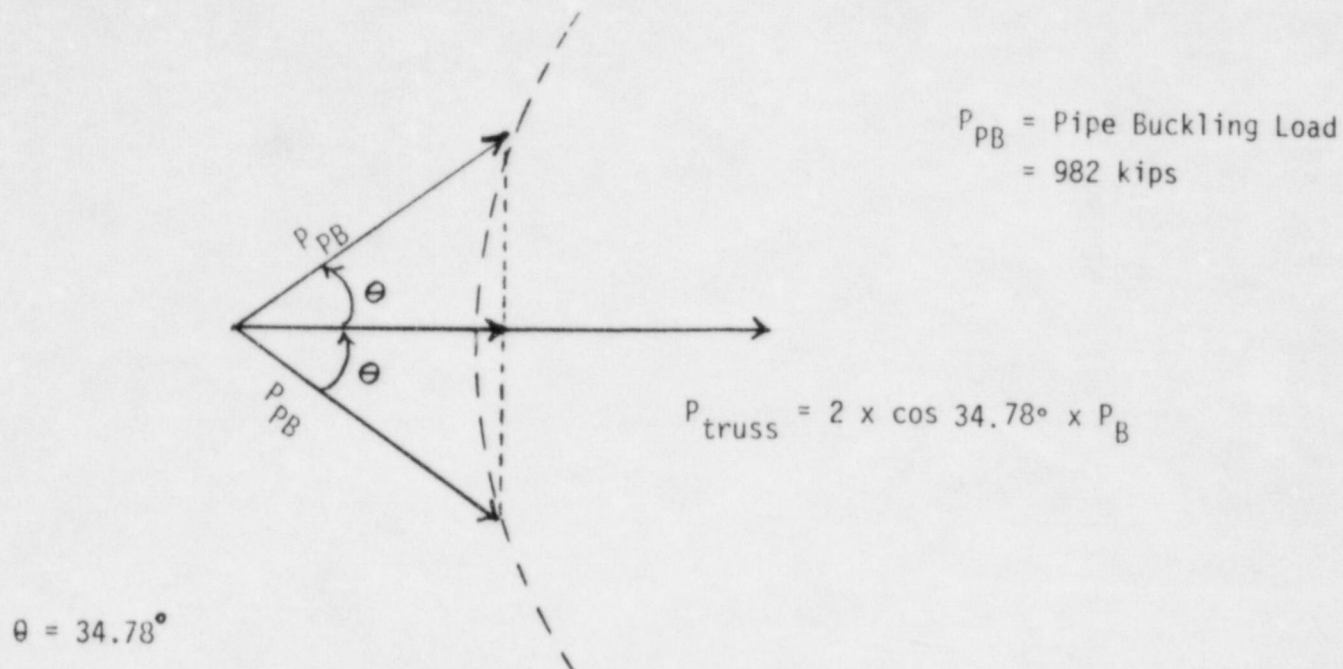


FIGURE 3-3: RESULTANT CAPACITY VECTOR FOR SINGLE "V" SHAPED PIPE TRUSS

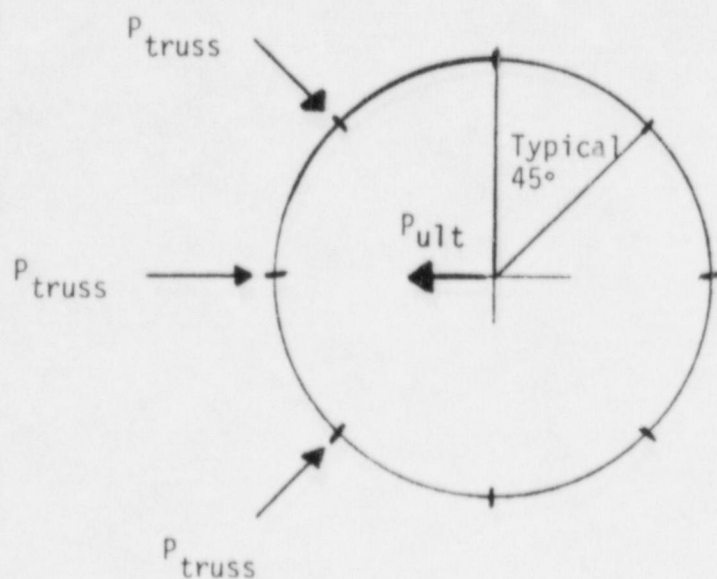


FIGURE 3-4. ULTIMATE LOAD CAPACITY FOR STAR TRUSS

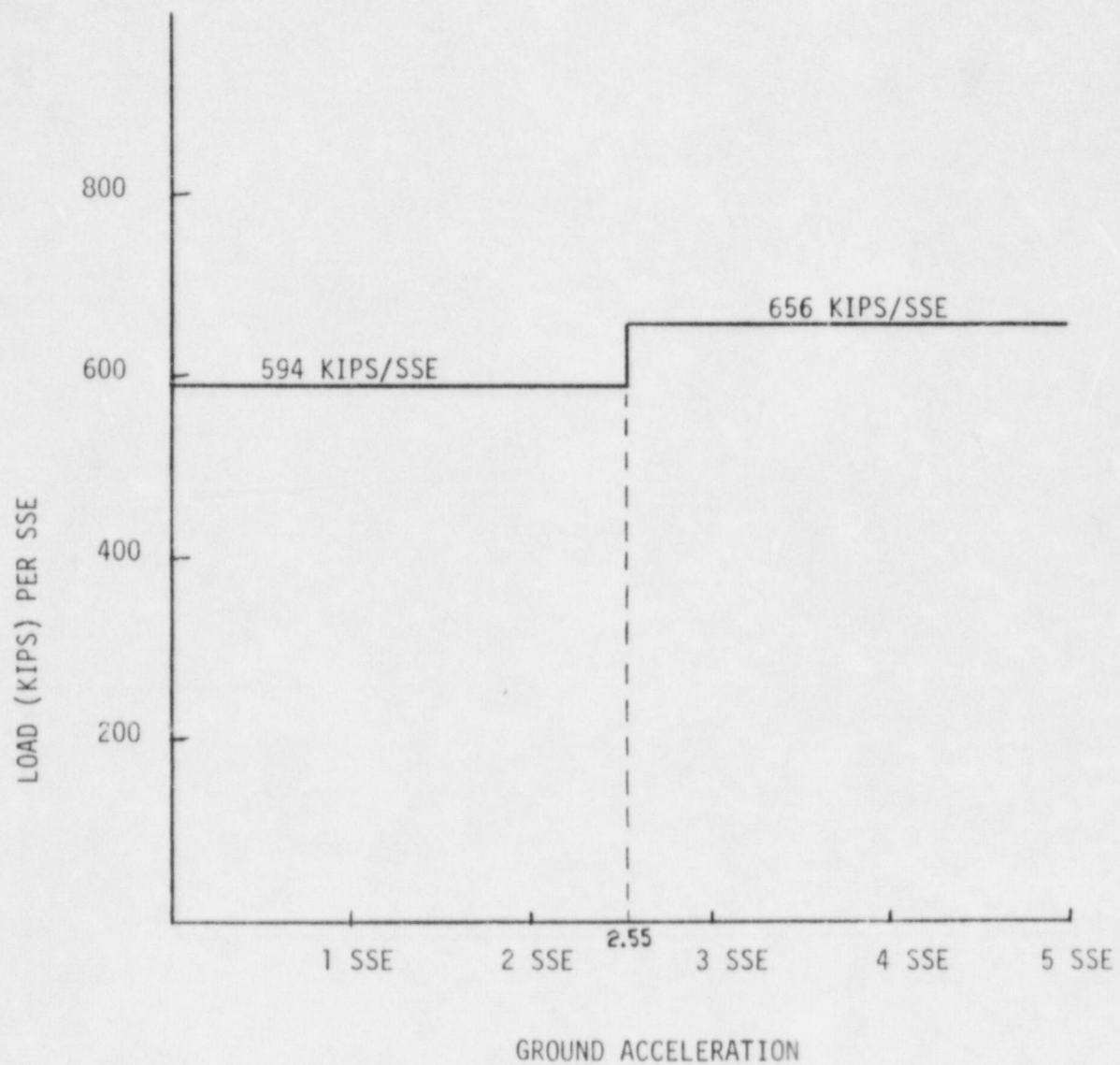


FIGURE 3-5. NONLINEAR LOADING ON STAR TRUSS SUPPORT SYSTEM



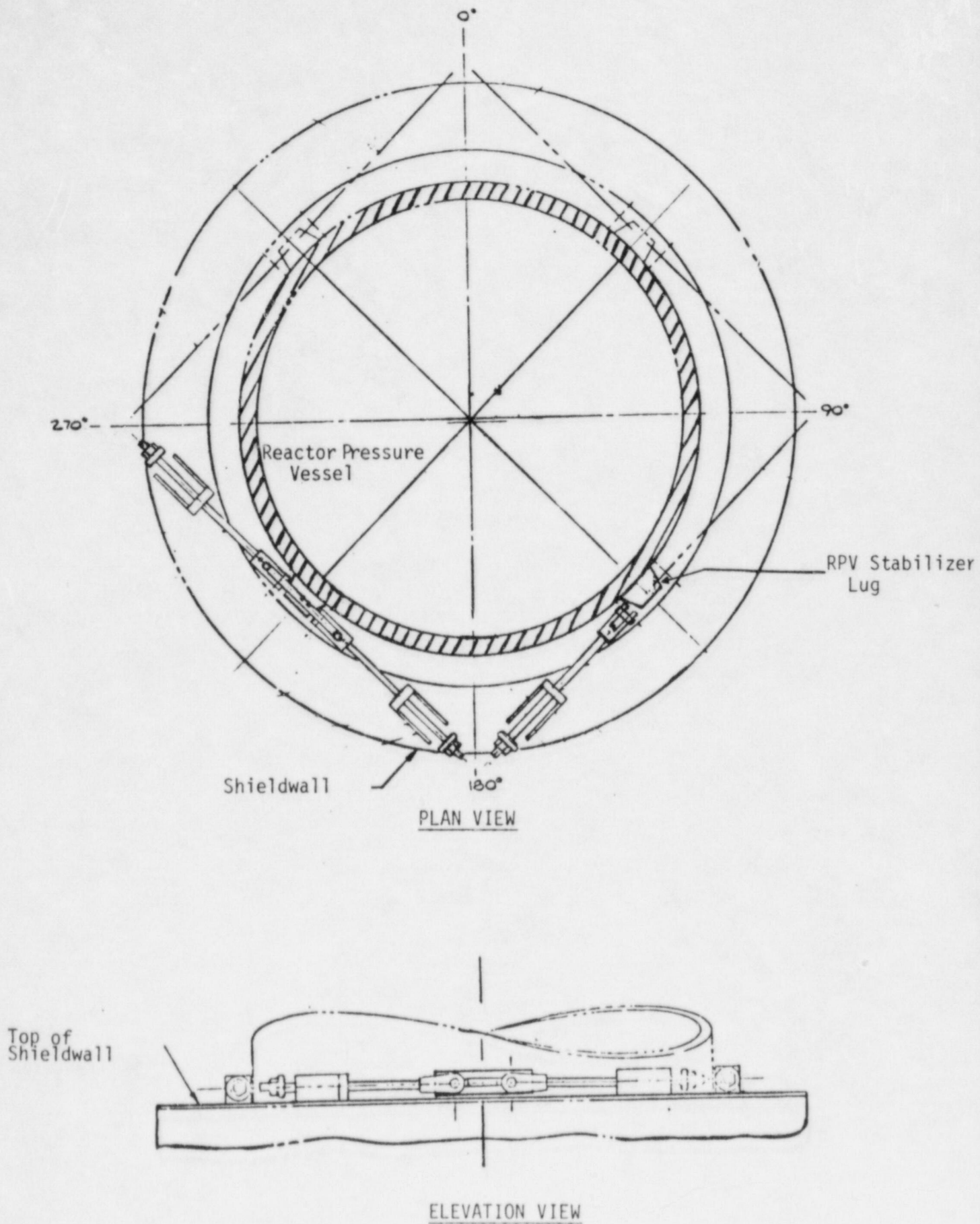
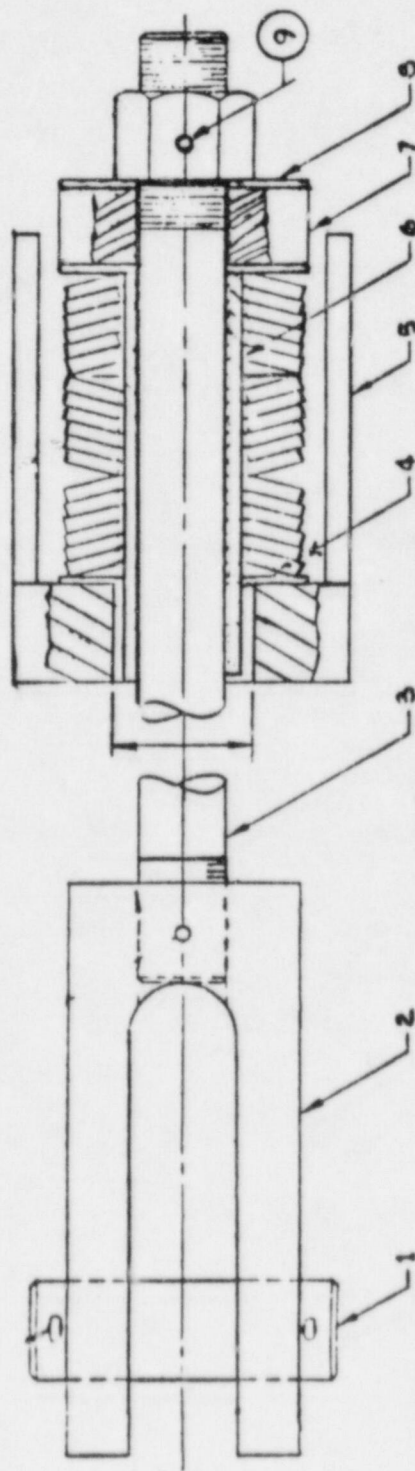


FIGURE 3-6. RPV STABILIZER CONFIGURATION  
3-38



1 = Clevis Pin  
2 = Clevis  
3 = Draw Bar

4 = Washer  
5 = Gusset Plate  
6 = Sleeve

7 = Collar  
8 = Washer  
9 = Set Screw

FIGURE 3-7. SCHEMATIC OF RPV STABILIZER COMPONENTS

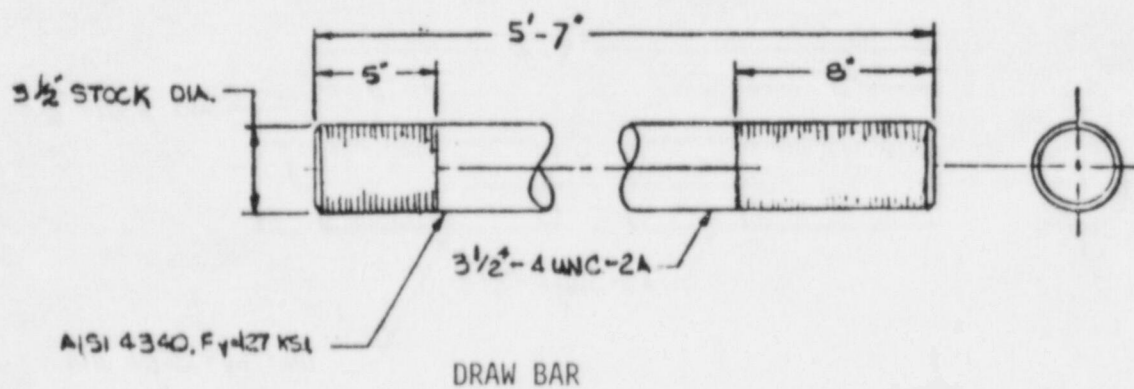
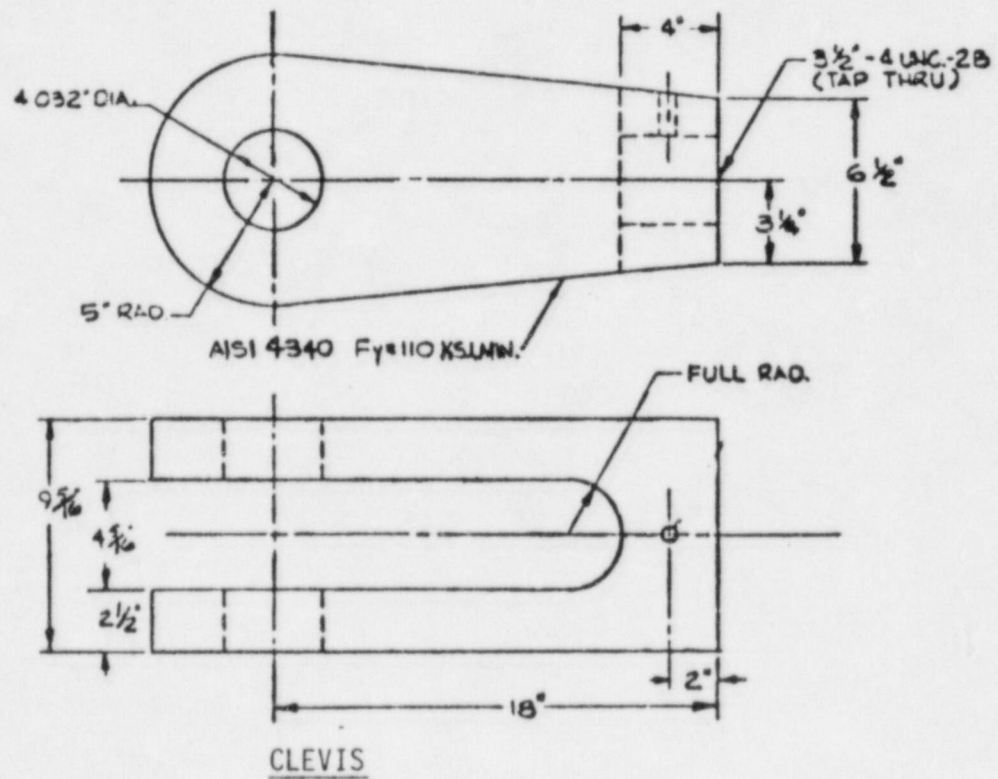
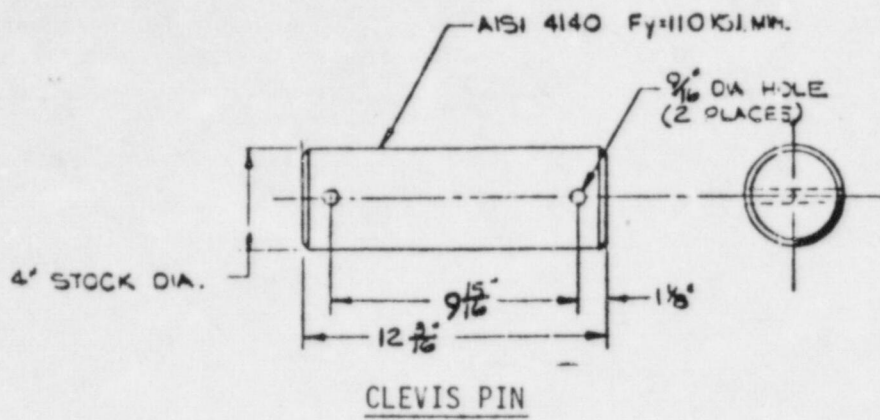


FIGURE 3-8. RPV STABILIZER CLEVIS PIN, CLEVIS AND DRAW BAR



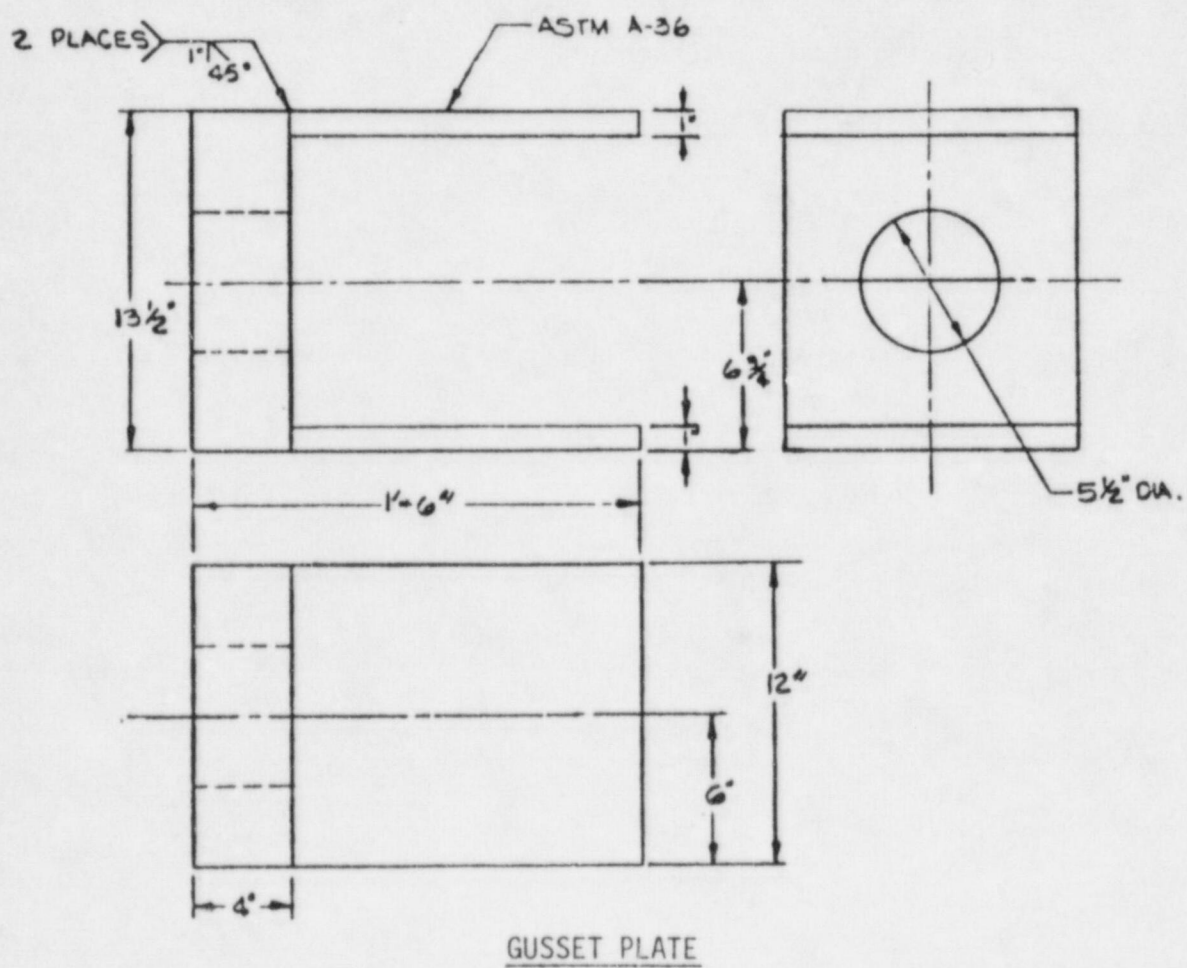


FIGURE 3-9. RPV STABILIZER GUSSET PLATE BRACKET

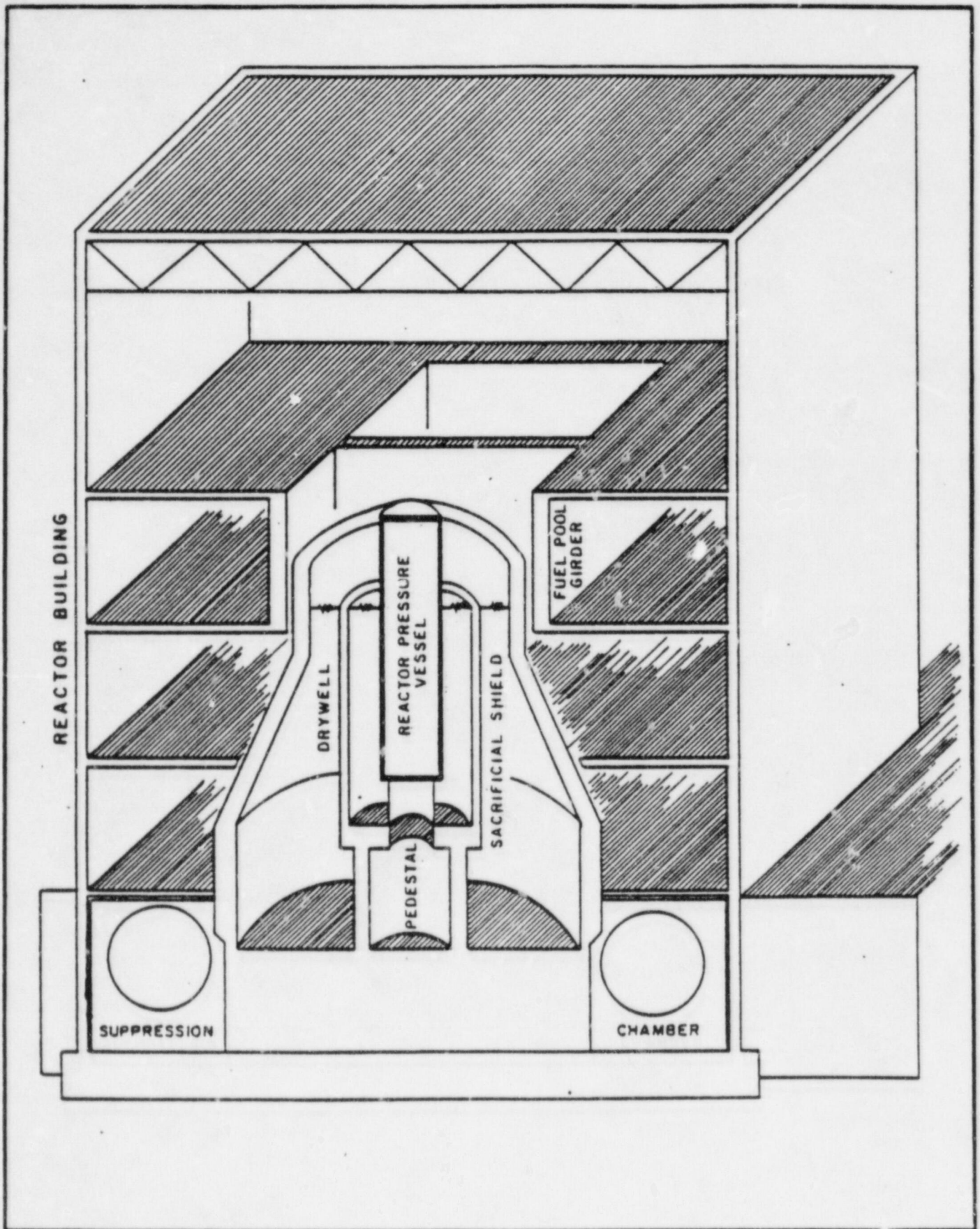


FIGURE 3-10. PERSPECTIVE VIEW OF CONTAINMENT STRUCTURE

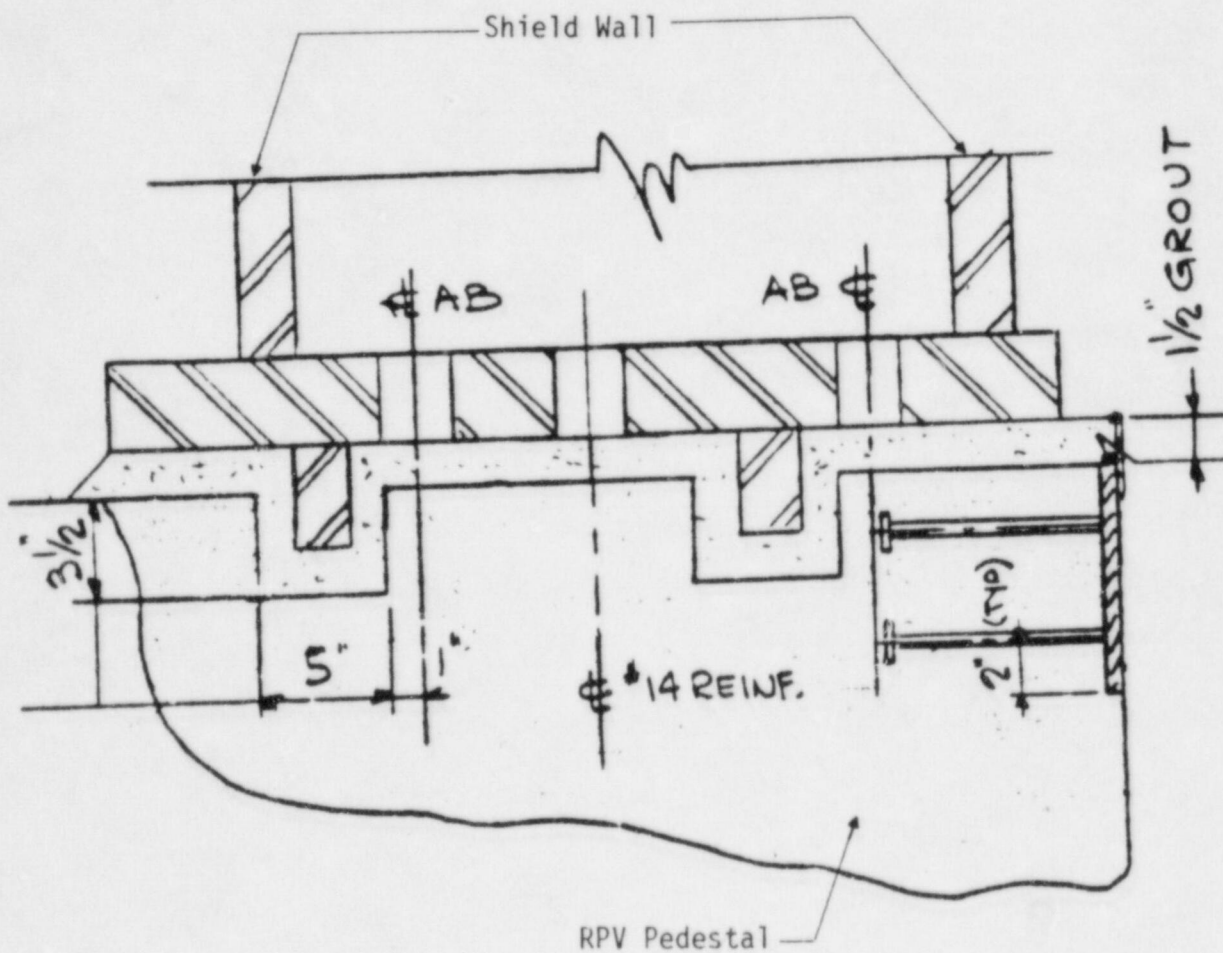
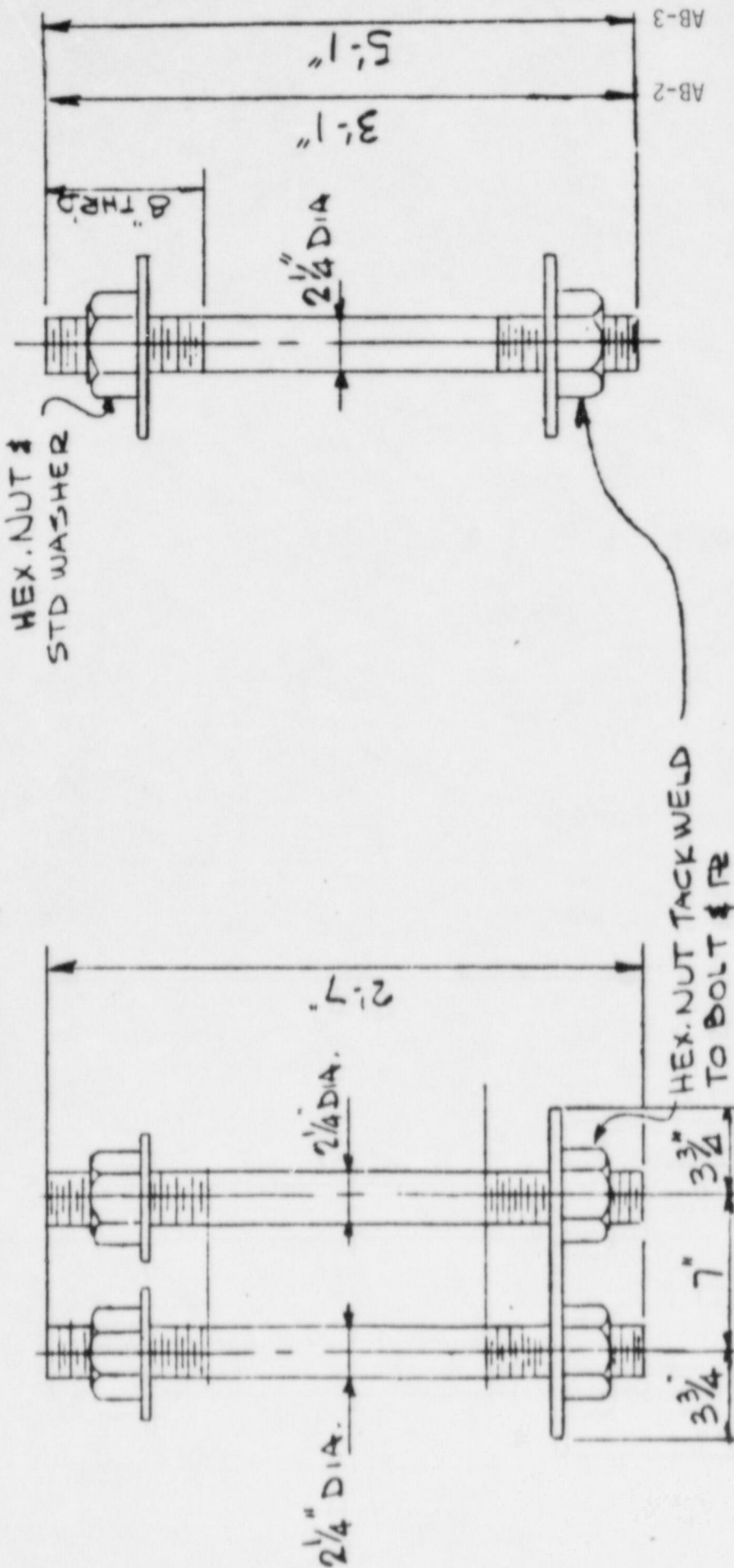


FIGURE 3-11. SHIELD WALL TO PEDESTAL INTERFACE





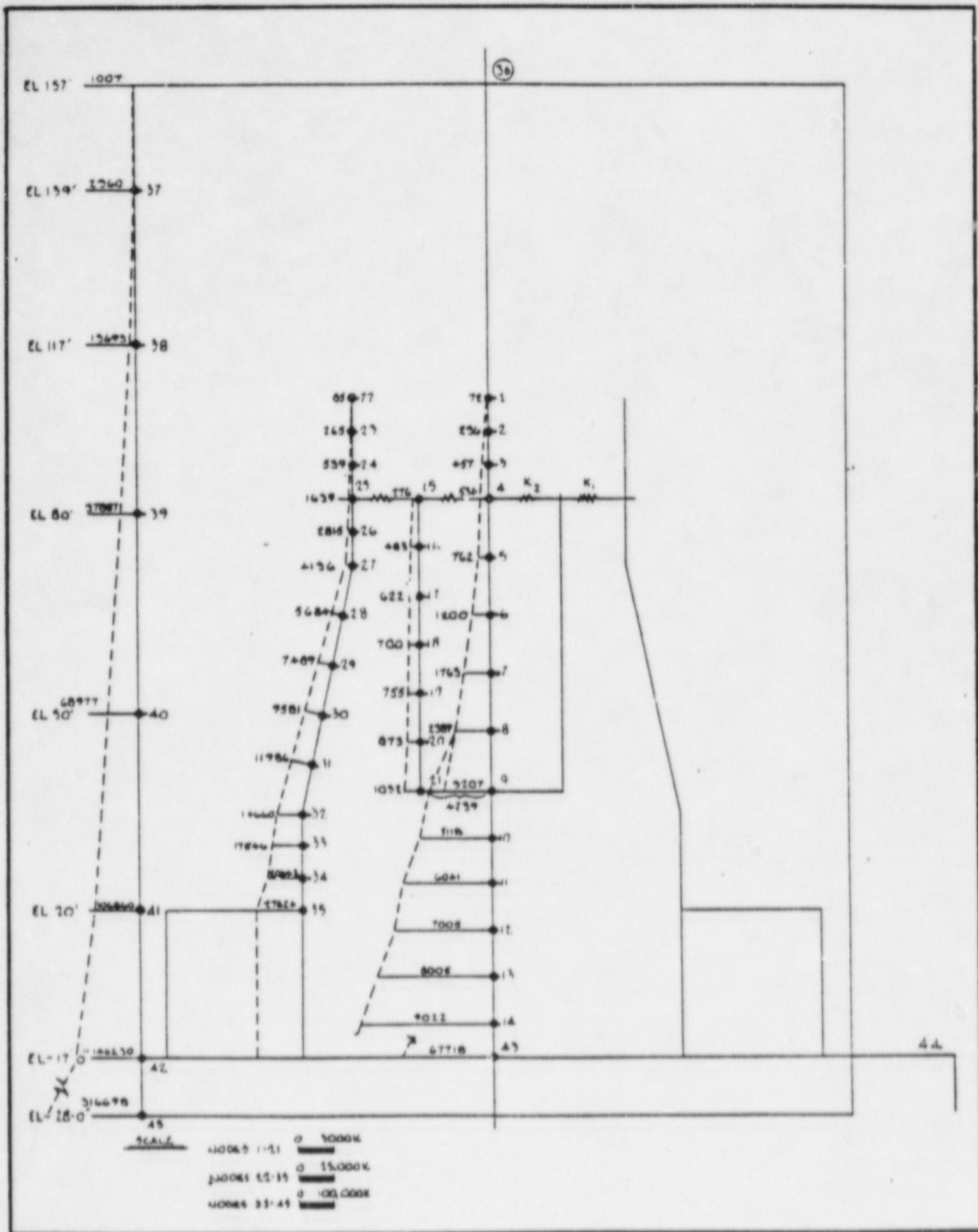
AT ELEV. 23'-2"  
SCALE 3/8" = 1'-0"



Ring Girder  
RPV Anchor Bolts

Shield Wall Anchor Bolts

FIGURE 3-13. ANCHOR BOLTS FOR RPV RING GIRDER AND SHIELD WALL







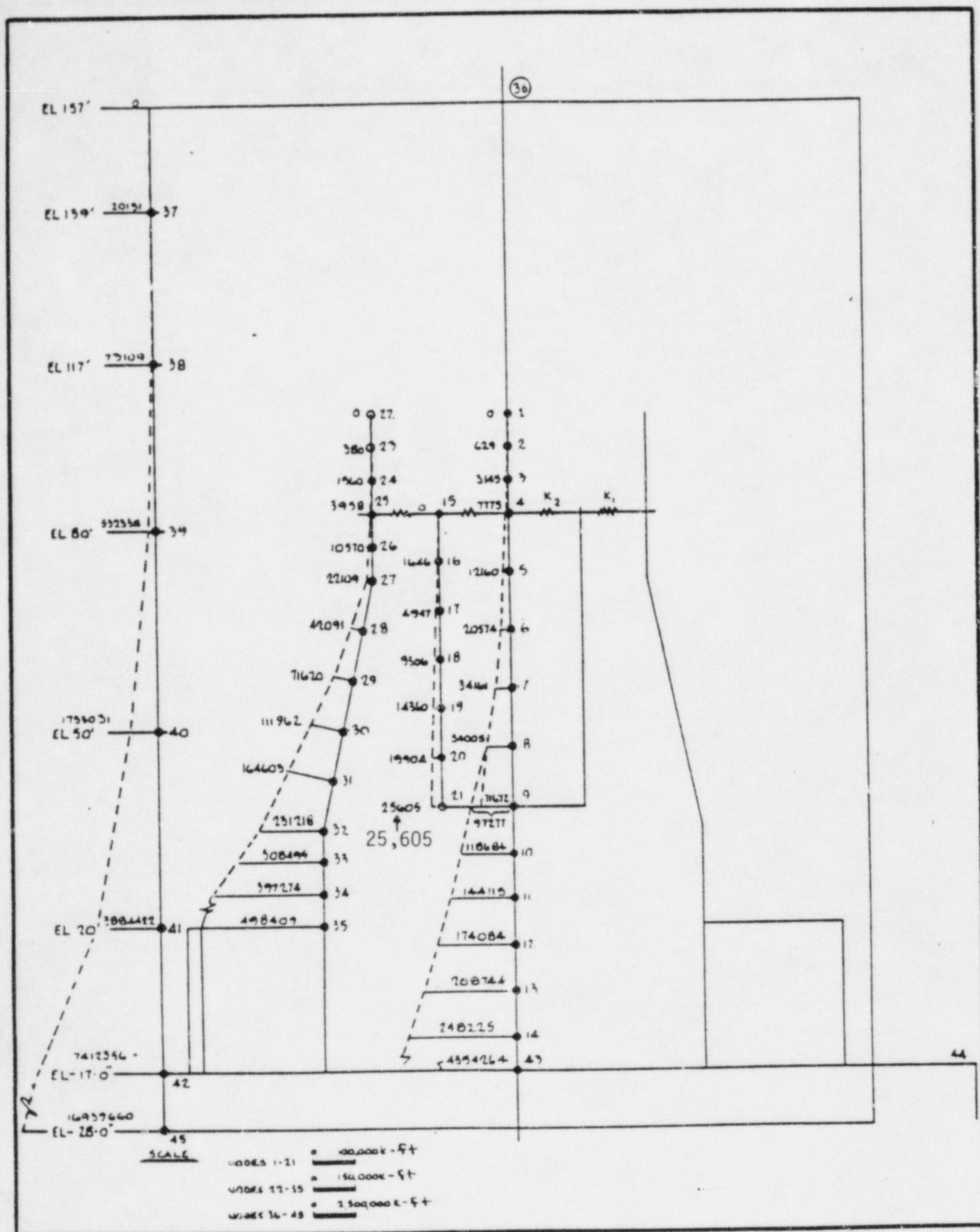


FIGURE 3-16. SUMMATION OF NODAL MOMENTS FOR SSE CONDITION - Y DIRECTION

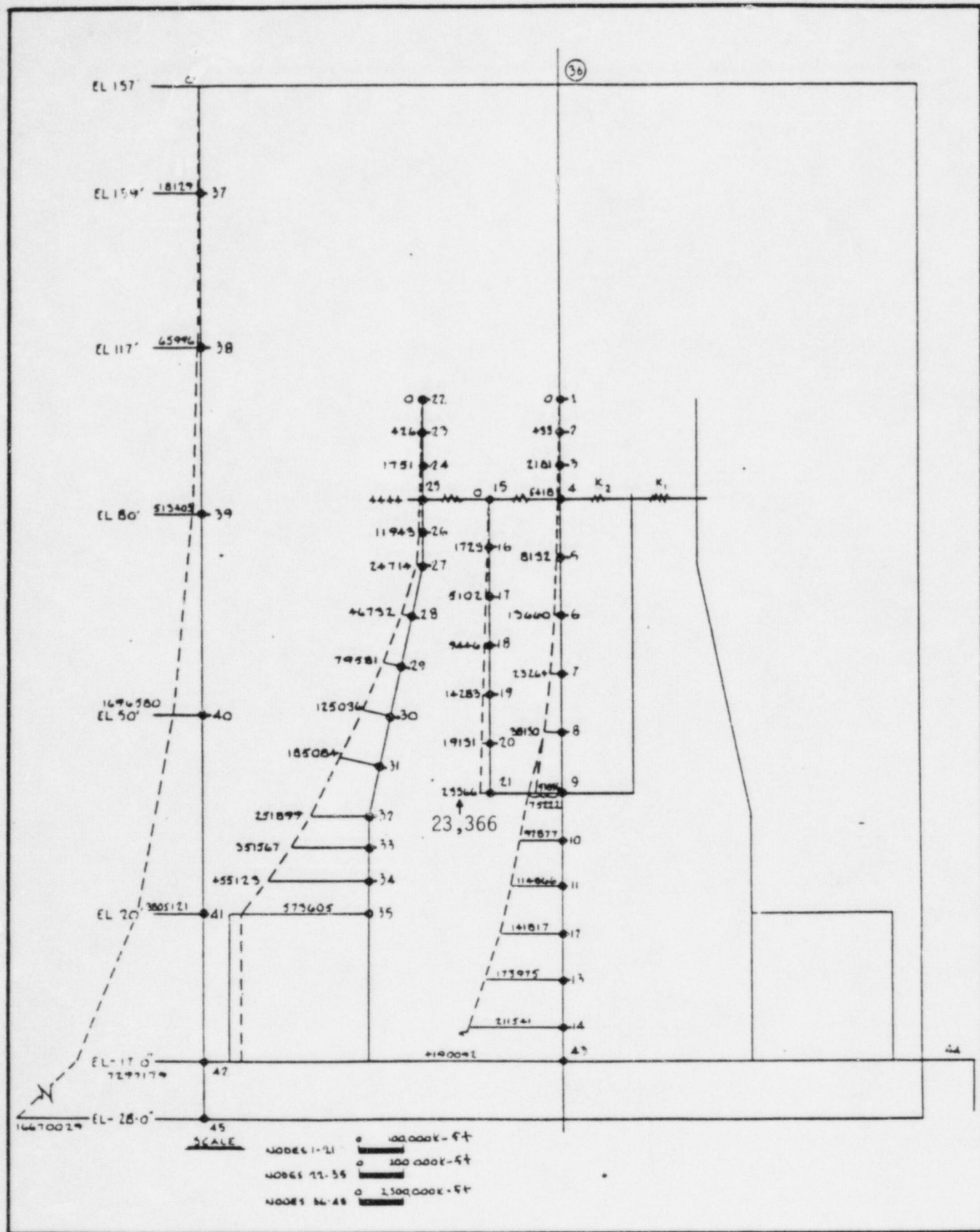


FIGURE 3-17: SUMMATION OF NODAL MOMENTS FOR SSE CONDITION - X DIRECTION



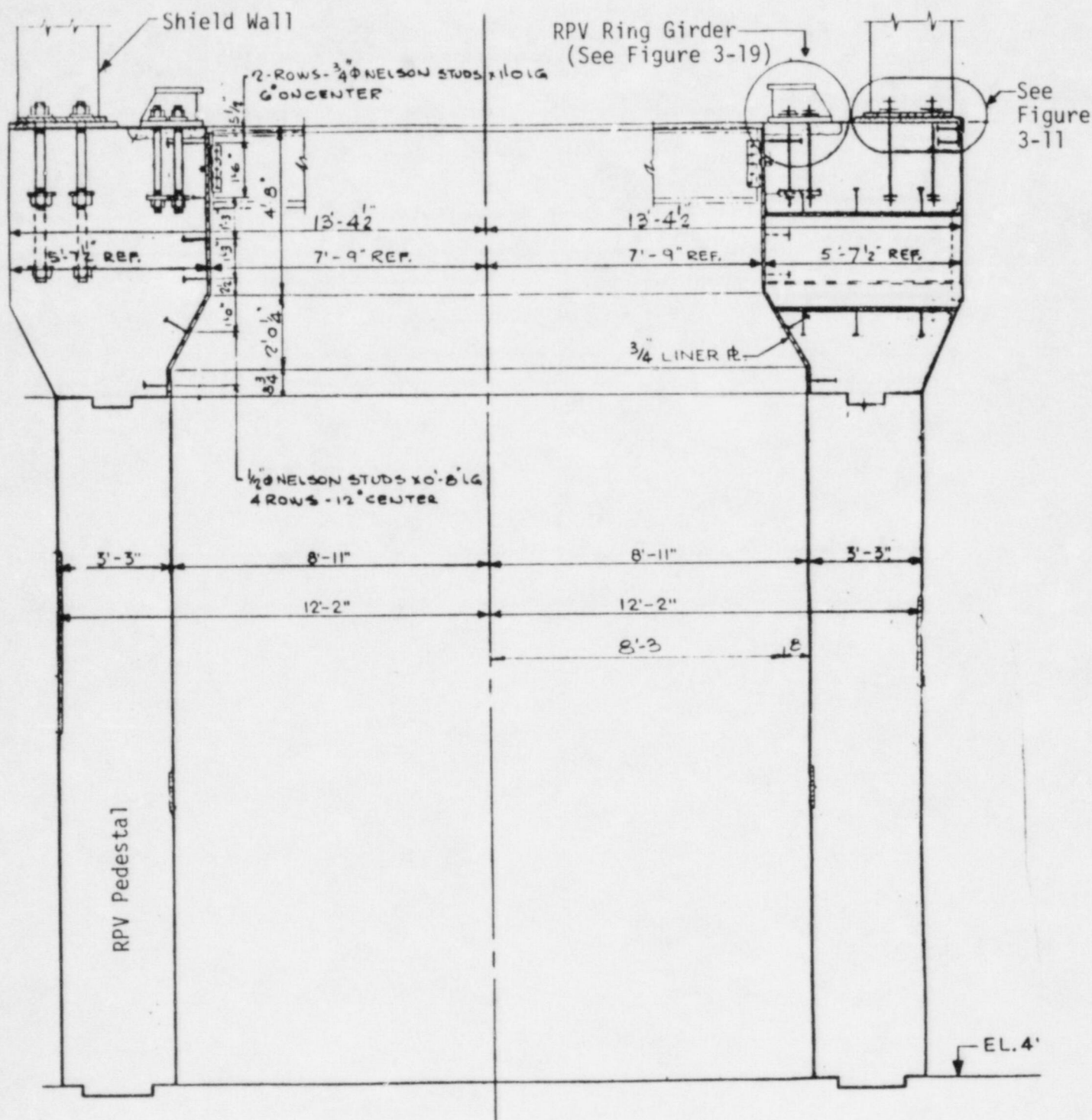


FIGURE 3-18. RPV SUPPORT PEDESTAL

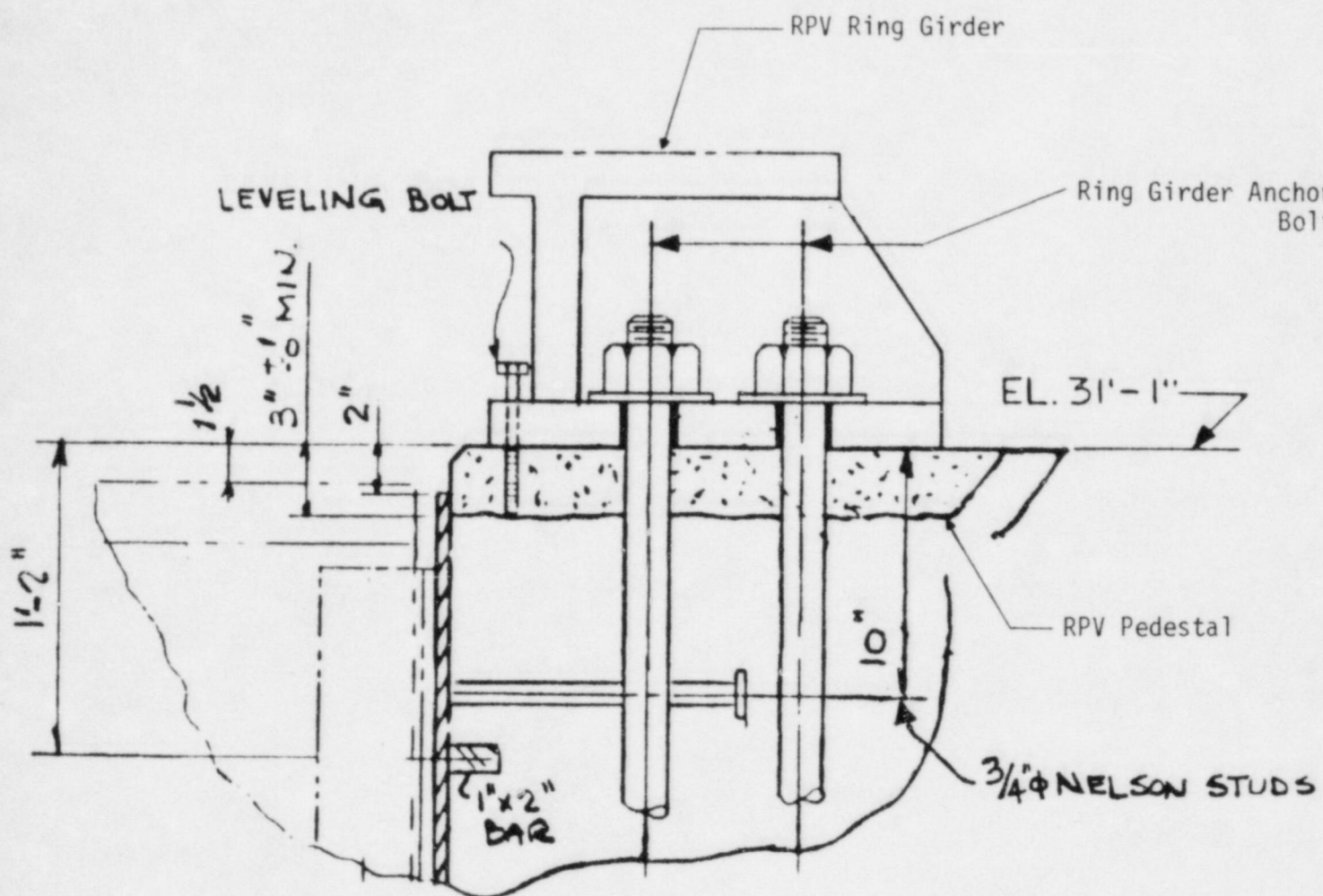


FIGURE 3-19. RPV RING GIRDER TO PEDESTAL ANCHORAGE

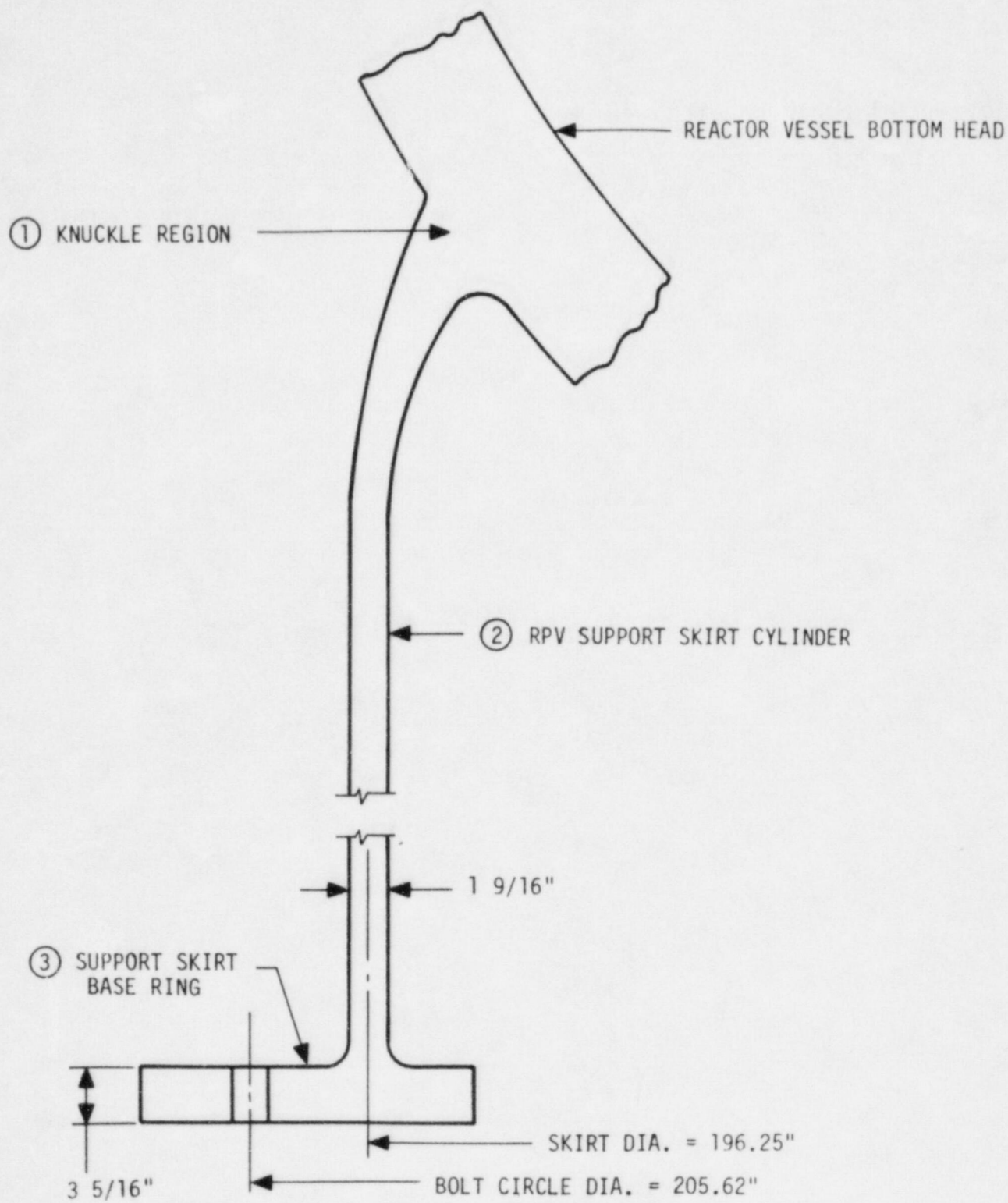
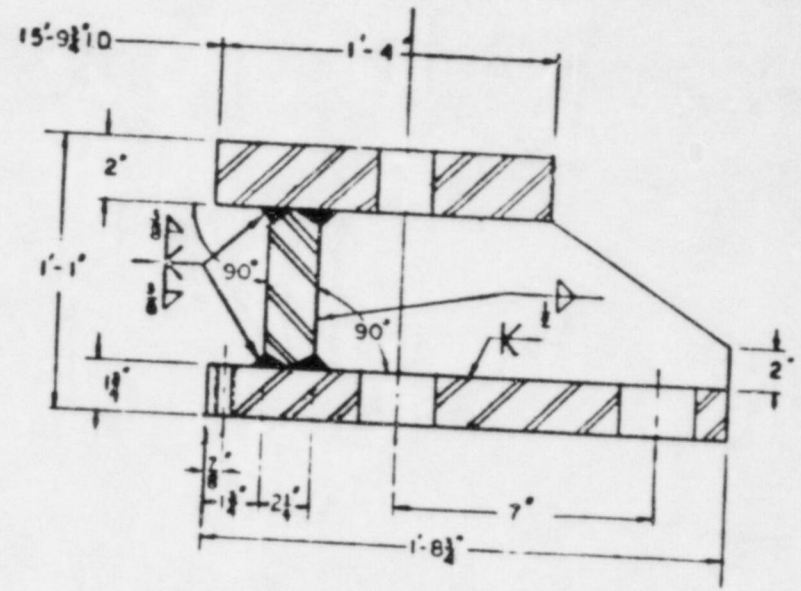
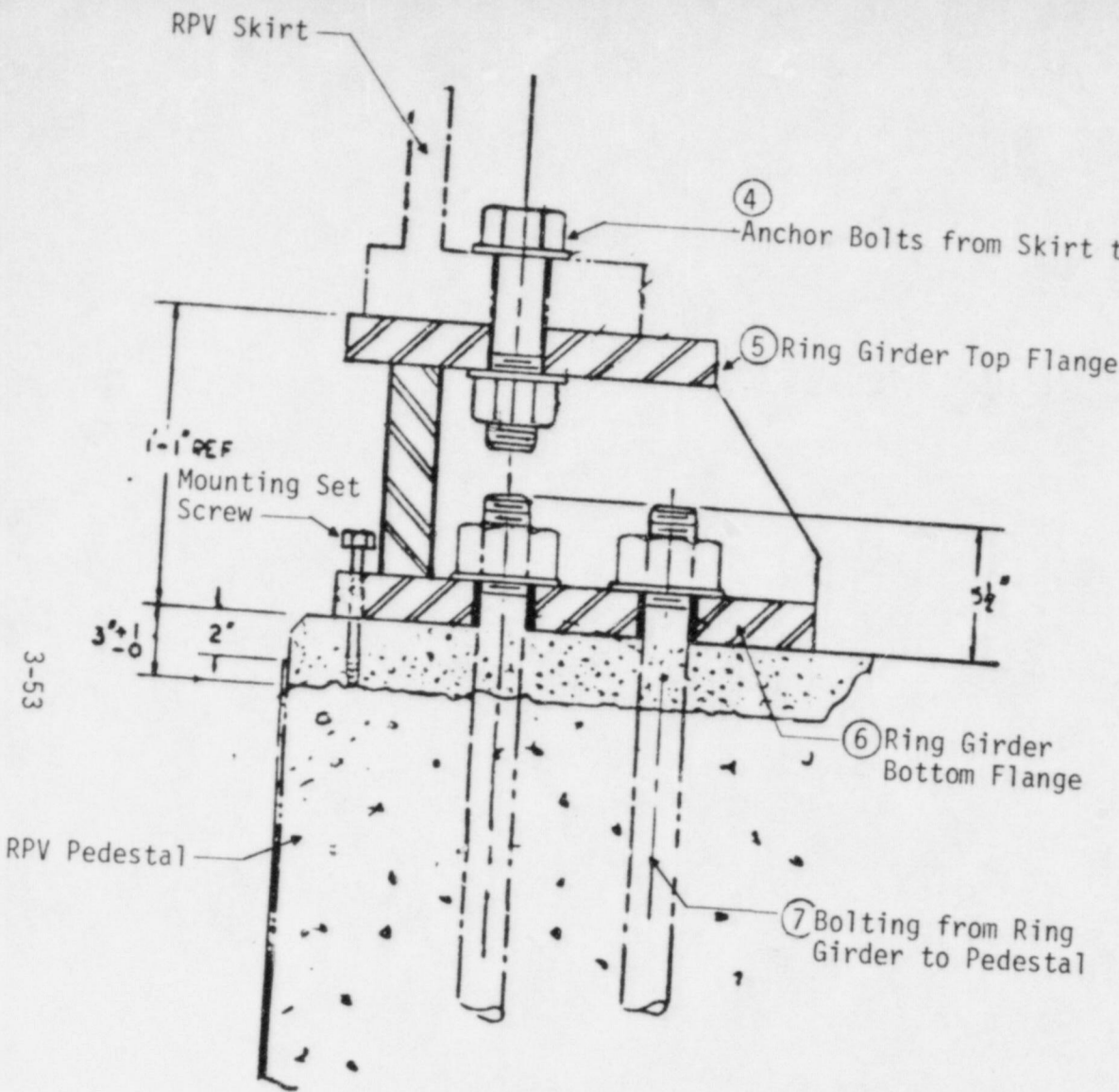


FIGURE 3-20. RPV SUPPORT SKIRT CONFIGURATION





Ring Girder Dimensions

FIGURE 3-21. RPV RING GIRDER AND ANCHORAGE

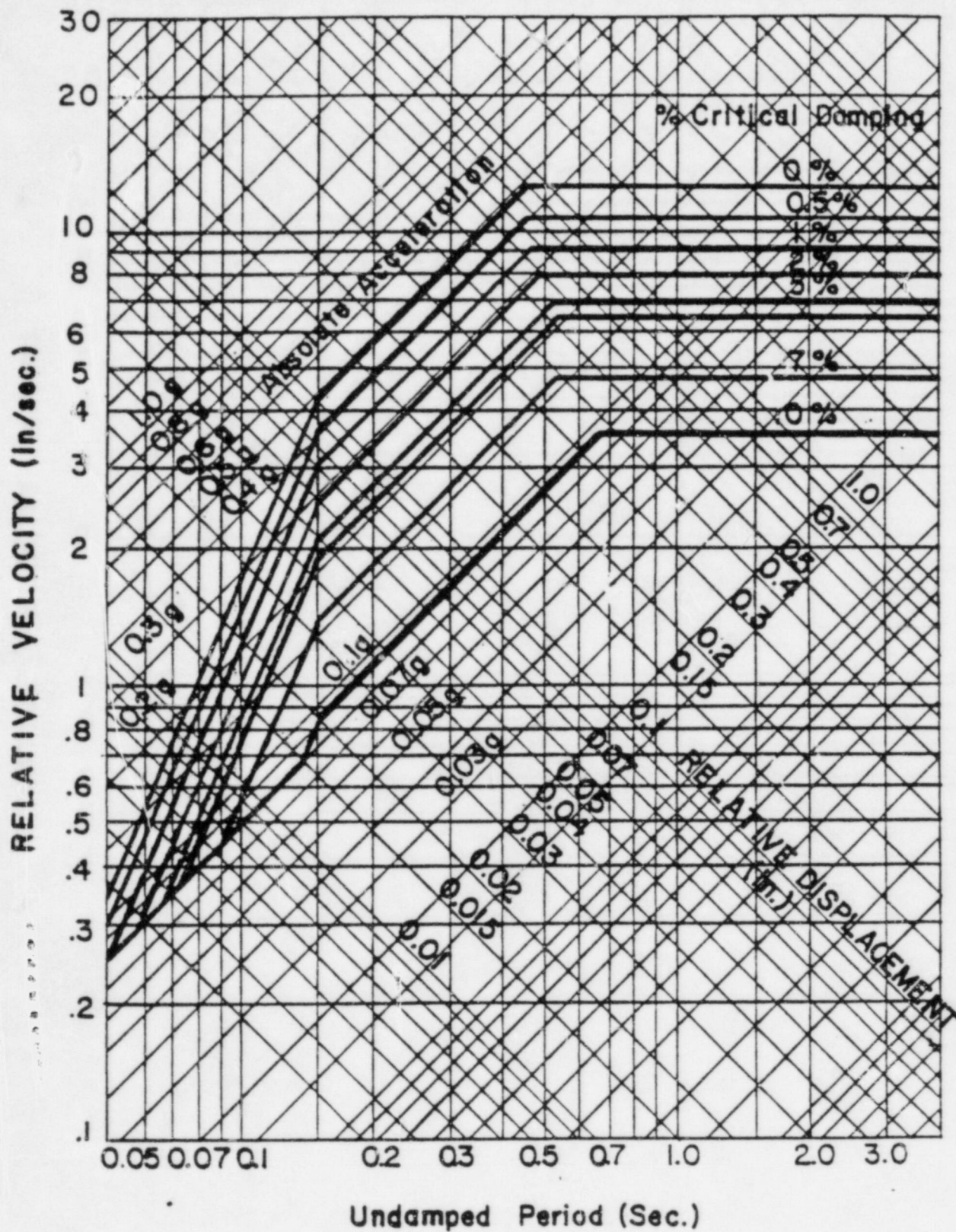


FIGURE 3-22. BRUNSWICK OBE DESIGN GROUND RESPONSE SPECTRA





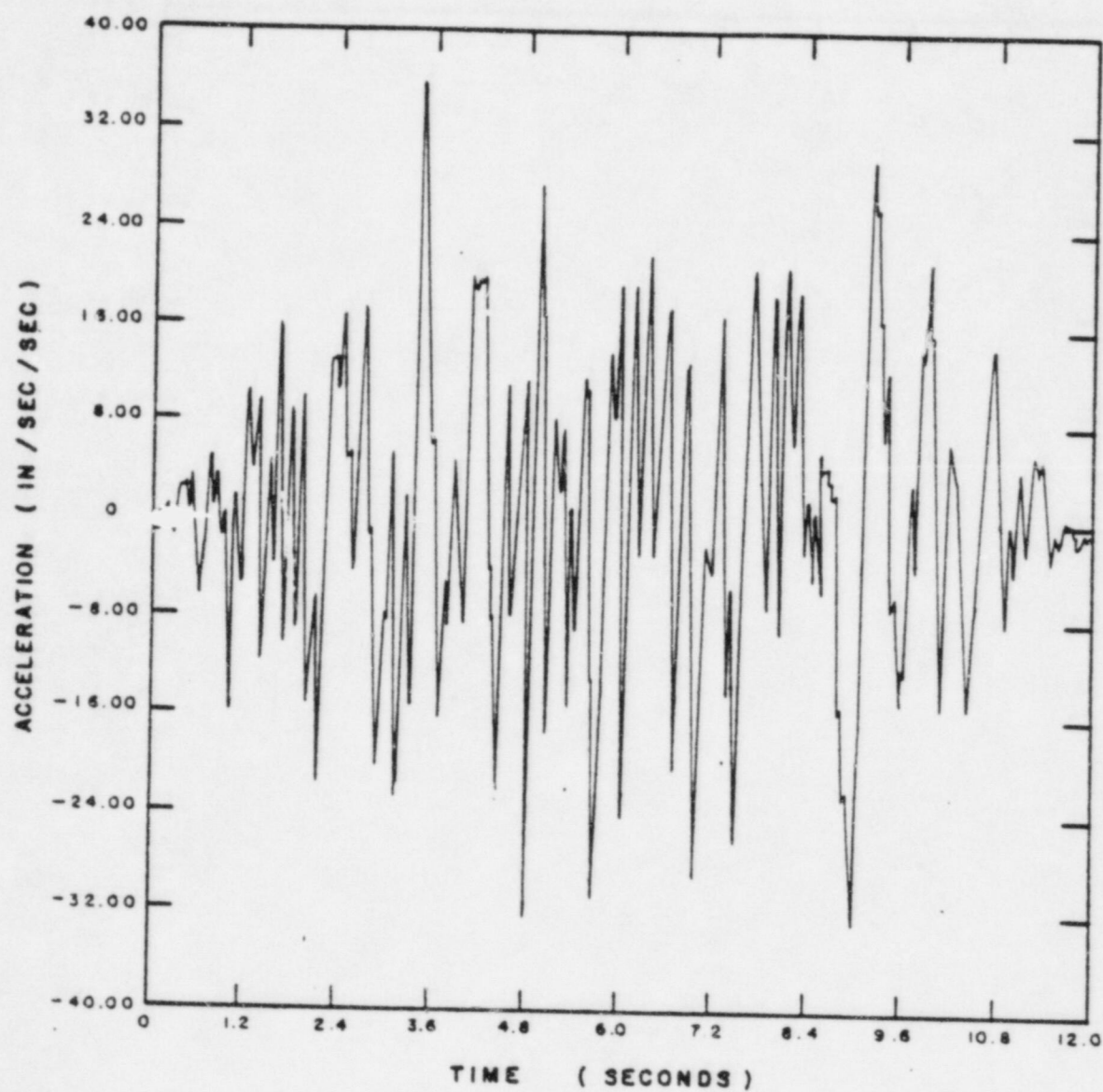


FIGURE 3-24. ARTIFICIAL TIME HISTORY FOR BRUNSWICK PLANT SITE

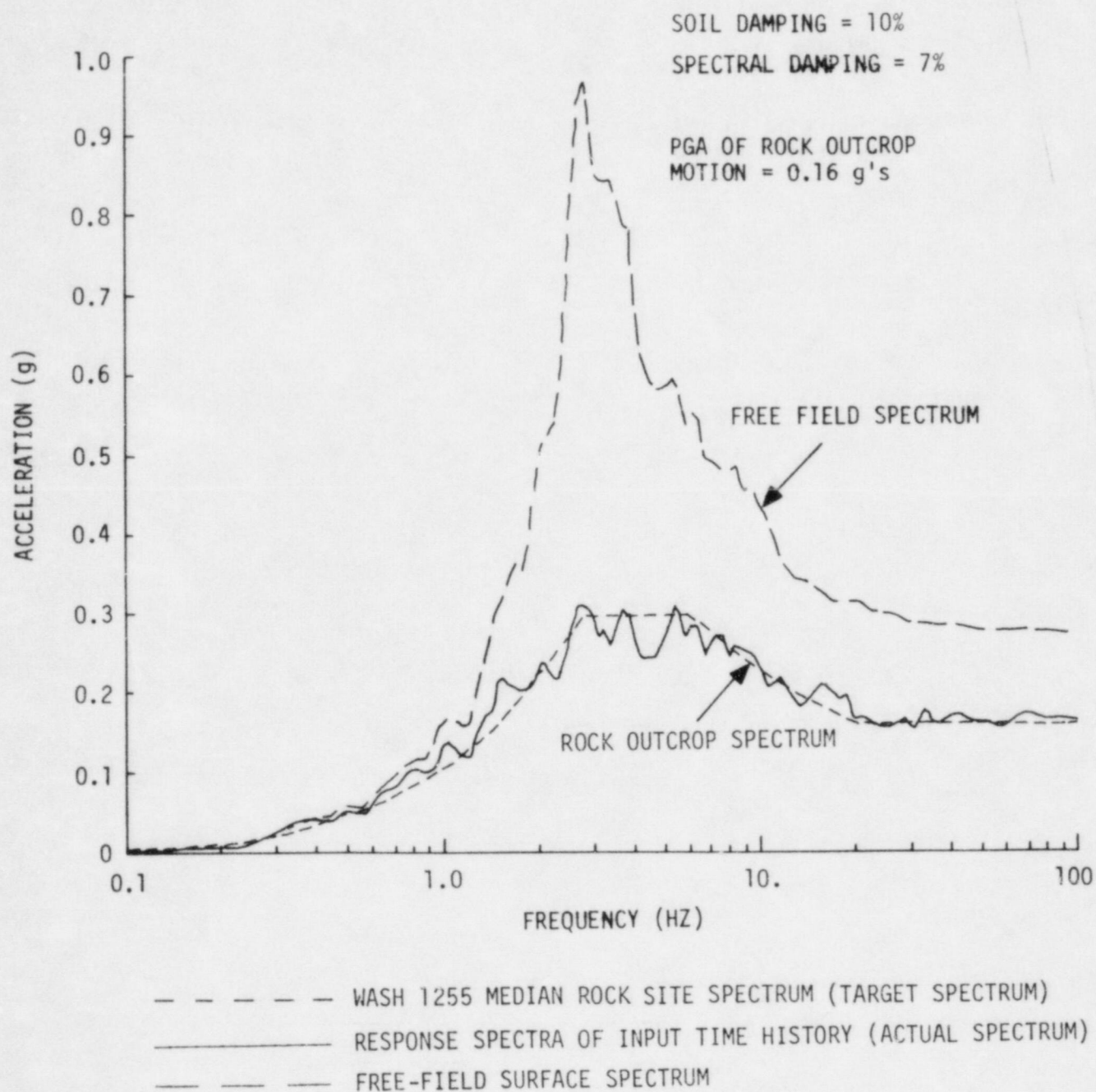


FIGURE 3-25. FREE-FIELD SURFACE RESPONSE SPECTRUM DUE TO WASH 1255 SPECTRUM APPLIED AT ROCK OUTCROP

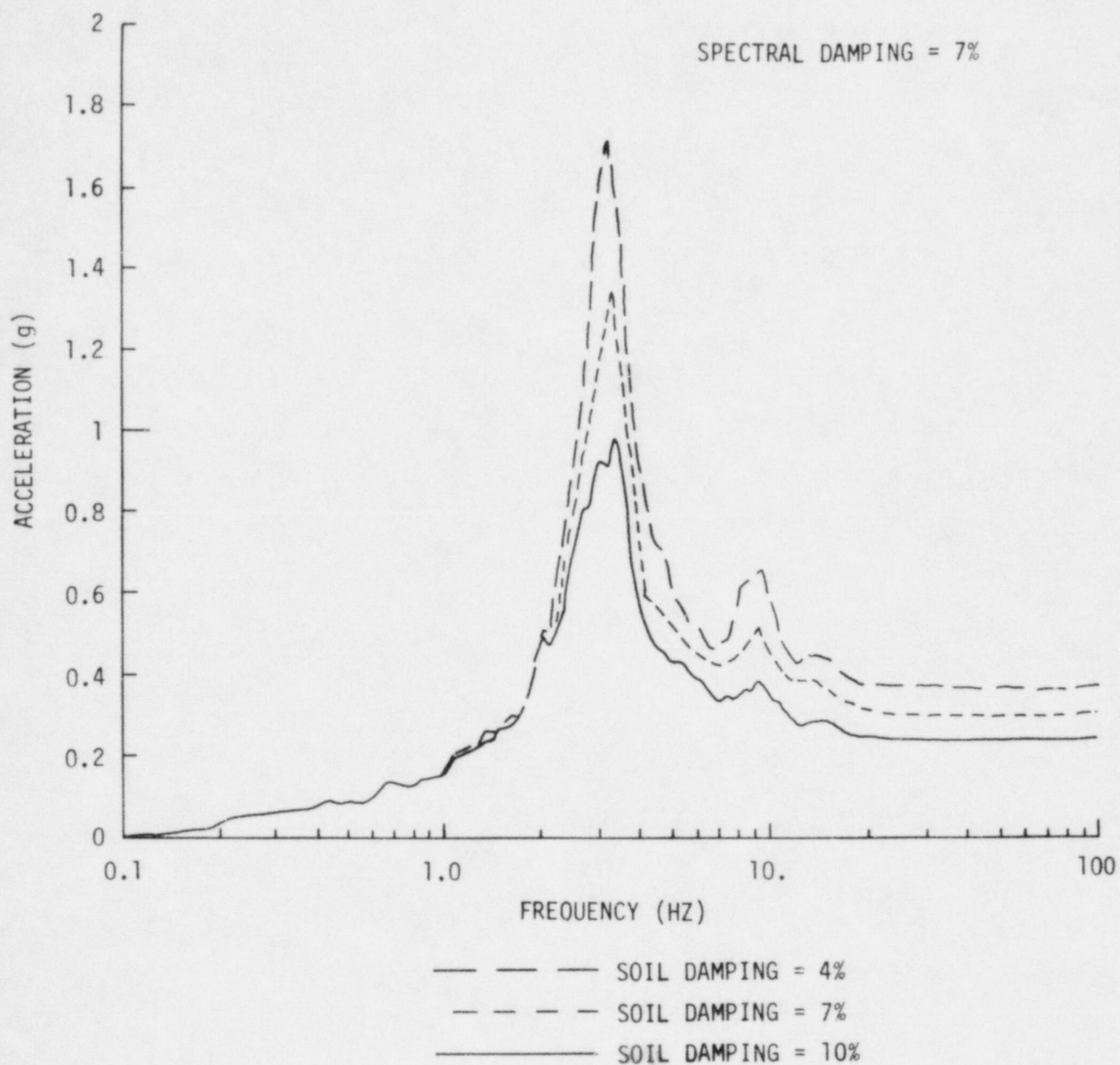


FIGURE 3-26. FREE-FIELD SURFACE SPECTRA DUE TO A BRUNSWICK DESIGN MOTION APPLIED TO THE BEDROCK LAYER



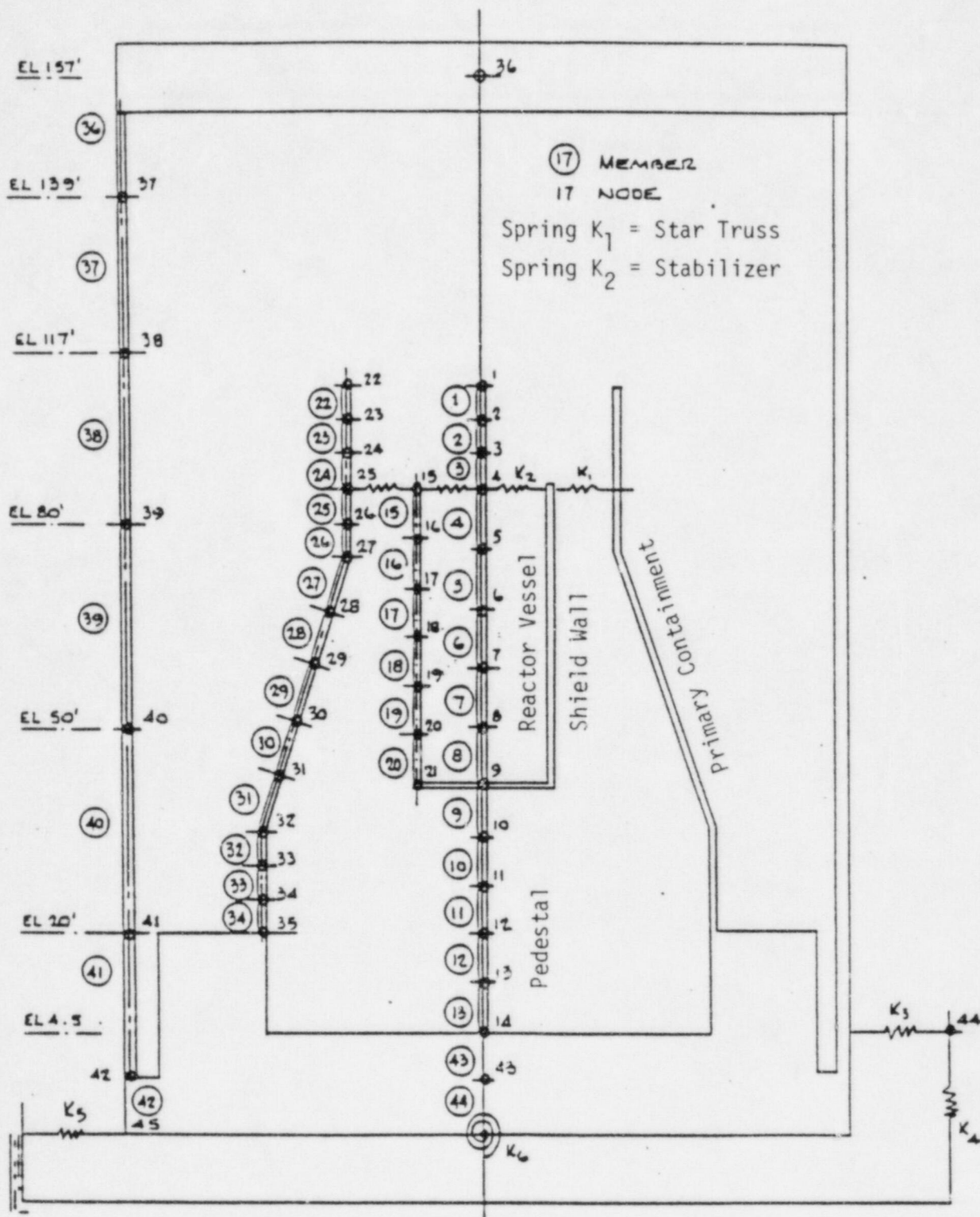
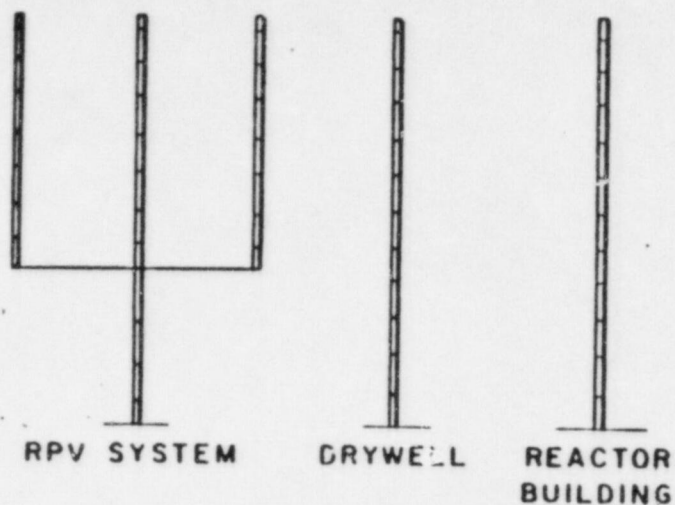
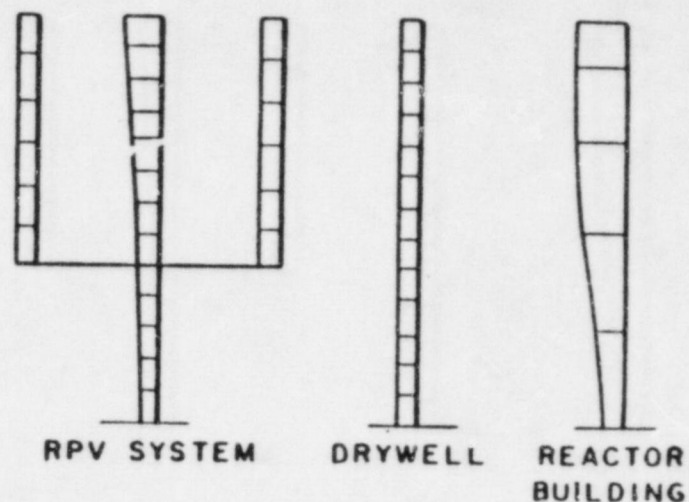


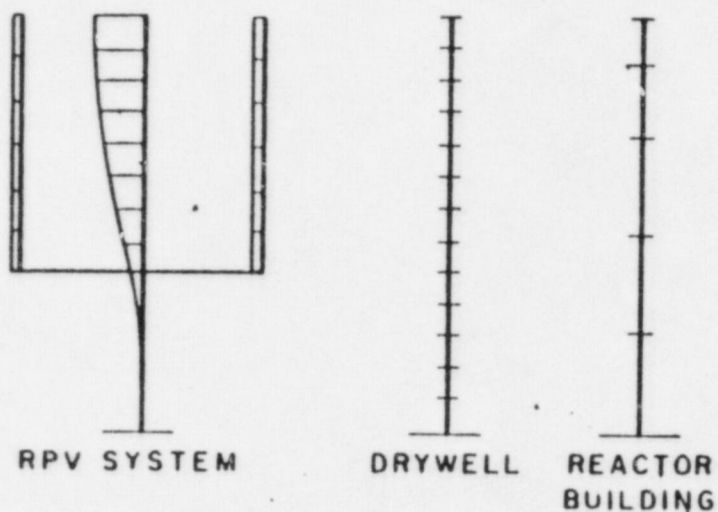
FIGURE 3-27. DYNAMIC MODEL OF REACTOR BUILDING



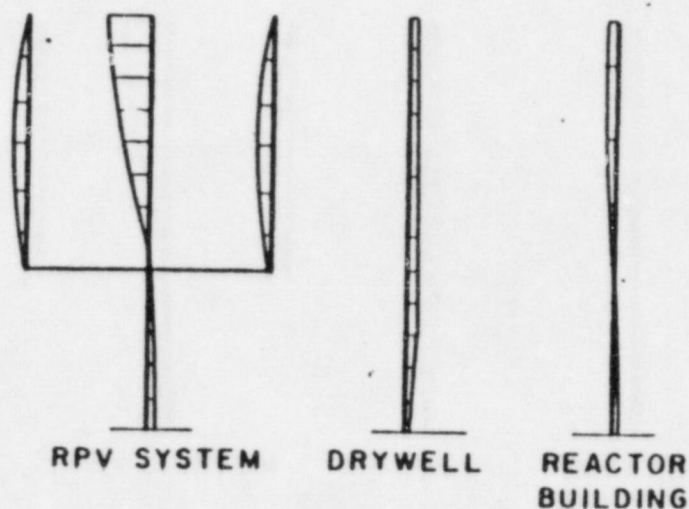
MODE - 1 (2.81 CPS)



MODE - 2 (3.28 CPS)



MODE - 3 (5.25 CPS)



MODE - 4 (5.62 CPS)

FIGURE 3-28. CONTAINMENT AND RPV SYSTEM MODE SHAPES

#### 4. GENERIC SEISMIC HAZARD CURVES

Ideally, site-specific seismic hazard curves should be used for a realistic estimation of DEGB probability. Since such site-specific seismic hazard curves are not available for the Brunswick site, generic seismic hazard curves have been utilized.

##### 4.1 BACKGROUND

The generic seismic hazard curves developed for our study of Westinghouse plants located east of the Rocky Mountains (Ravindra, et al, 1984) were utilized in this study. For the purpose of completeness, a brief description of the development of these hazard curves is given.

A total of six sites dispersed over the eastern and midwestern states were chosen. These are the sites for which formal seismic hazard analyses have been performed (Figure 4-1). Some of these analyses have been published (e.g., Zion and Indian Point Seismic Hazard Analyses), while others are part of PRA studies yet to be published. In order to preserve the anonymity of these seismic hazard studies, the plants with unpublished reports on seismic hazard studies have been labeled as A, B, C, and D.

All of these seismic hazard studies have been conducted by Dr. Robin McGuire of Dames and Moore. The salient assumptions and data (i.e., seismogenic regions, attenuation functions, activity rates, and upper bound magnitudes of earthquake) used in generating these seismic hazard curves have been reviewed thoroughly and accepted by the NRC and the peer reviewers during the Zion and Indian Point PRA studies. This methodology also explicitly treats the uncertainties in seismic hazard modeling and in the parameter values. Therefore, a family of seismic hazard curves is obtained for each site; a subjective probability value being assigned to each hazard curve to reflect the confidence in the hypothesis used to generate that curve.

Figure 4-2 shows the mean seismic hazard curves for the selected six sites. It may be observed that the mean hazard curves vary widely for different locations. It would not be appropriate to select an envelope of



these mean hazard curves as the mean generic hazard curve because it would be too conservative for plants located in most parts of the eastern and midwestern United States. Also, the Safe Shutdown Earthquake (SSE) levels of these plants vary from 0.10 to 0.25 peak ground acceleration. Hence, the seismic hazard curves must be normalized such that the peculiar features of seismicity of the region and the differences in SSE levels are not given undue importance. In this study, the hazard curves were normalized by dividing the peak ground acceleration by the larger of  $A_{SSE}$  or 0.15g. The use of 0.15g is justified because this is thought to be the currently acceptable minimum SSE in most parts of the eastern and midwestern United States. If this limit of 0.15g had not been introduced, the seismic hazard at some sites would have been disproportionately amplified in the sample of the six sites studied. Figure 4-3 shows the normalized mean seismic hazard curves at the chosen six sites.

#### 4.2 CURVE DEVELOPMENT PROCEDURE

The set of generic seismic hazard curves was developed using the following procedure.

The normalized seismic hazard curves for each of the six sites were pooled together as one population consisting of 40 seismic hazard curves. The subjective probability assigned to each curve in the original set (i.e., specific to the site) was divided by six, the number of sites included in this development of generic hazard curves. This means that each site was assigned equal weight. For the ease of further computation, the total set of 40 normalized hazard curves was condensed into five generic hazard curves with subjective probabilities of 0.1, 0.2, 0.4, 0.2, and 0.1, respectively. This was done by developing a subjective probability distribution of the probability of exceedance at each specified value of  $X$  (i.e.,  $A$  divided by the larger of  $A_{SSE}$  and 0.15g).

This subjective probability distribution was discretized into five regions with probabilities of 0.1, 0.2, 0.4, 0.2, and 0.1, respectively, and the centroid (giving the annual probability of exceedance of  $X$ ) of each region was

determined. By repeating this procedure for each  $X$  and joining the corresponding centroids, the set of five generic seismic hazard curves was obtained.

Figure 4-4 shows the generic seismic hazard curves that were used in the present study. For display purposes, Figure 4-5 shows the median generic hazard curve and the curves corresponding to 90% and 10% exceedance subjective probabilities. At a value of  $X=1$ , (i.e., at peak ground acceleration equal to  $A_{SSE}$  or  $0.15g$ ), the median annual frequency of exceedance is  $1.6 \times 10^{-4}$ ; the 90% to 10% exceedance subjective probability bounds on the annual probability of exceedance are  $3.7 \times 10^{-5}$  to  $5.2 \times 10^{-4}$ . These exceedance probabilities generally represent the bounds that most seismologists and hazard analysts believe are appropriate for eastern and midwestern U.S. sites. At higher values of  $X$ , these bounds become larger reflecting the greater degree of uncertainty.

Figure 4-1 shows the regions of the U.S. where the generic seismic hazard curves are deemed applicable.



FIGURE 4-1. REGION OF APPLICABILITY OF GENERIC SEISMIC HAZARD CURVES (RIGHT OF THE DASHED LINES)



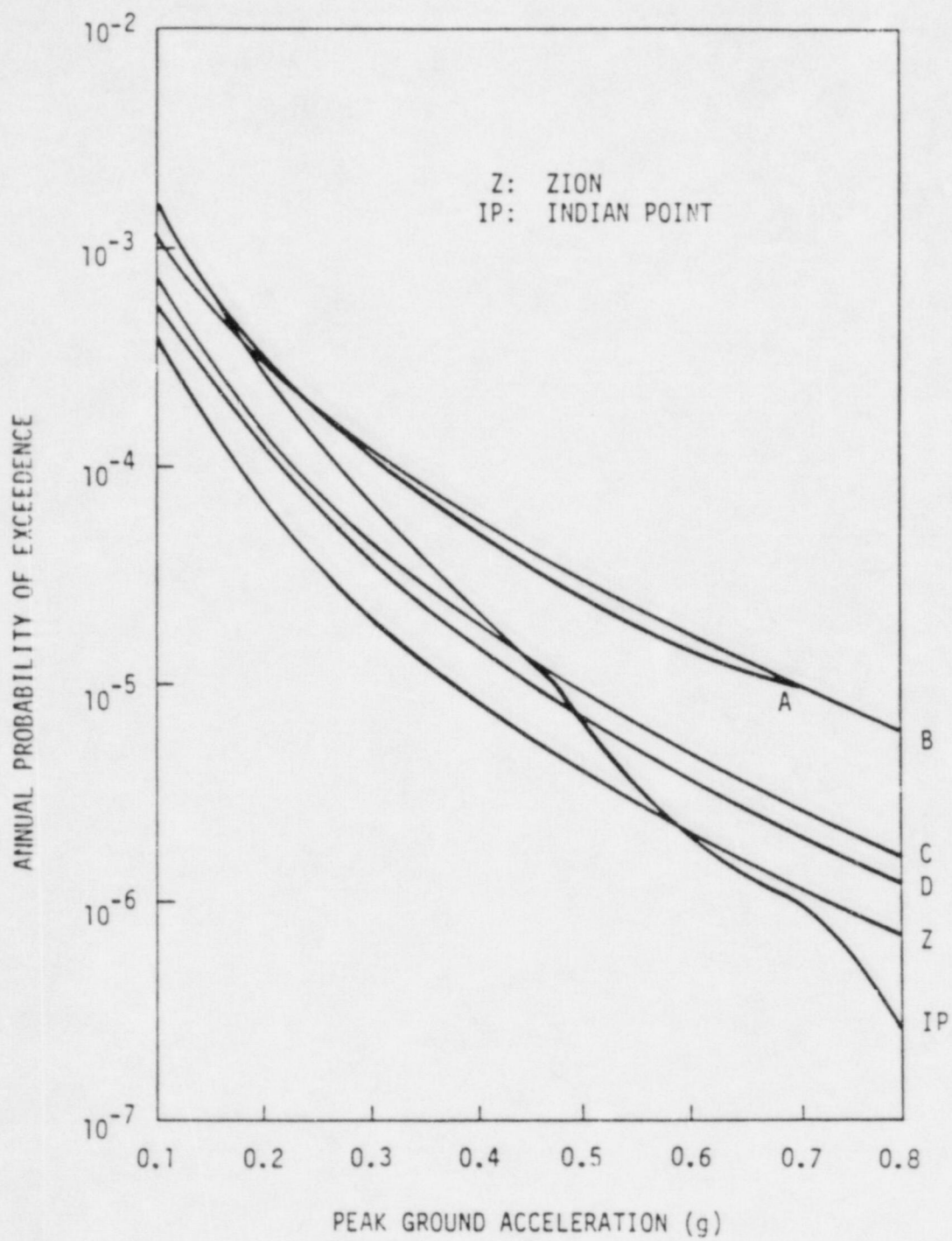


FIGURE 4-2. MEAN SEISMIC HAZARD CURVES

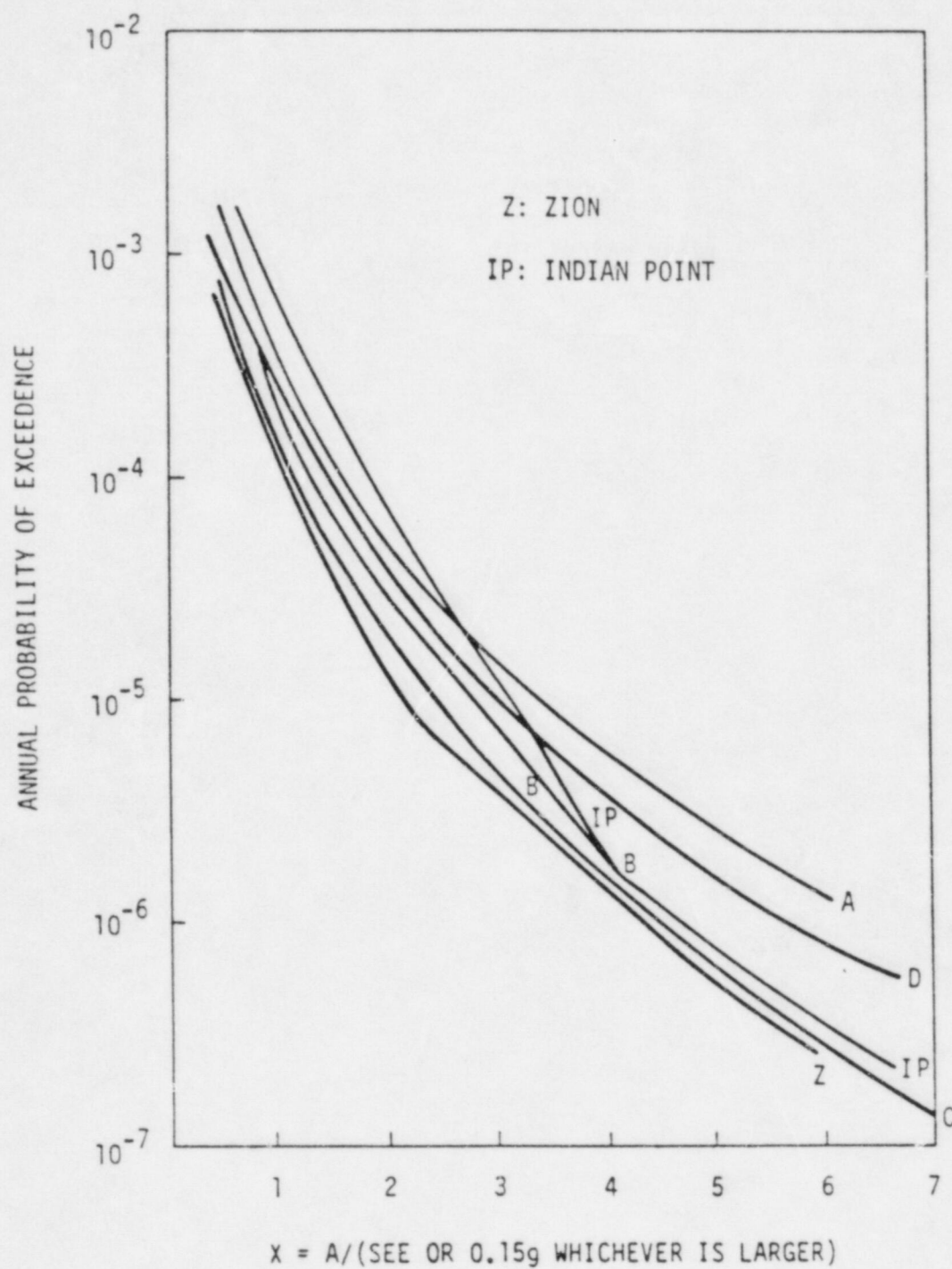


FIGURE 4-3. NORMALIZED MEAN HAZARD CURVES

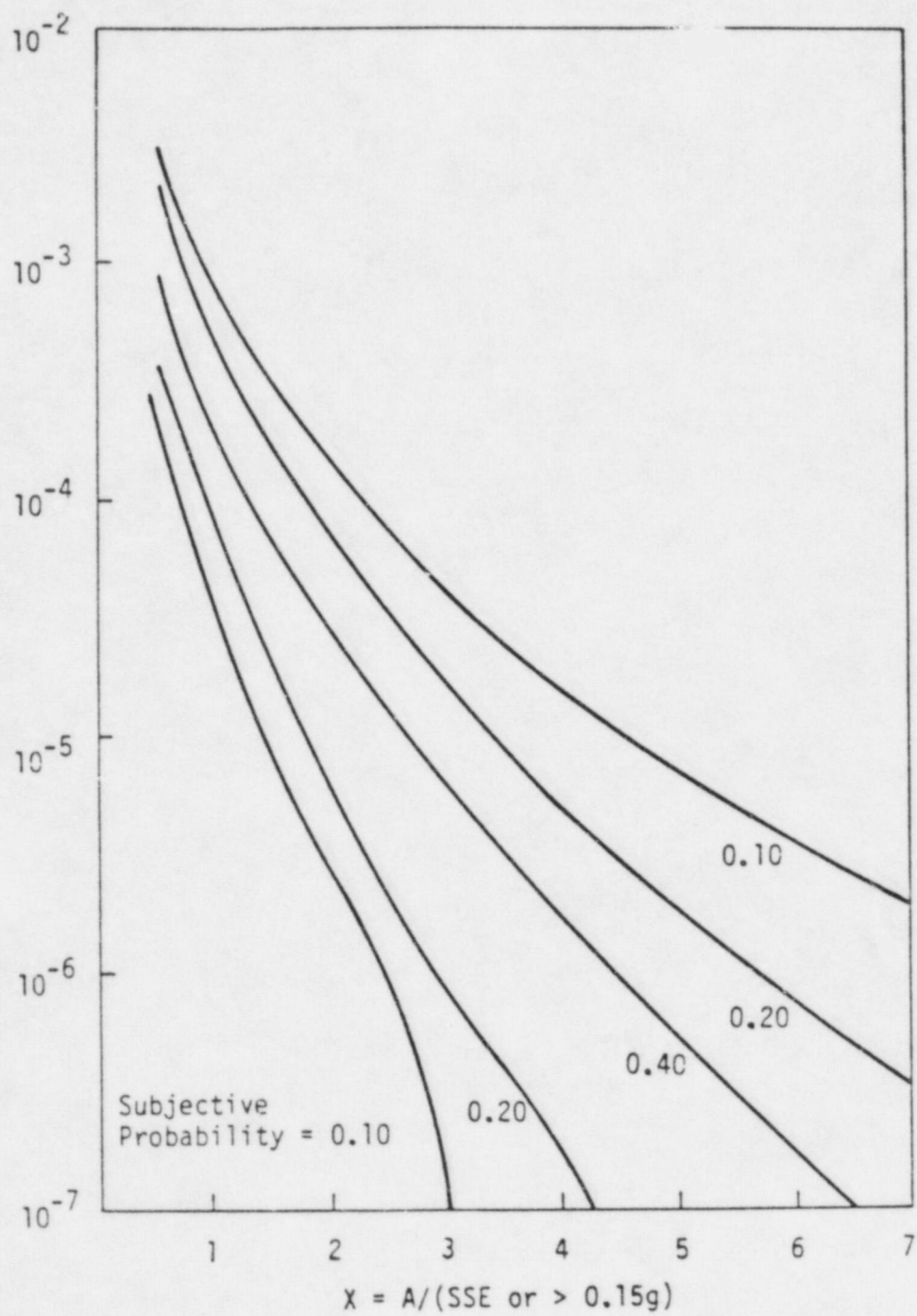


FIGURE 4-4. GENERIC SEISMIC HAZARD CURVES



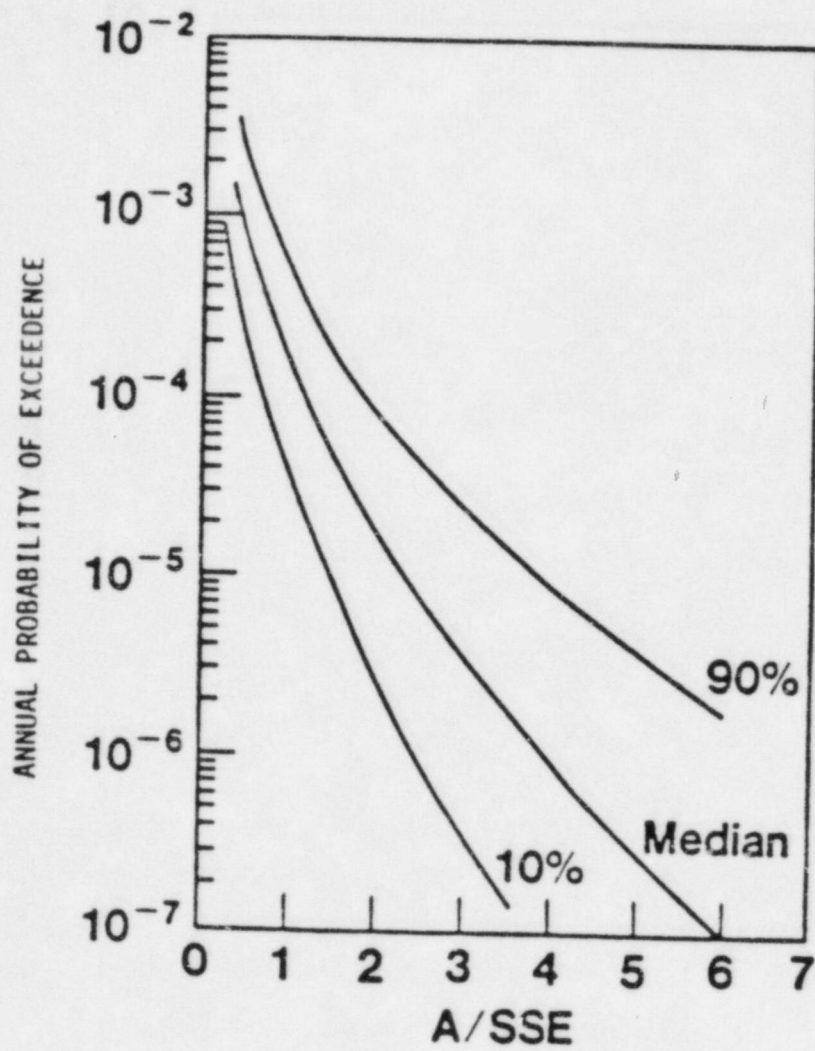


FIGURE 4-5. GENERIC SEISMIC HAZARD CURVES -  
MEDIAN AND 10% AND 90% CURVES

## 5. RESULTS AND CONCLUSIONS

The Brunswick Steam Electric Station was selected to be the trial plant on the Load Combination Program Probability of DEGB Project for GE Mark I Plant. The following subsections present the results and conclusions drawn from this study. The limitations concerning the use of these results in light of certain unresolved issues is also discussed.

### 5.1 PROBABILITY OF AN INDIRECT DEGB

As stated previously, it is assumed that the failure of any one of the RPV supports or of any of the major containment structures would result in DEGB. The RPV stabilizer and the star truss (between the shield wall and the drywell) were determined to be the weak link elements for Brunswick. Fragility curves for these two critical areas were derived in Chapter 3 and are shown in Figures 5-1 and 5-2. The calculated median capacity values of 1.92 g's (stabilizer) and 2.67 g's (star truss) are consistent with the high capacities calculated for the other GE plants during SMA's previous PRA studies. These high capacities stem from a combination of reasons:

1. Conservative design criteria which unnecessarily combines large loss-of-coolant loads with the seismic loads.
2. Conservative application of the design SSE at the bedrock instead of at the free-field.
3. Conservative response calculations (damping, etc.).
4. Utilization of design allowables which are substantially below the capacity limits of the component.

Plant level fragility curves for Brunswick were calculated using the SMA program SEISRISK. Figure 5-3 shows the median and 90% confidence bounds of the plant level fragility curves. Figure 5-4 shows the family of discretized curves which were used for the numerical convolution in SEISRISK.

By convolving the generic seismic hazard curves (Chapter 4) with the Brunswick plant level fragility curves, the probability of indirect DEGB was calculated. The median probability of an indirect DEGB is  $2.1 \times 10^{-8}$  per

reactor year and the 10% to 90% subjective probability interval on  $P_{DEGB}$  is  $2.5 \times 10^{-10}$  per reactor year to  $4.8 \times 10^{-7}$  per reactor year. Figure 5-5 shows a subjective histogram of  $P_{DEGB}$  for Brunswick.

## 5.2 COMPARISON WITH PREVIOUS STUDIES

There have been 3 comprehensive studies conducted by SMA to evaluate the probability of an indirect DEGB in the RCL piping in Westinghouse (plants east and west of the Rocky Mountains), Combustion Engineering, and Babcock and Wilcox plants. Table 5-1 compares the results for Brunswick to the range of results calculated for B&W, CE and W. The Brunswick  $P_{DEGB}$  for 10%, 50%, and 90% confidence is within the range of  $P_{DEGB}$  calculated for each of the other three plant types. The net result of Brunswick's  $P_{DEGB}$  is that the probability of an indirect DEGB occurring in the reactor coolant system piping at Brunswick is lower than that for the lowest capacity Westinghouse, Babcock and Wilcox and Combustion Engineering plants.

## 5.3 SENSITIVITY OF RESULTS

In the subsections which follow, the sensitivity of the results of this study to variation in important parameters such as the seismic hazard and gross errors are discussed.

### 5.3.1 Seismic Hazard

An important variable influencing the calculated  $P_{DEGB}$  value is the seismic hazard at the site. Plant-specific seismic hazard curves were not available for Brunswick, thus the generic seismic hazard curves were utilized in estimating  $P_{DEGB}$ . The wide spread of the uncertainty in these generic hazard curves is expected to cover all of the sites in the eastern and midwestern U.S. Past studies have shown that results generated from these generic hazard curves do not deviate greatly from those derived using plant specific hazard curves. It is generally expected that the calculated  $P_{DEGB}$  would be lower than that reported in Section 5.1 if site-specific hazard curves were used in the evaluation of the Brunswick plant.



### 5.3.2 Design and Construction Errors

The calculation of the probability of an indirect DEGB in this study has been based upon a comparison of the GE computed normal and seismic stresses and the stress levels judged to result in ultimate failure of the equipment supports for the most critical failure modes. This approach assumes that there are no undetected or uncorrected gross errors in the design and construction of the RCL equipment supports. Gross errors are very unlikely in an important system such as the reactor coolant system which is usually designed, fabricated, and installed under the careful supervision and Quality Assurance procedures of the reactor vendor. However, the topic of design and construction errors (DCE) in nuclear power plants has been broached on many different occasions. The concern is that potential gross DCEs may reduce the safety margins well below the calculated values and that the probability of an indirect DEGB may be significantly higher. This possibility was examined in depth in the Load Combination Research Program study of the Westinghouse reactors (Ravindra, et al., 1984). Several sensitivity studies were conducted to evaluate the significance of potential DEC's. It was concluded that only gross errors of implausible magnitude may substantially increase the calculated  $P_{DEGB}$  values. Design and construction errors were also addressed within the Babcock and Wilcox study (Ravindra, et al., 1985). Results were similar to those concluded from the Westinghouse study.

The two critical element failure modes for the Brunswick DEGB study are the draw bar nut failure on the stabilizer and the buckling failure of the star truss. Neither of these failure modes is judged to be vulnerable to design or construction errors of a large magnitude. The draw bar nut is made of A307 steel which is a very common ductile steel that does not undergo any exotic heat treating or fabrication process.

There are only four stabilizers at the PRV upper support and they are located such that they can be inspected with reasonable ease.

The star truss at the shield wall to drywell interface is a welded steel assembly of A36 steel tubes and plates. The failure mode projected for

the truss is buckling of the 10 inch extra strong pipe-beam members. Design and construction errors significantly effecting buckling capacity are not probable for the star truss for the following reasons:

1. The truss assembly is easy to inspect for construction deficiencies.
2. Pipe members are standard and require no special fabrication.
3. Heat treating is not applicable.
4. Welds are stronger than the pipe members and thus are not as critical.
5. Truss does not depend on possible attachment to the drywell (bumpers).
6. Columns are short and buckle plastically, thus, initial imperfections do not significantly affect buckling capacity.

The above arguments stipulate why design and construction errors are not expected to significantly influence the governing elements for the Brunswick indirect DEGB study. However, in order to assess the potential for the increased probability of an indirect DEGB as the result of a gross error in these other elements, the  $P_{DEGB}$  values were recalculated for the Brunswick facility assuming that the failure capacity of the two most critical areas (stabilizer and star truss) were reduced by 50%. A 50% reduction in capacity increases  $P_{DEGB}$  by about a factor of 40% or about one-and-one-half orders of magnitude. The median frequency of failure for the 50% reduction case is  $8.3 \times 10^{-7}$ . The 10% and 90% confidence bounds are  $2.5 \times 10^{-8}$  and  $8.5 \times 10^{-6}$ , respectively. These values are all still below the governing PWR plants, as noted in Table 5-1.

In view of the Quality Assurance and Quality Control procedures adopted for the reactor coolant system of GE reactors and the large margin in  $P_{DEGB}$  demonstrated for errors of significant magnitude the issue of gross design and construction errors appears to be relatively unimportant for the Brunswick nuclear power plant.

### 5.3.3 Low Fracture Toughness

The Nuclear Regulatory Commission funded a study related to the potential for low fracture toughness and lamellar tearing of NSSS component supports in nuclear power facilities. The results of the study were published in NUREG-0577 and identified structural materials which were potentially susceptible to low fracture toughness and therefore brittle failure. PWRs studied were ranked into three groups based upon whether or not such materials were used in the fabrication of major component supports.

BWRs were not included in the study but it is noted that some of the materials listed as having potentially low fracture toughness are included in the Brunswick NSSS supports that were determined to govern indirect DEGB. A-307 bolts and nuts and A-106 tubular products were identified as candidate materials for low fracture toughness. Both materials are very commonly used throughout nuclear power plants but it is deemed unlikely that the applications in Brunswick would be brittle.

The upper stabilizer has A-307 nuts which were found to be the governing element for PRV support. During plant operations the nuts are expected to be considerably above room temperature. The relationship between operating temperature and the nil-ductility transition temperatures are not known, therefore, it must be assumed that there is a very small potential for a brittle failure of the nuts by splitting in the hoop direction at loading less than the thread shear capacity.

The star truss material was unknown but was assumed to be made of A-106 pipe. The critical loading is in compression and it is inconceivable that a brittle failure could occur even in the event of low fracture toughness.

The sensitivity study conducted that assumed a 50% reduction in strength of both governing failure modes indicated that large margins still existed for Brunswick relative to  $P_{DEGB}$  computed for the governing PWR plants.



#### 5.3.4 Brunswick SSE Spectrum Application

The design analysis on Brunswick for seismic loads consisted of conservatively applying the SSE design spectrum at the bedrock level beneath the site shallow soil layer. A median centered analysis for the SSE would apply this spectrum at the free-field and subsequently deconvolve the loading through the soil and into the appropriate structure. This particular conservatism in the Brunswick design basis will not be present in the majority of the remaining GE Mark I reactor systems, and, thus, a sensitivity study was conducted to assess the  $P_{\text{DEGB}}$  for Brunswick without accounting for this factor. The spectral shape factors in Tables 3-4 and 3-5 were removed and a SEISRISK analysis performed. The new median, 90% probability values were:

$$P_{\text{DEGB}} (10\%) = 5.1 \times 10^{-10}$$

$$P_{\text{DEGB}} (50\%, \text{ median}) = 1.9 \times 10^{-7}$$

$$P_{\text{DEGB}} (90\%) = 2.8 \times 10^{-6}$$

These are still very low values and are likely more representative of other Mark I BWRs.

#### 5.4 SUMMARY AND CONCLUSIONS

In this study, the probability of an indirectly-induced DEGB of the reactor coolant system piping in the GE Mark I reactor system at Brunswick has been calculated. The seismic margins to ultimate failure of the major equipment and structures whose failure could lead to DEGB were calculated using design information provided by United Engineers and Constructors (plant Architect-Engineers) and Carolina Power and Light. Generic hazard curves were used along with the calculated seismic margins (fragilities) to compute the indirect DEGB probabilities.

Based upon insight gained and the results of this study, the following conclusions can be drawn:

1. The probability of an indirectly-induced DEGB in the reactor coolant system piping due to earthquakes is very low for the Brunswick Plant. Using very conservative assumptions, the 90% confidence value of  $P_{DEGB}$  is found to be less than  $5 \times 10^{-7}$  per year.
2. Sensitivity studies have shown that only very unlikely design and construction errors of implausible magnitude could substantially increase the  $P_{DEGB}$  values calculated in this study.
3. The Brunswick seismic design analysis was exceptionally conservative by application of the SSE design spectrum at bedrock. A sensitivity study which deleted the factor of conservatism associated with this SSE spectrum application was conducted for Brunswick and the resulting 90% confidence bound  $P_{DEGB}$  was still less than  $2 \times 10^{-6}$  per year. This sensitivity study is intended to be a reference for other GE Mark 1 reactor plants where more typical (less conservative) design criteria were utilized.

TABLE 5-1

COMPARISON OF  $P_{\text{DEGB}}$  FOR DIFFERENT TYPES OF NUCLEAR PLANTS

Plant Type	Probability of DEGB Per Year		
	Median Range	10% Prob. Range	90% Prob. Range
Brunswick (Mark I GE)	$2.0 \times 10^{-8}$	$2.5 \times 10^{-10}$	$4.8 \times 10^{-7}$
Babcock and Wilcox Plants	$1.1 \times 10^{-7}$ to $1.5 \times 10^{-17}$	$3.5 \times 10^{-8}$ to $1.3 \times 10^{-21}$	$1.1 \times 10^{-5}$ to $1.8 \times 10^{-12}$
Combustion Engineering Plants	$1.4 \times 10^{-6}$ to $4.6 \times 10^{-17}$	$5.0 \times 10^{-7}$ to $4.0 \times 10^{-19}$	$1.1 \times 10^{-5}$ to $3.2 \times 10^{-14}$
Westinghouse Plants	$3.3 \times 10^{-6}$ to (Note 1)	$2.3 \times 10^{-7}$ to (Note 1)	$2.3 \times 10^{-5}$ to (Note 1)

Note 1: The lowest probability of DEGB on Westinghouse Plants was not documented in NUREG/CR-3660. The lower bound was approximately in the same range as the B & W and CE Plants.



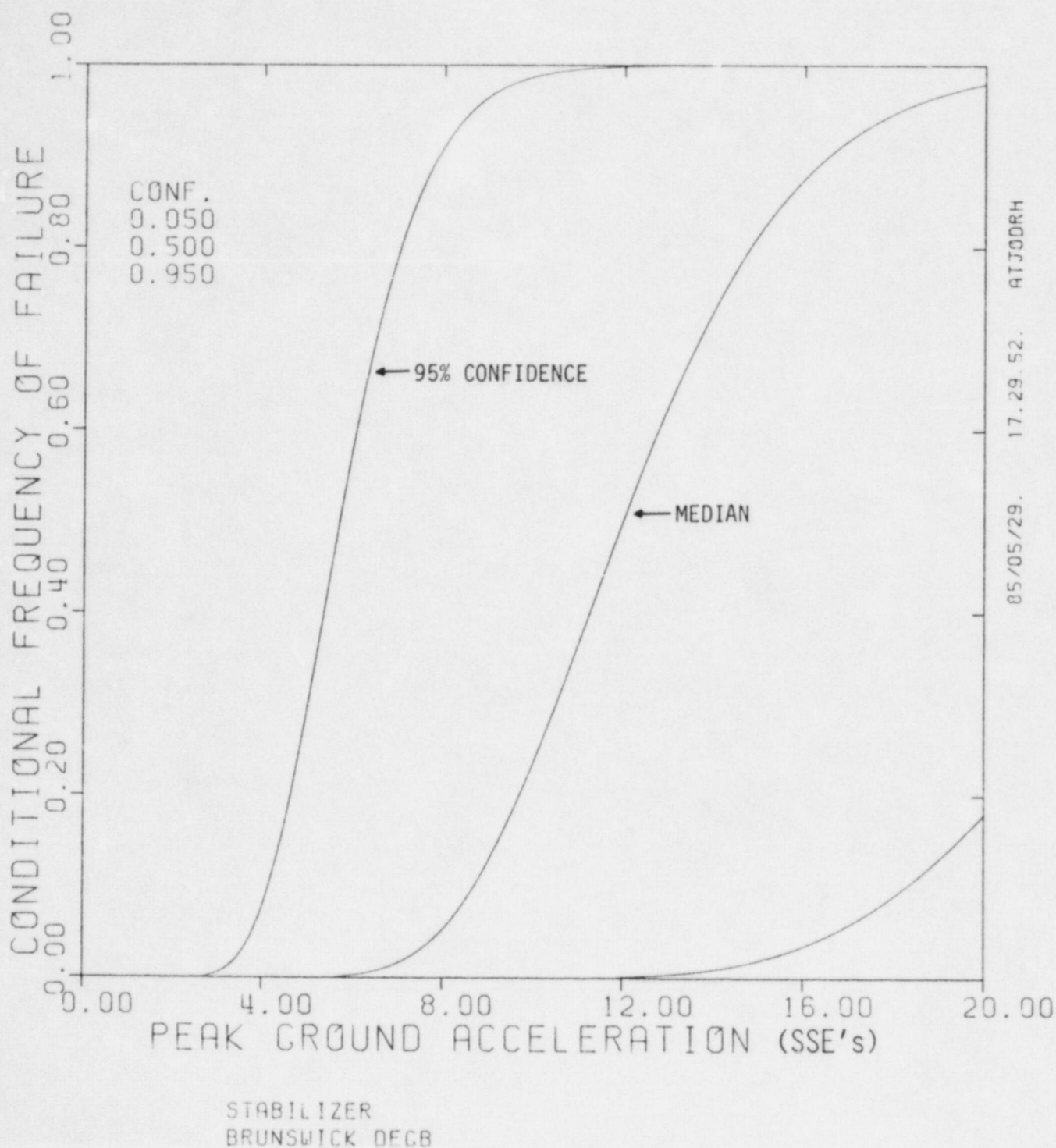
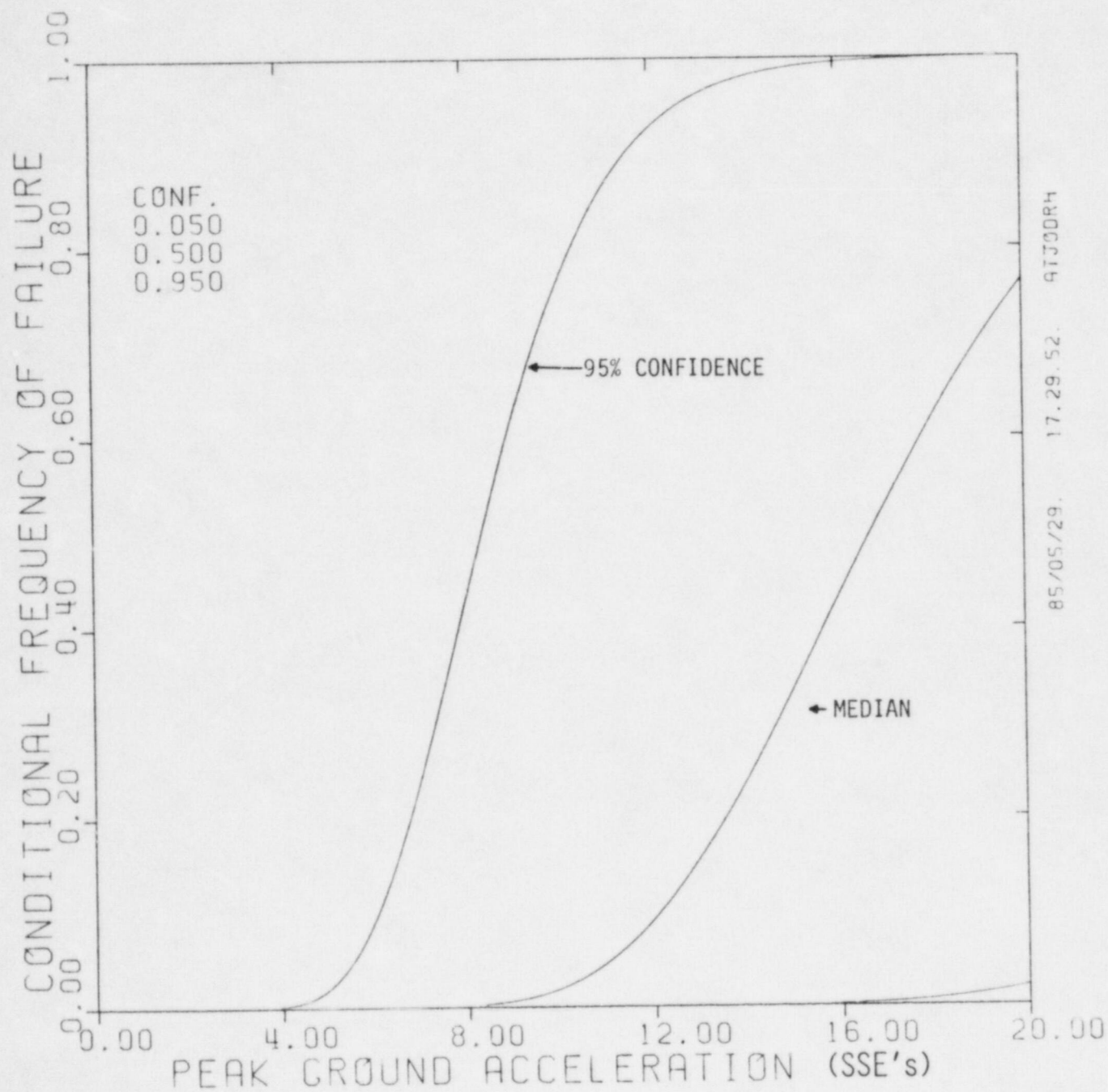


FIGURE 5-1. STABILIZER FRAGILITY CURVES



STAR TRUSS FAILURE  
BRUNSWICK DEGB

FIGURE 5-2. STAR TRUSS FRAGILITY CURVES

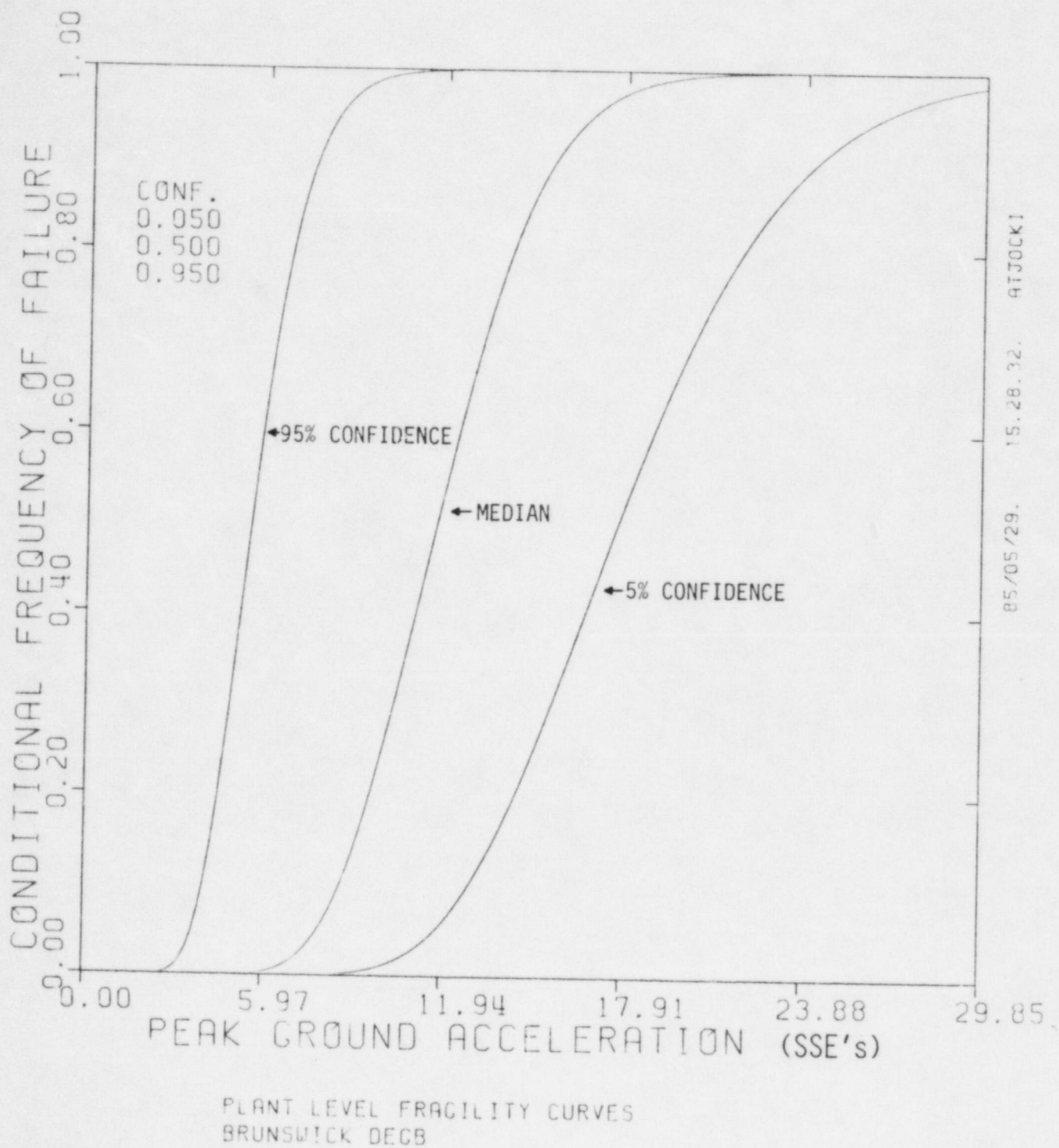
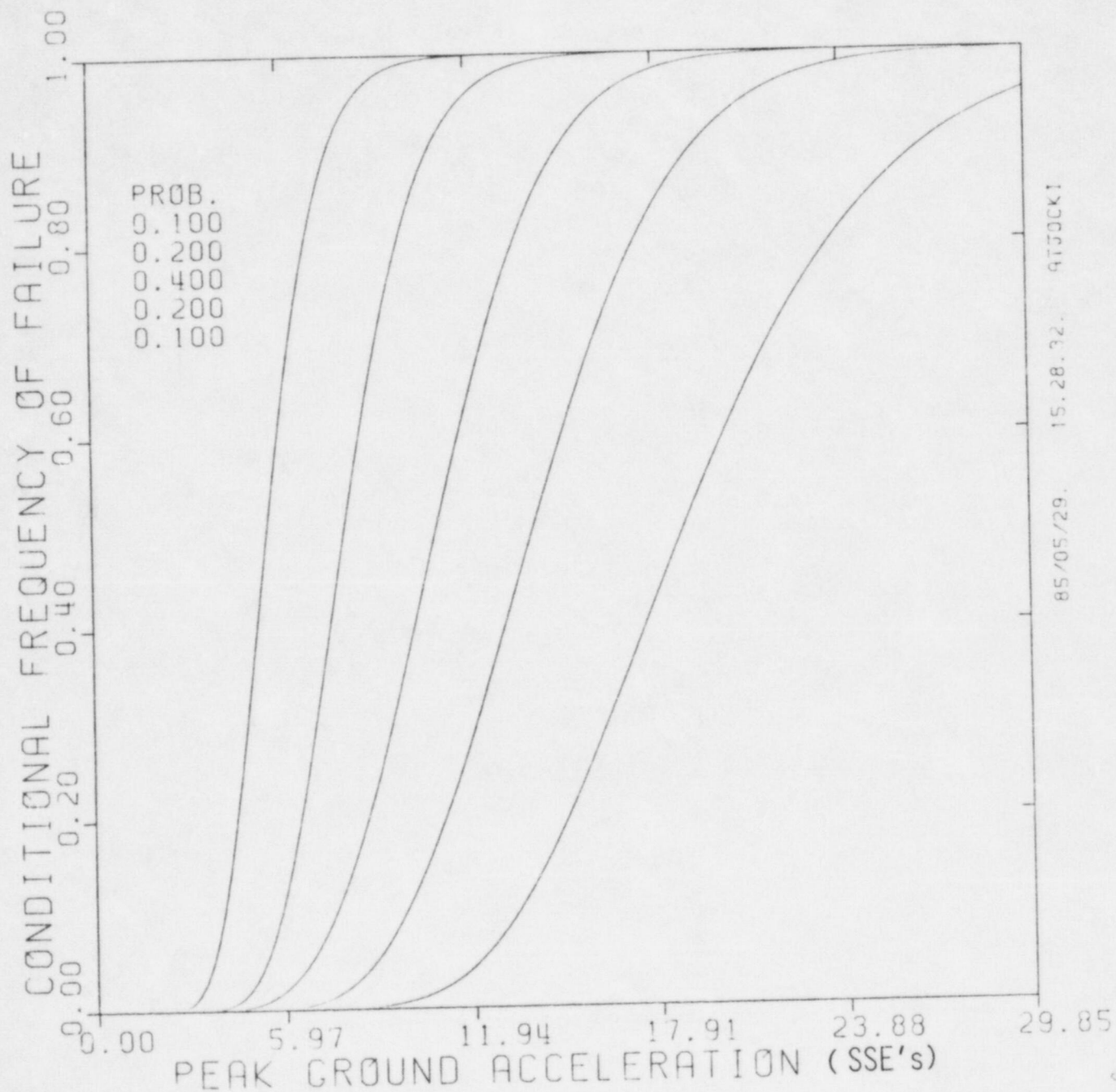


FIGURE 5-3. PLANT LEVEL FRAGILITY CURVES FOR BRUNSWICK



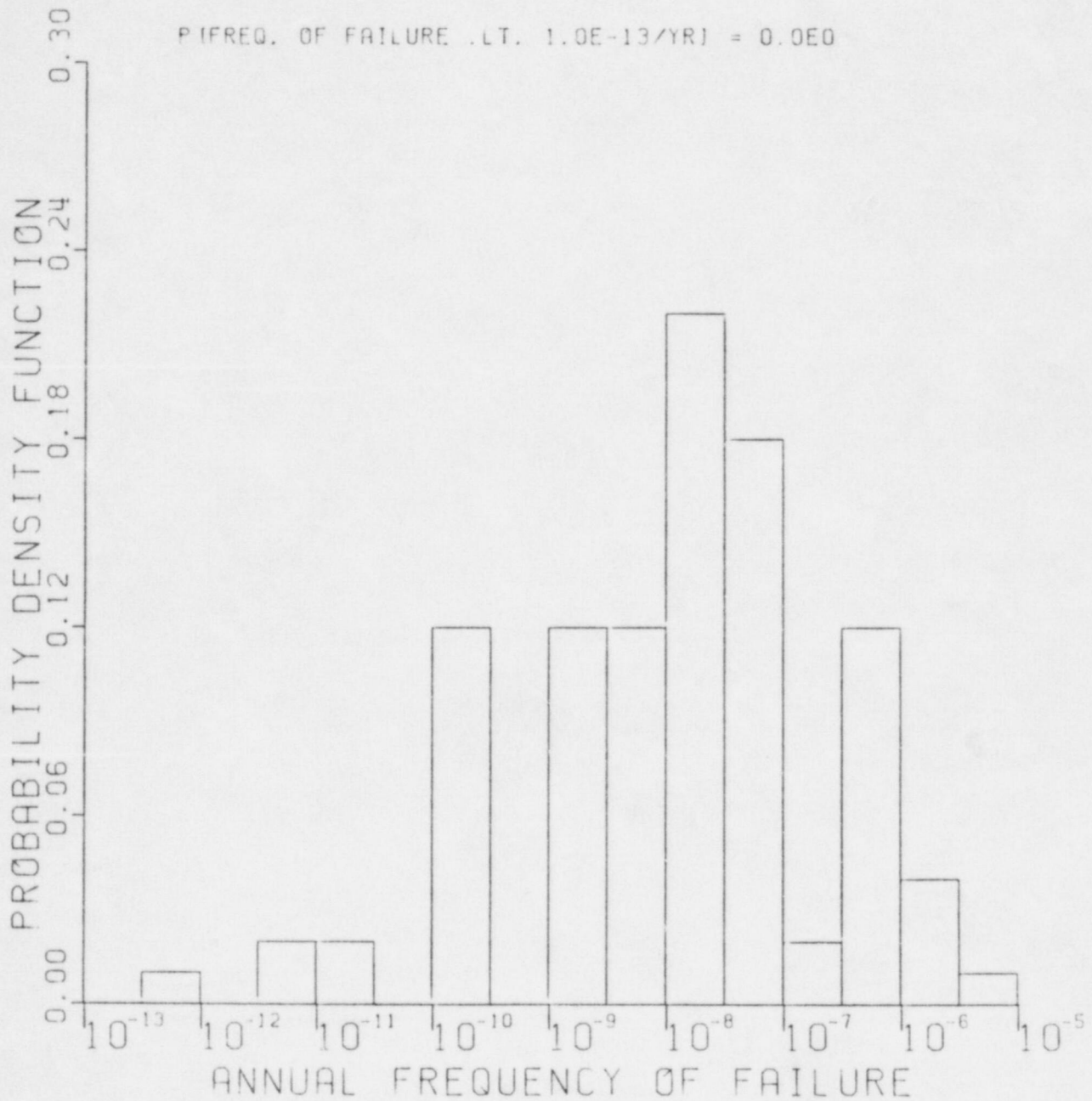


PLANT LEVEL FRAGILITY CURVES  
BRUNSWICK DECB

FIGURE 5-4. PLANT LEVEL FRAGILITY CURVES FOR BRUNSWICK

MEDIAN =  $2.1E-8$

P (FREQ. OF FAILURE .LT.  $1.0E-13$ /YR) = 0.000



BRUNSWICK DEGB

FIGURE 5-5. HISTOGRAM OF ANNUAL FREQUENCY OF DEGB FOR BRUNSWICK

## REFERENCES

1. Algermissen, S. T., et al, "Probabilistic Estimates of Maximum Acceleration and Velocity in Rock in the Contiguous United States", United States Department of the Interior Geological Survey, Open File Report 82-1033, 1982.
2. Babcock & Wilcox, Seismic Margin Study Report for Midland Units 1 and 2, 51-1140965-00, March, 1983.
3. Cornell, C. A., "Engineering Seismic Risk Analysis", Bulletin of the Seismological Society of America, Vol. 58, No. 5, pp. 1583-1605, 1968.
4. General Electric, "Reactor Vessel/Shield Wall Annulus Pressurization Following Pipe Break for the Brunswick Steam Electric Plant Units 1 and 2", NED0-24225, August, 1980.
5. Hadjian, A. H., C. B. Smith, A. Halder and P. Ibanex, "Variability in Engineering Aspects of Structural Modeling", Proc. 6th World Conference Earthquake Engineering, New Delhi, India, January, 1977.
6. Hall, D. H., "Proposed Steel Column Strength Criteria", ASCE, Journal of the Structural Division, April, 1981.
7. Joyner, W. B., and D. M. Boore, "Peak Horizontal Acceleration and Velocity from Strong Motion Records Including Records from the 1979 Imperial Valley, California, Earthquake", Bulletin of the Seismological Society of America, Vol. 71, No. 6, pp. 2011-2038, 1981.
8. Kennedy, R. P., et al, "Probabilistic Seismic Safety of an Existing Nuclear Power Plant", Nuclear Engineering and Design, Vol. 59, No. 2, August, 1980.
9. Kennedy, R. P. and M. K. Ravindra, "Seismic Fragilities for Nuclear Power Plant Risk Studies", presented at the Second CNSI (Committee on Safety of Nuclear Installations) Specialist Meeting on Probabilistic Methods in Seismic Risk Assessment for Nuclear Power Plants, Livermore, California, May, 1983 (submitted for publication in Nuclear Engineering and Design Journal).
10. NASA, "Buckling of Thin-Walled Circular Cylinders", Document #SP 8007 from the NASA Space Vehicles Design Criteria, 1965.
11. Newmark, N. M., "A Study of Vertical and Horizontal Earthquake Spectra", WASH 1255, prepared for USAEC, April, 1973.
12. Ravindra, M. K. and T. V. Galambos, "Load and Resistance Factor Design for Steel", Proc. ASCE, Journal of Structural Division, Vol. 104, No. ST9, Proc. Paper 14008, September, 1978, pp. 1337-1353.



13. Ravindra, M. K., R. D. Campbell, R. P. Kennedy and H. Banon, "Load Combination Program - Probability of Guillotine Break of Westinghouse Reactor Coolant Loop Piping Indirectly-Induced by Earthquakes", SMA 12208.30-R1-0, Structural Mechanics Associates, Inc., Newport Beach, California, January, 1984.
14. Ravindra, M. K., H. Banon, R. H. Sues and R. D. Thrasher, "Sensitivity Studies of Seismic Risk Models", SMA 15704.01-R1-0, Structural Mechanics Associates, Inc., Newport Beach, California, February, 1984.
15. Ravindra, M. K., R. D. Campbell, T. R. Kipp and R. H. Sues, "Load Combination Program Probability of Guillotine Break of Babcock and Wilcox Reactor Coolant Loop Piping Indirectly-Induced by Earthquakes", SMA 12211.05-R1, Structural Mechanics Associates, Newport Beach, California, April, 1985.
16. Riddeil, R. and N. M. Newmark, "Statistical Analysis of the Response of Nonlinear Systems Subjected to Earthquakes", Dept. of Civil Engineering, Report UILU 79-2016, University of Illinois, Urbana, Illinois, August, 1979.
17. Rodabaugh, E. C. and K. D. Desai, "Realistic Seismic Design Margins of Pumps, Valves, and Piping", NRC, NUREG/CR-2173, May, 1981.
18. Snaider, R. P., et al, "Potential for Low Fracture Toughness and Lamellar Tearing on Component Supports", NRC, NUREG-0577, Draft, October, 1980.

## NOMENCLATURE

<u>Symbol</u>	<u>Definition</u>
A	Peak ground acceleration; a random variable.
$A_C$	Ground acceleration capacity.
$A_{SSE}$	Safe shutdown earthquake peak horizontal ground acceleration.
a	Specific value of ground acceleration.
b	Richter slope parameter.
C	Capacity of a structural element, $C$ = median; $\bar{C}$ = mean, $\beta_C$ = logarithmic standard deviation.
d	Closest distance to the surface projection of the fault rupture.
F	Factor of safety; $F$ = median, $\bar{F}$ = mean.
$F_C$	Capacity factor.
$F_\delta$	Damping factor representing the variability in response due to difference in actual damping and design damping.
$F_{EC}$	Earthquake component combination factor accounting for the variability in response due to the method used in combining the earthquake components.
$F_M$	Modeling factor accounting for the uncertainty in response due to modeling assumptions.
$F_{MC}$	Mode combination factor accounting for the variability in response due to the method used in combining dynamic modes of response.
$F_{RE}$	Equipment response factor.
$F_{RS}$	Structure response factor.
$F_R$	Combined equipment and structure response factors.
$F_S$	Strength factor representing the ratio of ultimate strength (or strength at loss-of-function) to the stress calculated for reference earthquake acceleration ( $A_{SSE}$ ).

## NOMENCLATURE (Continued)

<u>Symbol</u>	<u>Definition</u>
$F_{SS}$	Spectral shape factor representing the variability in ground motion and the associated ground response spectra and how they affect the response.
$F_{SSI}$	Factor to account for the effect of soil-structure interaction.
$F_a$	Faulted allowable stress in buckling.
$F_u$	Specified ultimate capacity of snubber.
$F_{ult}$	Ultimate buckling strength of a column.
$f_A(a)da$	Frequency of occurrence of earthquakes with peak ground acceleration between $a$ and $a+da$ .
$l$	Length of column between support points.
$M$	Moment magnitude.
$m_b$	Bodywave magnitude.
$P_{DEGB}$	Probability of double-ended guillotine break
$P_N$	Normal operating load.
$P_T$	Total load on the structural element.
$R$	Response of structural element or equipment.
$r$	Radius of gyration, distance from the site to the earthquake source.
$S$	Strength of structural element for the particular failure mode.
$S_y$	Specified yield strength of material.
$X$	Normalized peak ground acceleration obtained by dividing $A$ by $A_{SSE}$ for the plant.
$B(\cdot), R$	Logarithmic standard deviation representing the inherent randomness of the variable specified in parenthesis.



NOMENCLATURE (Continued)

<u>Symbol</u>	<u>Definition</u>
$\beta(\cdot), U$	Logarithmic standard deviation representing the uncertainties in the parameter (median) describing the variable specified in parenthesis.
$\mu$	Ductility ratio.
$\lambda$	Slenderness parameter.

## GLOSSARY

Activity Rate	Mean annual rate of occurrence of earthquakes over a seismic source.
Attenuation	Decrease in the intensity of ground shaking with distance.
DEGB	A postulated event of an instantaneous double-ended guillotine break of the reactor coolant loop piping.
Factor of Safety	The ratio of the ground acceleration capacity A to the SSE acceleration used in plant design.
Failure Mode	The way in which a component may fail to perform its intended function. Examples of failure modes are excessive deformation, rupture of the pressure boundary, relay chatter and binding of a valve.
Fragility	Conditional probability that a structure or equipment would fail for a specified ground motion of response parameter value.
Ground Acceleration Capacity	The seismic capacity of a structure or equipment measures in terms of the peak ground acceleration value at which it would fail.
Inherent Randomness	The variability inherent to a physical phenomenon; it cannot be reduced by more detailed evaluation or by gathering of more data.
Magnitude	Magnitude is a measure of the size of an earthquake and is related to the energy released in the form of seismic waves. Richter magnitude (m) is equal to the common logarithm of the maximum trace amplitude (expressed in microns) written by a standard torsion seismometer (free period 0.8 sec, damping ratio about 50:1, and static magnitude of 2,800) at an epicentral distance of 100 km. The bodywave magnitude, m is a function of the bodywave amplitude to period ratio.
Seismic Hazard Analysis	The process of estimating the frequency distribution of the peak ground motion parameter value at the site due to earthquakes in the region.
Seismic Source	A fault or a seismotectonic province over which an earthquake may occur.

## GLOSSARY (Continued)

Uncertainty	Refers to the state of knowledge concerning a physical phenomenon; it can be reduced by a more detailed evaluation or by gathering of additional data.
Upperbound Magnitude	Magnitude of the largest earthquake that a seismic source is capable of producing.